University of Alberta

Effects of long-term inhibition of EAAT2 on the excitability of spinal dorsal horn neurons

by

Helena Jeonghyun Kim

A thesis submitted to the Faculty of Graduate Studies and Research
in partial fulfillment of the requirements for the degree of

Master of Science

Centre for Neuroscience

Spring 2011
Edmonton, Alberta

Examining Committee

Peter A. Smith, Pharmacology

Klaus Ballanyi, Physiology

Bradley J. Kerr, Anesthesiology and Pain Medicine

Abstract

This thesis examined the effects of long-term inhibition of excitatory amino acid transporter 2 (EAAT2) on the excitability of dorsal horn neurons in defined-medium organotypic slice cultures (DMOTCs). Previous reports suggest that inhibition of EAAT2 may be involved in development of neuropathic pain induced by brain-derived neurotrophic factor (BDNF). Experiments were carried out using confocal Ca^{2+} imaging to assess the excitability of dorsal horn neurons.

Long-term treatment with EAAT2 blocker, dihydrokainate (DHK), prominently increased the neuronal excitability. Long-term exposure to DHK had a significant effect on NMDA, AMPA and metabotropic glutamate subtype 1 ($mGluR_1$) receptors. Lastly, long-term treatment with BDNF and DHK increased activity of AMPA receptors but only DHK significantly increased activity of NMDA receptors. These findings suggest inhibition of EAAT2 and BDNF may have different pathways to promote neuropathic pain and modulating the activity of EAAT2 may be a novel therapeutic approach for neuropathic pain.

Acknowledgements

First, I would like to thank my supervisor, Peter Smith, for giving me the opportunity to work in his laboratory. I am truly grateful for his guidance and advice through the course of this degree. I cannot thank him enough for enabling me to develop a broad scope of training in the field of research and expand my interest in science.

I would like to thank Klaus Ballanyi for all the advice and suggestions regarding the imaging technique and my experiments. This thesis would not have been completed without them.

I would also like to thank Bradley Kerr for his ideas and suggestions for my experiments and all his help and advice regarding behavioural studies in NEURO 501. I truly appreciate his contributions toward my project.

Next, I would like to thank James Biggs for teaching me from day one regarding cell culture, imaging technique and everything else I should know to run experiments. Also, I must thank him for his patience throughout my learning process, answering my questions and helpful tips and suggestions.

I would like to thank Yishen Chen and Patrick Stemkowski for all the encouragement, advices and support regarding my experiments, courses and presentations. I would also like to thank Briana Napier for making solutions and culture preparations.

Lastly, I must thank Araya Ruangkittisakul and Bogdan Panaitescu for technical support regarding calcium imaging and all the help with my experiments. I would also like to thank Camille Olechowski for teaching me

techniques for behavioural studies and Shaona Acharjee for encouragement and advices on my experiments and research.

Table of Contents

List of Figures

List of Abbreviations

ALS - Amyotrophic lateral sclerosis

AM - Acetoxymethyl

ANOVA - Analysis of variance

AraC - Cytosine-β-d-arabino-furanoside

AMPA - α-amino-3-hydroxyl-5-methyl-4-isoxazole-propionate

BDNF - Brain-derived neurotrophic factor

CCI - Chronic constriction injury

CGRP - Calcitonin-gene related peptide

CL - Central lateral

CNS - Central nervous system

CNQX - 6-Cyano-7-nitroquinoxaline-2,3-dione

CTZ - Cyclothiazide

D-AP5 - D-(-)-2-Amino-5-phosphonopentanoic acid

DHK - Dihydrokinate

DHPG - (RS)-3,5-Dihydroxyphenylglycine

DMEM - Dulbecco's modified Eagle's medium

DMOTC - Defined-medium organotypic slice culture

DMSO - Dimethyl sulfoxide

DRG - Dorsal root ganglion

EAAC1 - Excitatory amino acid carrier 1

EAAT1 - Excitatory amino acid transporter 1

EAAT2 - Excitatory amino acid transporter 2

EAAT3 - Excitatory amino acid transporter 3

EAAT4 - Excitatory amino acid transporter 4

EAAT5 - Excitatory amino acid transporter 5

EPSC - Excitatory postsynaptic current

ERK - Extracellular-signal-regulated kinase

GABA - γ-aminobutyric acid

GLAST - Glutamate/aspartate transporter

GLT-1 - Glutamate transporter-1

GLY - Glycine

HBSS - Hanks' Balanced Salt Solution

IEM1460- N,N,N,-Trimethyl-5-[(tricyclo[3.3.1.13,7]dec-1-ylmethyl)amino]-1-pentanaminiumbromide hydrobromide

KCC2 - Potassium chloride cotransporter 2

LTP - Long-term potentiation

LY 367385 - (S)-(+)-a-Amino-4-carboxy-2-methylbenzeneacetic acid

mEPSC - Miniature excitatory postsynaptic current

mGluR - Metabotropic glutamate receptor

$mGluR_1$ - Metabotropic glutamate receptor subtype 1

$mGluR_5$ - Metabotropic glutamate receptor subtype 5

MK-801- dizocilpine

MPEP - 2-Methyl-6-(phenylethynyl)pyridine hydrochloride

MS-153 - (*R*)-(−)-5-methyl-1-nicotinoyl-2-pyrazoline

NGF - Nerve growth factor

NK1 – Neurokinin 1

NK2 – Neurokinin 2

NMDA - N-methyl-D-aspartic acid

NRM - Nucleus raphe magnus

NSAID - Nonsteroidal anti-inflammatory drug

OTC - Organotypic slice culture

p75NTR - p75 neurotrophin receptor

PAG - Periaqueductal gray

PKC - Protein kinase C

PLC - Phospholipase C

PNS - Peripheral nervous system

PSNL - Partial sciatic nerve ligation

PTX - Pertussis toxin

RPGL - Nucleus paragigantocellularis lateralis

RVM - Rostral ventral medulla

sEPSC – Spontaneous excitatory postsynaptic current

Trk - Tropomyosin-related kinase

VPI - Ventral posterior inferior nucleus

VPL - Ventral posterior lateral nucleus

CHAPTER 1 GENERAL INTRODUCTION

1.1 Definition of Pain

Pain is regarded as an unpleasant sensory and emotional experience associated with actual or potential tissue damage, or described in terms of such damage (Merskey and Spear 1967; International Association for the Study of Pain). It is generally classified into two categories: acute and chronic pain. Acute or nociceptive pain is perceived by stimulation of a subpopulation of sensory neurons known as nociceptors, in response to noxious stimuli (Woolf, 1991). This type of pain is transient and serves to protect one's body (Woolf, 1991; Iadarola and Caudle, 1997). On the contrary, chronic pain, such as neuropathic pain, is long-lasting (lasting more than 3-6 months) and persists after the injury is healed thus has no physiological function (Woolf and Salter, 2000; Merskey and Bogduk; 1994; Woolf, 1991). Therefore this type of pain has a substantial impact on one's quality of life.

1.2 Nociceptive Pathways

Pain signalling pathways begin with excitation of primary afferent neurons in response to noxious stimuli (Woolf, 1991; Ji and Woolf, 2001; Nestler et al., 2001). The primary afferent neurons relay the nociceptive information via a train of action potentials which are transmitted along their axons to the dorsal horn of the spinal cord (Nestler et al., 2001). From the dorsal horn, the nociceptive information ascends to various higher centres of the brain but mainly to brainstem, thalamus and then to cortex where the information is processed (Ji and Woolf, 2001; Nestler et al., 2001).

1.2.1 Classification of primary afferent neurons

The primary afferent neurons which have their cell bodies located in dorsal root ganglia (DRG) are classified by their axonal diameter, degree of axonal myelination and conduction velocity (Snider and McMahon, 1998; Grudt and Perl, 2002; Nestler et al., 2001). Aβ fibres of large primary afferent neurons have diameter of 10μm or greater, are heavily myelinated and have a conduction velocity of 30m/s or greater (Almeida and Tufik, 2003). These fibres are low-threshold cutaneous mechanoreceptors that respond to light touch and bending of hairs (Woolf and Doubell, 1994; Nestler et al., 2001). Aδ fibres of medium-sized neurons have diameter of 2-5μm, are thinly myelinated and a conduction velocity of 6-30m/s (Burgess and Perl, 1967; Nestler et al., 2001). These fibres are activated by high intensity mechanical or thermal stimuli (Nestler et al., 2001). The Aδ fibres consist of high threshold mechanoreceptors and thermal receptors that react to high (45-53°C) and low (-15°C) temperatures (Almeida and Tufik, 2003). Lastly, C-fibres of small primary afferent neurons have an axonal diameter of 0.5-1.5μm, lack myelination and have a conduction velocity of 0.5-2m/s (Nestler et al., 2001; Almeida and Tufik, 2003). These fibres, known as the polymodal nociceptors, are activated by noxious chemical, mechanical and thermal stimuli (Bessou and Perl, 1969; Campero et al., 1996; Nestler et al., 2001).

Activated Aδ fibres in response to a noxious stimulus are responsible for a rapid and sharp sensation of a “first pain” (Almeida and Tufik, 2003; Nestler et al., 2001). C fibres propagate the nociceptive information slower than Aδ fibres

therefore are responsible for the sensation of "second pain" (Nestler et al., 2001; Almeida and Tufik, 2003).

1.2.2 Dorsal Horn Structure

The grey matter of the spinal cord is classified into 10 laminae where each lamina is composed of neurons with various shapes and sizes (Rexed, 1952; Bishop, 1980). Laminae I-VI comprise the dorsal horn which receives inputs from primary afferent fibres (Rexed, 1952; Nestler et al., 2001). Primary afferent neurons carrying nociceptive information form synapses in the dorsal horn neurons in laminae I, II, IV and V (Figure 1-1; Bishop, 1980; Nestler et al., 2001).

The superficial dorsal horn which consists of lamina I (marginal zone) and II (*substantia gelatinosa*) is an important component in processing nociceptive information and is the region where most Aδ and C fibres terminate (Bishop,1980). Lamina I neurons are primarily nociceptive and classified into three types (Christensen and Perl, 1970; Bishop, 1980). The lamina I nociceptive neurons consist of local excitatory and inhibitory interneurons and projections neurons which terminate in the higher centres in the brain (Dougherty et al., 2005). It has been reported that only a small percentage of the neurons are projection neurons (Spike et al., 2003). In contrast, lamina II interneurons form excitatory and inhibitory circuits (Pearson, 1952; Santos et al., 2007, Lu and Perl, 2003; Lu and Perl, 2005; Zheng et al., 2010). Moreover, it has been

reported that some lamina II neurons project to and synapse with lamina I neurons (Lu and Perl, 2005).

Lamina II neurons have been categorized into several groups according to the morphology and electrophysiology (Grudt and Perl, 2002; Lu et al., 2007; Lu et al., 2009). Islet neurons are oriented in rostro-caudal direction and the action potential firing pattern is characterized as a tonic discharge in response to a depolarizing pulse. Central neurons have moderately dense arborisation in rostro-caudal direction and are divided into transient and tonic central neurons. The transient central neurons fire action potentials briefly in the beginning following a depolarizing pulse whereas the tonic central neurons fire continuous action potentials. Vertical neurons are oriented in rostro-caudal direction and display either delayed or tonic action potential discharges. Lastly, radial neurons, whose dendrites project in all directions, display delayed firing of action potentials in response to a depolarization pulse. In summary, the classification of the lamina II neurons suggests that each group is associated with specific functions to modulate and integrate nociceptive inputs (Lu and Perl, 2005; Grudt and Perl, 2002).

1.2.3. Ascending and Descending Pain Pathways

From the dorsal horn, the nociceptive information ascends to higher centres such as thalamus and brainstem (Nestler et al., 2001). In primates, the axons of the dorsal horn neurons cross the midline and ascend in the anterolateral quadrant of the spinal cord (Willis, 1985). There are several

different ascending pathways which the axons can travel through. The pathways include the spinothalamic tract, spinoreticular tract, spinomesencephalic tract, spinocervical tract, spinohypothalamic tract, spinoparabrachial tract, spinolimbic tract and postsynaptic dorsal column pathway (Willis, 1985; Willis and Westlund, 1997; Almeida and Tufik, 2003**;** Nestler et al., 2001). Among these pathways, the spinothalamic tract is considered to be the major ascending pathway (Kostyuk et al., 2001). The higher centres of the brain where the axons terminate include periaqueductal gray (PAG), parabrachial region of the brainstem and various thalamic nuclei such as ventral posterior lateral nucleus (VPL), ventral posterior inferior nucleus (VPI), the central lateral (CL) nucleus and medial thalamic nucleus (Willis and Westlund, 1997). Therefore the axonal termination to various regions of the brain indicates that the projections can regulate autonomic, endocrine, motivational, affective and alerting responses (Almeida and Tufik, 2003).

In contrast to the ascending pathways, descending pathways are regarded as the analgesic pathways which modulate nociceptive transmission (Willis and Westlund, 1997). The descending pathways originate from various regions including PAG and several nuclei of the rostral ventral medulla (RVM) such as the nucleus raphe magnus (NRM) and the nucleus paragigantocellularis lateralis (RPGL; Basbaum and Fields, 1984; Vanegas and Schaible; 2004). These pathways terminate in the spinal dorsal horn where they directly inhibit the projection neurons or modulate the activity of excitatory and inhibitory interneurons in the dorsal horn (Vanegas and Schaible, 2004; Fields et al., 1991).

1.3 Neuropathic Pain

The study of neuropathic pain is one of the major challenges in the field of chronic pain. In the United States, up to 56 million adults (28% of adult population) suffer from chronic pain and 4 million of these people suffer from neuropathic pain (US Census Bureau, 2007; Burgoyne, 2007). Moreover, chronic pain exerts a burden to the society due to the costs involved. In the US, $150 billion are spent annually for chronic pain and $40 billion is attributed to neuropathic pain (Gilron and Coderre, 2007). The costs are comprised of not only health care resources but loss of productivity and disability compensation as well (Turk, 2002).

Analgesics such as nonsteroidal anti-inflammatory drugs (NSAIDs) and opioids are common treatments for acute pain but they are not effective in neuropathic pain (Max et al., 1988; Gilron and Coderre, 2007; Arner and Meyerson, 1988). Despite the lack of efficacy, it has been reported that common analgesics are being used extensively among patients with neuropathic pain thus raising concerns relating to opiod dependence (Vo et al., 2009; Berger et al., 2004). Current therapy for the management of neuropathic pain includes the anti-allodynic gabapentinoids, pregabalin and gabapentin, antidepressants such as amitriptyline and venlafaxine, dissociative anaesthetics such as ketamine and transient exposures to capsaicin that is thought to damage or desensitize primary afferent fibers (Moulin et al., 2007; Gilron et al., 2006; McCleane, 2004). Unfortunately, all of these treatments are associated with marked undesirable effects which reduce patient compliance. For example, gabapentinoids promote

drowsiness and dizziness, amitriptyline produces cardiovascular disturbances, ketamine produces unpleasant hallucinations and capsaicin produces marked acute pain (Moulin et al., 2007; Gilron et al., 2006; McCleane, 2004). Therefore, finding an effective treatment for neuropathic pain with minimal or no side effect is crucial.

Neuropathic pain is initiated by an injury or dysfunction in the central (CNS) or peripheral nervous system (PNS; Merskey and Bogduk, 1994; International Association for the Study of Pain). Some of the causes of neuropathic pain include viral infection, diabetes, autoimmune diseases and peripheral nerve trauma (Nestler et al., 2001; Pitcher and Henry, 2008; Chen and Pan, 2002; Kim et al., 1997). Common symptoms of neuropathic pain induced by a peripheral nerve injury include hyperalgesia, which is an enhanced response to a noxious stimulus, allodynia, which is a generation of painful sensation in response to a non-painful stimuli and causalgia, which is spontaneous burning pain (Kim et al., 1997; Basbaum and Woolf, 1999; Nestler et al., 2001).

1.3.1 Mechanisms of Neuropathic Pain

In neuropathic pain conditions due to neural damage, changes occur at molecular and cellular levels (Costigan and Woolf, 2000; Costigan et al., 2009). Although some of the changes that occur are adaptive (i.e. changes in the receptors to balance the loss of input), many of the changes are maladaptive (Costigan et al., 2009). Various maladaptive modifications occur following the neural damage (Costigan et al., 2009). One of the maladaptive changes is

generation of ectopic action potentials that are not initiated by a stimulus and results in spontaneous pain (Wall and Gutnick, 1974; Bridges et al., 2001; Costigan et al., 2009). It has been suggested that the spontaneous pain may occur from ectopic discharges in both nociceptors and low threshold myelinated Aβ afferents (Bostock et al., 2005; Campbell et al., 1988).

Disinhibition is another change that occurs in neuropathic pain conditions. In normal conditions, dorsal horn neurons control the nociceptive input via γ-aminobutyric acid (GABA) and glycine (GLY) receptor-mediated inhibition (Costigan et al., 2009). It has been reported that a disinhibition mechanism is involved following peripheral nerve injury (Coull et al., 2003). The mechanism involves a reduction in the expression of potassium chloride cotransporter 2 (KCC2) in lamina I nociceptive neurons which results in a disruption of anion gradient (Coull et al., 2003; Price et al., 2005). The change in the anion gradient causes $GABA_A$/Gly receptor-mediated postsynaptic depolarization of the lamina I neurons (Coull et al., 2003). Furthermore, brain-derived neurotrophic factor (BDNF) released from activated spinal microglia in lamina I neurons induces downregulation of KCC2 (Coull et al., 2005).

Moreover, hyperexcitability of dorsal horn neurons occurs following nerve injury and this is known as “central sensitization” (Woolf, 1983; Woolf and Chong, 1993; Scholz and Woolf, 2002; Bridges et al., 2001). In addition to the hyperexcitability, central sensitization is also manifested by lowered activation thresholds of action potentials which in turn increase discharge rate of afferents with each stimulus and increased response to afferent inputs, known as

the “wind-up”, which may be responsible for development of hyperalgesia (Bridges et al., 2001; Costigan and Woolf, 2000; Woolf and Salter, 2000). Therefore, investigation of the mediators involved in central sensitization may be important in finding potential treatments for neuropathic pain.

1.3.2 Central sensitization: chemical mediators

Increase in excitability of primary afferent neurons as a result of peripheral nerve injury promotes an increase in release of chemical mediators including neurotransmitters and neuropeptides (Figure 1-2; Woolf, 1991). Glutamate is the major neurotransmitter released from primary afferents (Bridges et al., 2001; Nestler et al., 2001). Furthermore, neuropeptides such as calcitonin-gene related peptide (CGRP) and tachykinins including substance P and neurokinin A are also present in the terminals of the primary afferents (Woolf, 1991; Nestler et al., 2001; Latremoliere and woolf, 2009). These neuropeptides are released by high-intensity stimulation of primary afferents (Nestler et al., 2001). Moreover, they are believed to participate in generation of central sensitization (Latremoliere and woolf, 2009). CGRP, found in subsets of Aδ and C fibres, enhances the actions of substance P and contributes in generation of central sensitization (Nestler et al., 2001; Mao et al., 1992; Sun et al., 2004; Sun et al., 2003). Substance P binds to neurokinin 1 (NK1) receptor and neurokinin A binds to neurokinin 2 (NK2) receptor (Nestler et al., 2001). Substance P is co-released with glutamate from nociceptive afferents, innervates mostly to lamina II (Nestler et al., 2001; De Biasi and Rustioni, 1988; Dougherty

et al., 1994; Khasabov et al., 2002). Therefore, in addition to the neurotransmitters, the neuropeptides released by primary afferent neurons in a hyperexcitated state following a peripheral nerve injury could likely result in modifications which could contribute to the generation of central sensitization.

1.4 Brain-Derived Neurotrophic Factor (BDNF)

BDNF is a neurotrophin and located in terminals of nociceptive afferent neurons (Latremoliere and woolf, 2009). Neurotrophins are growth factors which maintain neuronal survival and growth (Obata and Noguchi, 2006). Other neurotrophins include nerve growth factor (NGF), neurotrophin-3 and 4/5 (Obata and Noguchi, 2006).

The neurotrophin receptors are divided into two categories. They are tropomyosin-related kinase (Trk) receptor which is a high-affinity tyrosine kinase receptor and p75 neurotrophin receptor (p75NTR) which is a low affinity receptor and a member of tumor necrosis factor receptor family (Obata and Noguchi, 2006; Patapoutian and Reichardt, 2001). All neurotrophins bind to p75NTR (Obata and Noguchi, 2006) However, not all neurotrophins bind to the family of Trk receptors which is classified into TrkA, TrkB and TrkC receptors (Obata and Noguchi, 2006). BDNF binds specifically to TrkB receptors which are expressed in many regions of CNS and PNS including the superficial dorsal horn (Patapoutian and Reichardt, 200; Bradbury et al., 1998).

BDNF is found and acts on numerous regions of the brain (McAllister et al., 1999). It is also found in nociceptive afferent neurons and synthesized in the

DRG and anterogradely transported to the terminals of the neurons (Obata and Noguchi, 2006; Michael et al., 1997; Zhou and Rush, 1996). It has been indicated that BDNF is co-stored with CGRP and substance P in dense-core vesicles and released into the dorsal horn (Salio et al. 2007; Obata and Noguchi, 2006). Furthermore, anterograde transport of BDNF is increased following a nerve injury (Tonra et al., 1998).

After binding to TrkB receptor, BDNF activates various signalling pathways via extracellular-signal-regulated kinases (ERK) and protein kinase C (PKC; Slack et al., 2004). It has been reported that a high-frequency stimulation of nociceptive afferents in a specific pattern releases BDNF in the dorsal horn (Lever et al., 2001). BDNF released to the dorsal horn phosphorylates N-methyl-D-aspartic acid (NMDA) receptor subunit NR1 in the dorsal horn and potentiates the responses of the NMDA receptors (Slack and Thompson, 2002; Kerr et al., 1999; Slack et al., 2004). Moreover, Zou et al. (2000) have reported that the NR1 subunit was phosphorylated following noxious stimulation. Because of these findings, numerous studies have correlated BDNF with generation of neuropathic pain. Intrathecal injection of BDNF induced thermal hyperalgesia in mice (Groth and Aanonsen, 2002). Nociceptive behaviours were significantly attenuated after reduction of BDNF expression by the use of antisense BDNF oligonucleotides (Groth and Aanonsen, 2002). Furthermore, similar dorsal horn neuron type-specific changes were seen following long-term exposure of the dorsal horn neurons to BDNF and chronic constriction injury (CCI) of rat sciatic nerve (Lu et al., 2007; Lu et al., 2009).

Studies have reported that spinal microglia are activated following peripheral nerve injury induced by formalin injection, spinal and partial sciatic nerve ligation (PSNL; Fu et al., 1999; Coyle, 1998; Jin et al., 2003). Activated microglia synthesize and release various chemical mediators such as cytokines and neurotrophic factors that can act on dorsal horn neurons (Figure 1-3; Inoue, 2006; Kreutzberg, 1996; Hanisch, 2002). It has been observed that BDNF is also released from activated spinal microglia following nerve injury (Dougherty et al., 2000; Ikeda et al., 2001; Biggs et al., 2010). Therefore BNDF has an important role in inducing pain signalling and eliciting central sensitization, resulting in a development of neuropathic pain.

1.5 Glutamate Transporters

Glutamate is an abundant amino acid and the major excitatory amino acid neurotransmitter in CNS (Featherstone and Shippy, 2008). It is involved in many processes such as cellular metabolism, synaptic plasticity and excitatory synaptic transmission including transmission of nociceptive information (Danbolt, 2001; Mayer and Westbrook, 1987; Basbaum and Woolf, 1999; Featherstone and Shippy, 2008). Furthermore, glutamate is involved with the generation of hypersensitivity after tissue injury (Danbolt, 2001). Glutamate as a neurotransmitter acts on glutamate receptors including NMDA, α-amino-3-hydroxyl-5-methyl-4-isoxazole-propionate (AMPA)/kainate and metabotropic glutamate receptors (mGluR; Tao et al., 2005).

It is important to maintain extracellular glutamate concentration at a physiological level as excess glutamate can result in neuronal death via excitotoxicity (Danbolt, 2001). Resting extracellular glutamate concentration is less than 1μM and excitotoxicity can occur at extracellular glutamate concentration of 20 μM or less (Nicholls and Attwell, 1990; Bouvier et al., 1992; Featherstone and Shippy, 2008). Glutamate is not metabolized extracellularly, therefore an appropriate glutamate removal mechanism must be present to ensure the survival of neurons. The glutamate removal mechanism is mediated by a group of proteins known as glutamate transporters (Danbolt, 2001).

1.5.1 Properties of glutamate transporters

Glutamate transporters are a family of membrane transport proteins and responsible for glutamate uptake from the synaptic cleft (Tao et al., 2005). It is suggested that the glutamate transporters cotransport three Na^+ ions, one H^+ ion and countertransports one K^+ ion (Zerangue and Kavanaugh, 1996). The transporters alternate between two conformations: the outward conformation exposes the glutamate-binding site to the extracellular space and the inward conformation flips the glutamate-binding site to the cytoplasm (Tzingounis and Wadiche, 2007). The two conformations are necessary for continual inward transport of glutamate (Tzingounis and Wadiche, 2007). It has been reported that the glutamate transporter is a homomeric trimer with a bowl-shaped structure (Yernool et al., 2004).

There are five isoforms of glutamate transporters: excitatory amino acid transporter 1 (EAAT1) which is also called glutamate/aspartate transporter (GLAST), excitatory amino acid transporter 2 (EAAT2), also called glutamate transporter-1 (GLT-1), excitatory amino acid transporter 3 (EAAT3) which is also known as excitatory amino acid carrier 1(EAAC1), excitatory amino acid transporter 4 (EAAT4) and excitatory amino acid transporter 5 (EAAT5; Danbolt, 2001; Storck et al., 1992; Tanaka, 1993; Pines et al., 1992; Kanai and Hediger, 1992; Fairman et al., 1995; Arriza et al., 1997).

EAAT1 and EAAT2 are expressed predominantly in glial cells. However, EAAT1 is more localized to Bergmann glia of cerebellum and EAAT2 is expressed throughout forebrain, cerebellum and spinal cord (Danbolt, 2001; Rothstein et al., 1994). EAAT3, EAAT 4 and EAAT5 are located predominantly in neurons of brain and spinal cord (Rothstein et al., 1994; Kugler and Schmitt, 1999). EAAT3 is found throughout the CNS, EAAT4 is located in mostly in Purkinje cells of cerebellum and EAAT5 is found in rods and bipolar cells of retina (Rothstein et al., 1994; Kugler and Schmitt, 1999; Dehnes et al., 1998; Arriza et al., 1997; Pow and Barnett, 2000).

1.5.2 Glutamate transporters in nociceptive signalling pathways

Glutamate transporters control the intensity and duration of glutamate receptor activation (Sung et al., 2003). It has been reported that altered expression of glutamate transporters can result in neurodegenerative diseases

such as epilepsy, amyotrophic lateral sclerosis (ALS) and stroke (Dunlop et al., 2003; Sheldon and Robinson, 2007).

Many studies have demonstrated the role of glutamate transporters in nociceptive processing. Intrathecal injection of glutamate transporter blockers resulted in spontaneous nociceptive behaviours and mechanical and thermal hyperalgesia in rats (Liaw et al., 2005; Weng et al., 2006). Moreover, topical application of glutamate transporter blocker onto the dorsal horn of lumbar spinal cord produced an increase in spontaneous nociceptive behaviours and evoked responses to electrical stimulation of the spinal dorsal root (Weng et al., 2006). Riluzole, a positive regulator of glutamate transporters, significantly reduced thermal hyperalgesia and mechanical allodynia in CCI (Sung et al., 2003). Therefore, the role of glutamate transporters is crucial as they prevent excessive activation of glutamate receptors which can lead to various pathological conditions (Sung et al., 2003).

1.5.3 Excitatory amino acid transporter 2 (EAAT2)

EAAT2, which is expressed mainly in astrocytes, has an important role in glutamate uptake and termination of synaptic transmission (Beart and O'Shea, 2007; Robinson, 1998; Robinson and Dowd, 1997; Rothstein et al., 1996). The glutamate taken up by the astrocytes is converted to glutamine by glutamine synthetase and the glutamine is then transported into neurons (Figure 1-4; Sonnewald et al., 1997). EAAT2 is the major glutamate transporter in CNS and is responsible for 90% of glutamate uptake (Haugeto et al., 1996). In the spinal

cord, EAAT2 is widely distributed within the dorsal horn (Sung et al., 2003). Therefore, examining the actions of EAAT2 on nociceptive transmission is important especially in neuropathic pain conditions.

Previous studies using various animal models have reported that downregulation of EAAT2 correlates with neuropathic pain conditions (Weng et al., 2005; Cata et al., 2006; Weng et al., 2006). The two peripheral nerve injury models, PSNL and CCI in rats resulted in a significantly reduced expression of EAAT2 in the dorsal horn (Xin et al., 2009; Sung et al., 2003). Furthermore, the expression of EAAT2 in the spinal cord decreased following taxol-induced mechanical hyperalgesia (Weng et al., 2005). Also, the spinal EAAT2 gene transfer via recombinant adenovirus significantly decreased mechanical hyperalgesia and allodynia (Maeda et al., 2008). Therefore these findings support that EAAT2 likely is a vital component in preventing excessive activation of glutamate receptors following nociceptive stimuli. This also indicates that downregulation of EAAT2 is likely involved in generation of central sensitization.

1.5.4 Classification of Glutamate receptors

Due to the action of EAAT2 in clearance of extracellular glutamate, it has effects on activation of the glutamate receptors including AMPA/kainate, NMDA and mGlu receptors (Figure 1-4). The ionotropic receptors, AMPA/kainate and NMDA receptors, are tetramers formed from different sets of subunits (Featherstone and Shippy, 2008).

AMPA receptors are assembled from combinations of GluR1, GluR2, GluR3 and GluR4 subunits and kainate receptors are formed from GluR5, GluR6, GluR7, KA1 and KA2 subunits (Kew and Kemp, 2005). The permeability to Ca^{2+} of AMPA receptors is controlled by the GluR2 subunit. An AMPA receptor that lacks GluR2 subunit is permeable to Ca^{2+} whereas a presence of GluR2 subunit prevents Ca^{2+} from passing through the receptor (Kew and Kemp, 2005).

NMDA receptors are formed from NR1, NR2 and NR3 subunits (Kew and Kemp, 2005). The NR1 subunit binds to the co-agonist, glycine and NR2 subunit binds to glutamate (Kew and Kemp, 2005). The NMDA receptor is highly permeable to Ca^{2+} and has a voltage-dependent Mg^{2+} block (Cull-Candy et al., 2001).

Unlike the ionotropic receptors, the mGluRs are members of G-protein coupled receptors therefore involved in second messenger-mediated signal transduction pathways (Pin and Duvoisin, 1995; Kew and Kemp, 2005).There are eight types of mGluRs and they are divided into three "groups" (Pin and Duvoisin, 1995; Fagni et al., 2004). Group I mGluRs include $mGluR_1$ and $mGluR_5$ and are mainly localized post-synaptically (Fagni et al., 2004). These receptors couple G_q/G_{11} protein to phospholipase C (PLC) which then results in intracellular Ca^{2+} release (Fagni et al., 2004; Bhave et al., 2001, Nestler et al., 2001). Group II mGluRs which consists of $mGluR_2$ and $mGluR_3$, and group III which consists of $mGlu_4$, $mGlu_7$ and $mGlu_8$ are mostly found in axon terminals (Fagni et al., 2004). Both group II and group III receptors inhibit of adenylyl

cyclase activity via G_i/G_o (Kew and Kemp, 2005). All of the mGluRs except $mGluR_6$ which is expressed in retina are found in the CNS in both neurons and glia (Kew and Kemp, 2005; Nakajima et al., 1993).

1.5.5 Glutamate receptors in nociceptive signalling

Activation of the AMPA, NMDA and mGlu receptors in dorsal horn neurons is associated with pain transmission and chronic pain (Bleakman et al., 2006; Nie and Weng, 2009; Aanonsen and Wilcox, 1987; Kontinen and Meert, 2002; Davies and Watkins, 1983; Ren amd Dubner, 2007; Galik et al., 2008). All subunits of AMPA receptors are highly expressed in the superficial laminae of dorsal horn (Furuyama et al., 1993). Moreover, Ca^{2+}-permeable AMPA receptors are highly expressed in the superficial laminae dorsal horn neurons (Engelman et al., 1999). Numerous studies have indicated that AMPA receptors are involved in chronic pain states. In a CCI model, intrathecal injection of AMPA receptor antagonist attenuated thermal hyperalgesia and mechanical allodynia (Garry et al., 2003). Furthermore, intraperitoneal administration of AMPA receptor antagonists reduced formalin and thermal-induced nociceptive behaviours (Nishiyama et al., 1999).

There have been studies that reported on the role of NMDA receptors in chronic pain. Intraplantar and intrathecal injections of NMDA produced nociceptive behaviours and produced thermal hyperalgesia and mechanical allodynia (Zhou et al., 1996; Coderre and Melzack, 1992). Therefore, NMDA receptor blockers are currently used as analgesics for neuropathic pain.

Ketamine, a NMDA receptor antagonist and an intravenous anaesthetic, is used for neuropathic pain but it does not provide a high efficacy and can produce psychomimetic side effects (Gilron et al., 2006; Hocking and Cousins, 2003). Moreover, dizocilpine (MK-801), another NMDA receptor antagonist, also has side effects such as hallucinations and sedation (Bleakman et al., 2006).

Studies have reported that group I mGluRs are highly expressed in superficial dorsal horn (Fortuhi et al., 1993; Valerio et al., 1997; Vidnyanszky et al., 1994). The group I mGluRs are implicated in capsaicin-induced hyperexcitability of spinal cord neurons (Neugebauer et al., 1999). Furthermore, intrathecal injection of group I mGluR agonist produced hyperalgesia and spontaneous nociceptive behaviours and intrathecal administration of group I mGluR antagonist reduced development of mechanical allodynia and cold hyperalgesia (Fisher and Coderre, 1998; Fisher et al., 1998). Therefore these results indicate that mGluRs may also be a key component in promoting central sensitization in addition to the ionotropic receptors.

1.5.6 Effects of glutamate transporters on glutamate receptors

Inhibition of glutamate transporters elicits nociceptive behaviours and these behaviours are attenuated by NMDA and AMPA/kainate receptor antagonists (Liaw et al., 2005). Furthermore, inhibition of glutamate uptake significantly increased the amplitude and duration of mGluR-dependent slow excitatory postsynaptic current (EPSC) in dorsal horn neurons (Galik et al., 2008). It has been reported that long-term potentiation (LTP) induced by

NMDA receptors involves the insertion of new and/or altered AMPA receptors in the postsynaptic membrane (Derkach et al., 2007; Ji et al., 2008). Therefore, this raises the possibility that activation of NMDA receptors by inhibition of glutamate uptake may result in the insertion of AMPA receptors in the postsynaptic membrane of excitatory neurons of the dorsal horn. Since NMDA receptor antagonists used for neuropathic pain tend to produce side effects, as an alternative to the receptor antagonists, activation of glutamate transporters may be a potential route for treatment of neuropathic pain.

1.6 Organotypic Slice Culture of Spinal Cords

To examine the effects of long-term inhibition of EAAT2 and exposure to BDNF in dorsal horn neurons, the most appropriate *in vitro* technique had to be used. Acute tissue slices are easy to prepare and maintain the cytoarchitecture of the tissue of origin, thus they are a useful tool to study cell to cell communication (Gahwiler et al., 1997; Guerineau et al., 1997). However, these slices are short-lived therefore they are difficult to work with for long-term studies (Gahwiler et al., 1997; Guerineau et al., 1997). As an alternative, organotypic slice cultures (OTCs) were developed to enable to run both short- and long-term experiments (Gahwiler, 1981; Gahwiler et al., 1997; Guerineau et al., 1997).

There are a numerous studies that used OTCs with different methods. The roller-tube method allows the culture to be maintained for several weeks (Gahwiler et al., 1981). The procedure for this method involves plating the slice

on a glass coverslip which is then placed into a culture tube with the culture medium. The tube is incubated in a roller drum which rotates continuously at a specific speed and angle to allow proper feeding and aeration. Moreover, the rotation enables the slice to spread and flatten thus result in a thin slice often with a monolayer thickness.

The alternative "Stoppini" method involves the slice placed on a porous membrane at the interface between air and medium (Stoppini et al., 1991). This method produces similar results obtained from the roller-tube method but results in thicker slices. It is a simple method which preserves the organization of the slice and can be used for long-term studies which are comparable to the roller-tube method.

Although both methods are ideal for OTCs, the slices developed by the Stoppini method are a few layers thick and can be problematic for imaging as accessibility of individual neurons is difficult. Therefore, the roller-tube method was used to prepare organotypic spinal cord slice cultures in this project.

A problem that may arise with the OTCs is serum-containing medium (Gahwiler et al., 1997; Lu et al., 2006). Such medium contains undefined trophic components and cytokines which could lead to inaccurate interpretation of effects especially the effects following a long-term treatment with specific agonists or antagonists (Lu et al., 2006). Therefore, defined-medium organotypic slice culture (DMOTC) with serum-free medium was used in this project (Lu et al., 2006).

1.7 Hypothesis

Previous studies have examined the role of glutamate transporters and BDNF in central sensitization. They have indicated that both release of BDNF and downregulation of EAAT2 in the dorsal horn are associated with generation of central sensitization (Groth and Aanonsen, 2002; Yajima et al., 2005; Mannion et al., 1999; Matayoshi et al., 2005; Thompson et al., 1999; Weng et al., 2005; Cata et al., 2006; Weng et al., 2006; Xin et al., 2009; Sung et al., 2003). Preliminary data indicate that downregulation of EAAT2 occurs in a concentration dependent manner in presence of BDNF (Figure 1-5; unpublished data obtained from Kerr laboratory). This correlation reinforces the suggestion that downregulation of EAAT2 is involved in central sensitization induced by chemical mediators such as BDNF.

Sung et al. (2003) have indicated that EAAT2 expression was significantly decreased from the seventh day following CCI. Moreover, BDNF released into the dorsal horn remained at a high level for seven days following a nerve injury (Ha et al., 2001; Miletic and Miletic, 2001). Therefore, a long-term application of BDNF or EAAT2 blocker in the DMOTC of dorsal horn spinal cord was used in this project to mimic the *in vivo* results.

The objective of this project was to investigate the role of EAAT2 in regulating the excitability of spinal dorsal horn by the application of the EAAT2 blocker, dihydrokainate (DHK). Both acute (5 min) and chronic (5-6 d) treatments of DHK were performed on the DMOTC. Effects of pharmacological block were assessed in DHK treated neurons (chronic treatment) and activation

of glutamate receptors were compared in both DHK and BDNF treated neurons (chronic treatment).

Similar to the changes in glutamate receptor activity in LTP, increased activation of NMDA receptors by inhibition of glutamate uptake may result in the insertion of AMPA receptors in the dorsal horn. Therefore, my hypothesis is that there will be an increase in the activity of specific types of the glutamate receptors following long-term application of DHK. Furthermore, I hypothesize that the long-term inhibition of EAAT2 will function similar to a long-term exposure to BDNF as BDNF concentration dependent downregulation of EAAT2 was observed (Fig 1-5). Confocal Ca^{2+} imaging technique was used to assess the excitability of dorsal horn neurons in all experiments.

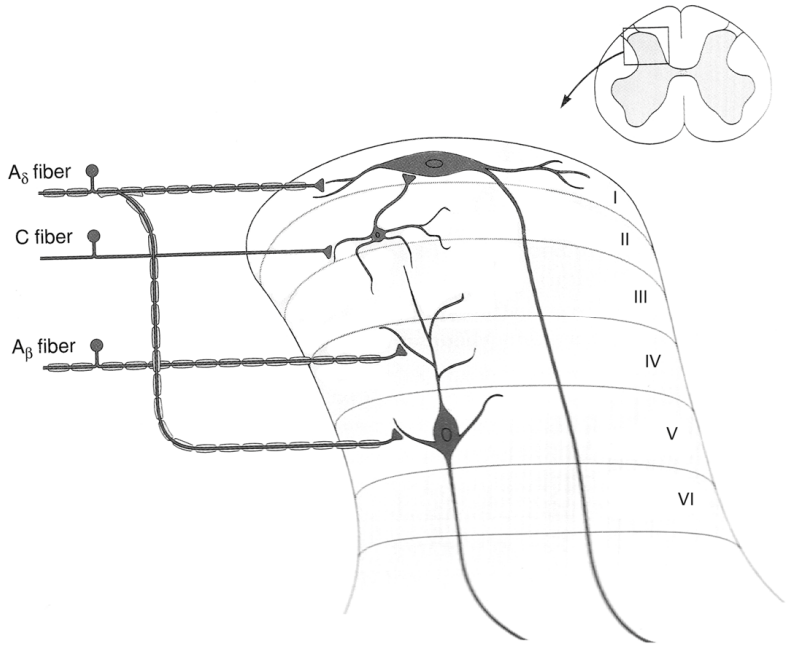

Figure 1-1. Laminae of the dorsal horn of the spinal cord with a possible synaptic arrangement of Aβ, Aδ and C fibres (modified from Nestler et al., 2001).

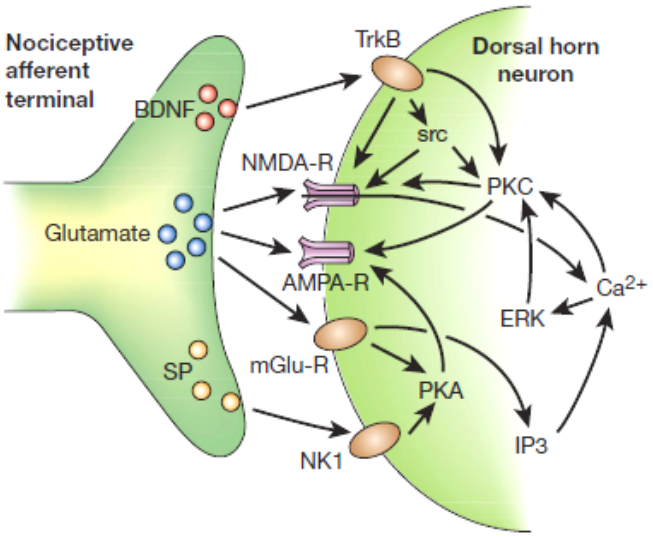

Figure 1-2. Schema of induction of central sensitization (modified from Scholz and Woolf, 2002).

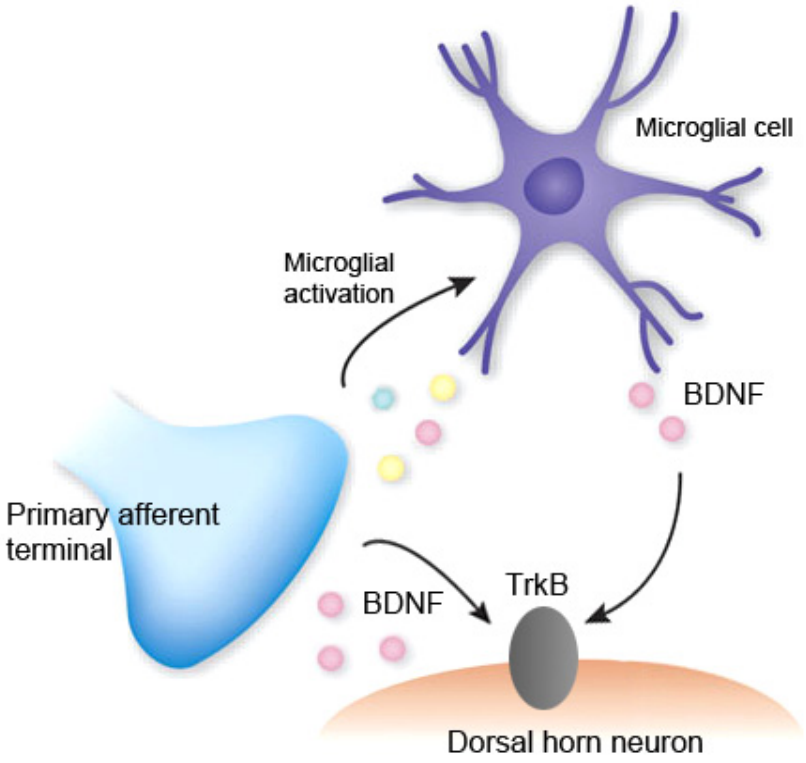

Figure 1-3. BDNF released from primary afferent terminals and activated microglia bind to TrkB receptor in the dorsal horn neuron (modified from Scholz and Woolf, 2007).

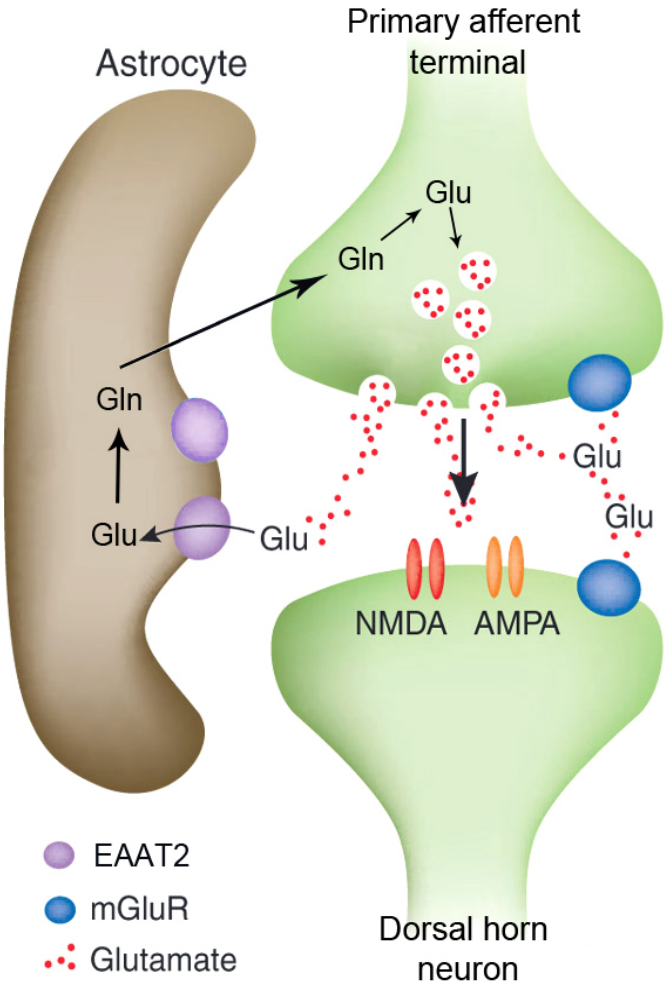

Figure 1-4. Schema of glutamate uptake by EAAT2 and actions of glutamate on glutamate receptors (modified from Weinberger, 2007).

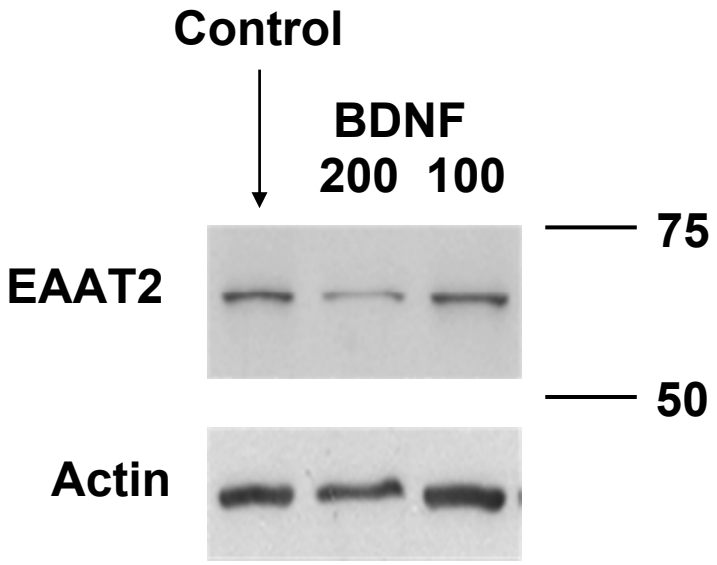

Figure 1-5. Western Immunoblot for EAAT2 shows concentration dependent downregulation of EAAT2 in spinal cord cultures following exposure to BDNF 100 or 200ng/ml (unpublished data obtained from Kerr laboratory).

1.8 References

Aanonsen LM & Wilcox GL (1987). Nociceptive action of excitatory amino acids in the mouse: effects of spinally administered opioids, phencyclidine and sigma agonists. *J Pharmacol Exp Ther* **243**, 9-19.

Almeida TF, Roizenblatt S, & Tufik S (2004). Afferent pain pathways: a neuroanatomical review. *Brain Res* **1000**, 40-56.

Arner S & Meyerson BA (1988). Lack of analgesic effect of opioids on neuropathic and idiopathic forms of pain. *Pain* **33**, 11-23.

Arriza JL, Eliasof S, Kavanaugh MP, & Amara SG (1997). Excitatory amino acid transporter 5, a retinal glutamate transporter coupled to a chloride conductance. *Proc Natl Acad Sci U S A* **94**, 4155-4160.

Ballerini L & Galante M (1998). Network bursting by organotypic spinal slice cultures in the presence of bicuculline and/or strychnine is developmentally regulated. *Eur J Neurosci* **10**, 2871-2879.

Barbour B, Brew H, & Attwell D (1988). Electrogenic glutamate uptake in glial cells is activated by intracellular potassium. *Nature* **335**, 433-435.

Basbaum AI & Fields HL (1984). Endogenous pain control systems: brainstem spinal pathways and endorphin circuitry. *Annu Rev Neurosci* **7**, 309-338.

Basbaum AI & Woolf CJ (1999). Pain. *Curr Biol* **9**, R429-R431.

Beart PM & O'Shea RD (2007). Transporters for L-glutamate: an update on their molecular pharmacology and pathological involvement. *Br J Pharmacol* **150**, 5-17.

Berger A, Dukes EM, & Oster G (2004). Clinical characteristics and economic costs of patients with painful neuropathic disorders. *J Pain* **5**, 143-149.

Berthele A, Boxall SJ, Urban A, Anneser JM, Zieglgansberger W, Urban L, & Tolle TR (1999). Distribution and developmental changes in metabotropic glutamate receptor messenger RNA expression in the rat lumbar spinal cord. *Brain Res Dev Brain Res* **112**, 39-53.

Bessou P & Perl ER (1969). Response of cutaneous sensory units with unmyelinated fibers to noxious stimuli. *J Neurophysiol* **32**, 1025-1043.

Bhave G, Karim F, Carlton SM, & Gereau RW (2001). Peripheral group I metabotropic glutamate receptors modulate nociception in mice. *Nat Neurosci* **4**, 417-423.

Biggs JE, Lu VB, Stebbing MJ, Balasubramanyan S, & Smith PA (2010). Is BDNF sufficient for information transfer between microglia and dorsal horn neurons during the onset of central sensitization? *Mol Pain* **6**, 44.

Bishop B (1980). Pain: its physiology and rationale for management. Part I. Neuroanatomical substrate of pain. *Phys Ther* **60**, 13-20.

Bleakman D, Alt A, & Nisenbaum ES (2006). Glutamate receptors and pain. *Semin Cell Dev Biol* **17**, 592-604.

Bostock H, Campero M, Serra J, & Ochoa JL (2005). Temperature-dependent double spikes in C-nociceptors of neuropathic pain patients. *Brain* **128**, 2154-2163.

Bouvier M, Szatkowski M, Amato A, & Attwell D (1992). The glial cell glutamate uptake carrier countertransports pH-changing anions. *Nature* **360**, 471-474.

Bradbury EJ, King VR, Simmons LJ, Priestley JV, & McMahon SB (1998). NT-3, but not BDNF, prevents atrophy and death of axotomized spinal cord projection neurons. *Eur J Neurosci* **10**, 3058-3068.

Braschler UF, Iannone A, Spenger C, Streit J, & Luscher HR (1989). A modified roller tube technique for organotypic cocultures of embryonic rat spinal cord, sensory ganglia and skeletal muscle. *J Neurosci Methods* **29**, 121-129.

Brennan F, Carr DB, & Cousins M (2007). Pain management: a fundamental human right. *Anesth Analg* **105**, 205-221.

Bridges D, Thompson SW, & Rice AS (2001). Mechanisms of neuropathic pain. *Br J Anaesth* **87**, 12-26.

Burgess PR & Perl ER (1967). Myelinated afferent fibres responding specifically to noxious stimulation of the skin. *J Physiol* **190**, 541-562.

Burgoyne DS (2007). Prevalence and economic implications of chronic pain. *Manag Care* **16**, 2-4.

Campbell JN, Raja SN, Meyer RA, & Mackinnon SE (1988). Myelinated afferents signal the hyperalgesia associated with nerve injury. *Pain* **32**, 89-94.

Campero M, Serra J, & Ochoa JL (1996). C-polymodal nociceptors activated by noxious low temperature in human skin. *J Physiol* **497 (Pt 2)**, 565-572.

Cata JP, Weng HR, Chen JH, & Dougherty PM (2006). Altered discharges of spinal wide dynamic range neurons and down-regulation of glutamate transporter expression in rats with paclitaxel-induced hyperalgesia. *Neuroscience* **138**, 329-338.

Chen SR & Pan HL (2002). Hypersensitivity of spinothalamic tract neurons associated with diabetic neuropathic pain in rats. *J Neurophysiol* **87**, 2726-2733.

Cho HJ, Kim SY, Park MJ, Kim DS, Kim JK, & Chu MY (1997). Expression of mRNA for brain-derived neurotrophic factor in the dorsal root ganglion following peripheral inflammation. *Brain Res* **749**, 358-362.

Christensen BN & Perl ER (1970). Spinal neurons specifically excited by noxious or thermal stimuli: marginal zone of the dorsal horn. *J Neurophysiol* **33**, 293-307.

Coderre TJ & Melzack R (1992). The contribution of excitatory amino acids to central sensitization and persistent nociception after formalin-induced tissue injury. *J Neurosci* **12**, 3665-3670.

Costigan M, Scholz J, & Woolf CJ (2009). Neuropathic pain: a maladaptive response of the nervous system to damage. *Annu Rev Neurosci* **32**, 1-32.

Costigan M & Woolf CJ (2000). Pain: molecular mechanisms. *J Pain* **1**, 35-44.

Coull JA, Beggs S, Boudreau D, Boivin D, Tsuda M, Inoue K, Gravel C, Salter MW, & de KY (2005). BDNF from microglia causes the shift in neuronal anion gradient underlying neuropathic pain. *Nature* **438**, 1017-1021.

Coull JA, Boudreau D, Bachand K, Prescott SA, Nault F, Sik A, De KP, & de KY (2003). Trans-synaptic shift in anion gradient in spinal lamina I neurons as a mechanism of neuropathic pain. *Nature* **424**, 938-942.

Coyle DE (1998). Partial peripheral nerve injury leads to activation of astroglia and microglia which parallels the development of allodynic behavior. *Glia* **23**, 75-83.

Cull-Candy S, Brickley S, & Farrant M (2001). NMDA receptor subunits: diversity, development and disease. *Curr Opin Neurobiol* **11**, 327-335.

Danbolt NC (2001). Glutamate uptake. *Prog Neurobiol* **65**, 1-105.

Davies J & Watkins JC (1983). Role of excitatory amino acid receptors in mono- and polysynaptic excitation in the cat spinal cord. *Exp Brain Res* **49**, 280-290.

De BS & Rustioni A (1988). Glutamate and substance P coexist in primary afferent terminals in the superficial laminae of spinal cord. *Proc Natl Acad Sci U S A* **85**, 7820-7824.

Dehnes Y, Chaudhry FA, Ullensvang K, Lehre KP, Storm-Mathisen J, & Danbolt NC (1998). The glutamate transporter EAAT4 in rat cerebellar Purkinje cells: a glutamate-gated chloride channel concentrated near the

synapse in parts of the dendritic membrane facing astroglia. *J Neurosci* **18**, 3606-3619.

Derkach VA, Oh MC, Guire ES, & Soderling TR (2007). Regulatory mechanisms of AMPA receptors in synaptic plasticity. *Nat Rev Neurosci* **8**, 101-113.

Dougherty KD, Dreyfus CF, & Black IB (2000). Brain-derived neurotrophic factor in astrocytes, oligodendrocytes, and microglia/macrophages after spinal cord injury. *Neurobiol Dis* **7**, 574-585.

Dougherty KJ, Sawchuk MA, & Hochman S (2005). Properties of mouse spinal lamina I GABAergic interneurons. *J Neurophysiol* **94**, 3221-3227.

Dougherty PM, Palecek J, Paleckova V, & Willis WD (1994). Neurokinin 1 and 2 antagonists attenuate the responses and NK1 antagonists prevent the sensitization of primate spinothalamic tract neurons after intradermal capsaicin. *J Neurophysiol* **72**, 1464-1475.

Dunlop J, Beal MH, She Y, & Howland DS (2003). Impaired spinal cord glutamate transport capacity and reduced sensitivity to riluzole in a transgenic superoxide dismutase mutant rat model of amyotrophic lateral sclerosis. *J Neurosci* **23**, 1688-1696.

Edmonds B, Gibb AJ, & Colquhoun D (1995). Mechanisms of activation of glutamate receptors and the time course of excitatory synaptic currents. *Annu Rev Physiol* **57**, 495-519.

Engelman HS, Allen TB, & MacDermott AB (1999). The distribution of neurons expressing calcium-permeable AMPA receptors in the superficial laminae of the spinal cord dorsal horn. *J Neurosci* **19**, 2081-2089.

Fagni L, Ango F, Perroy J, & Bockaert J (2004). Identification and functional roles of metabotropic glutamate receptor-interacting proteins. *Semin Cell Dev Biol* **15**, 289-298.

Fairman WA, Vandenberg RJ, Arriza JL, Kavanaugh MP, & Amara SG (1995). An excitatory amino-acid transporter with properties of a ligand-gated chloride channel. *Nature* **375**, 599-603.

Featherstone DE & Shippy SA (2008). Regulation of synaptic transmission by ambient extracellular glutamate. *Neuroscientist* **14**, 171-181.

Fields HL, Heinricher MM, & Mason P (1991). Neurotransmitters in nociceptive modulatory circuits. *Annu Rev Neurosci* **14**, 219-245.

Fisher K & Coderre TJ (1998). Hyperalgesia and allodynia induced by intrathecal (RS)-dihydroxyphenylglycine in rats. *Neuroreport* **9**, 1169-1172.

Fisher K, Fundytus ME, Cahill CM, & Coderre TJ (1998). Intrathecal administration of the mGluR compound, (S)-4CPG, attenuates hyperalgesia and allodynia associated with sciatic nerve constriction injury in rats. *Pain* **77**, 59-66.

Fotuhi M, Sharp AH, Glatt CE, Hwang PM, von KM, Snyder SH, & Dawson TM (1993). Differential localization of phosphoinositide-linked metabotropic glutamate receptor (mGluR1) and the inositol 1,4,5-trisphosphate receptor in rat brain. *J Neurosci* **13**, 2001-2012.

Fu KY, Light AR, Matsushima GK, & Maixner W (1999). Microglial reactions after subcutaneous formalin injection into the rat hind paw. *Brain Res* **825**, 59-67.

Furuyama T, Kiyama H, Sato K, Park HT, Maeno H, Takagi H, & Tohyama M (1993). Region-specific expression of subunits of ionotropic glutamate receptors (AMPA-type, KA-type and NMDA receptors) in the rat spinal cord with special reference to nociception. *Brain Res Mol Brain Res* **18**, 141-151.

Gahwiler BH (1981). Organotypic monolayer cultures of nervous tissue. *J Neurosci Methods* **4**, 329-342.

Gahwiler BH, Capogna M, Debanne D, McKinney RA, & Thompson SM (1997). Organotypic slice cultures: a technique has come of age. *Trends Neurosci* **20**, 471-477.

Galik J, Youn DH, Kolaj M, & Randic M (2008). Involvement of group I metabotropic glutamate receptors and glutamate transporters in the slow excitatory synaptic transmission in the spinal cord dorsal horn. *Neuroscience* **154**, 1372-1387.

Garry EM, Moss A, Rosie R, Delaney A, Mitchell R, & Fleetwood-Walker SM (2003). Specific involvement in neuropathic pain of AMPA receptors and adapter proteins for the GluR2 subunit. *Mol Cell Neurosci* **24**, 10-22.

Gilron I & Coderre TJ (2007). Emerging drugs in neuropathic pain. *Expert Opin Emerg Drugs* **12**, 113-126.

Gilron I, Watson CP, Cahill CM, & Moulin DE (2006). Neuropathic pain: a practical guide for the clinician. *CMAJ* **175**, 265-275.

Groth R & Aanonsen L (2002). Spinal brain-derived neurotrophic factor (BDNF) produces hyperalgesia in normal mice while antisense directed against

either BDNF or trkB, prevent inflammation-induced hyperalgesia. *Pain* **100**, 171-181.

Grudt TJ & Perl ER (2002). Correlations between neuronal morphology and electrophysiological features in the rodent superficial dorsal horn. *J Physiol* **540**, 189-207.

Guerineau NC, McKinney RA, Debanne D, Mollard P, & Gahwiler BH (1997). Organotypic cultures of the rat anterior pituitary: morphology, physiology and cell-to-cell communication. *J Neurosci Methods* **73**, 169-176.

Ha SO, Kim JK, Hong HS, Kim DS, & Cho HJ (2001). Expression of brain-derived neurotrophic factor in rat dorsal root ganglia, spinal cord and gracile nuclei in experimental models of neuropathic pain. *Neuroscience* **107**, 301-309.

Hanisch UK (2002). Microglia as a source and target of cytokines. *Glia* **40**, 140-155.

Haugeto O, Ullensvang K, Levy LM, Chaudhry FA, Honore T, Nielsen M, Lehre KP, & Danbolt NC (1996). Brain glutamate transporter proteins form homomultimers. *J Biol Chem* **271**, 27715-27722.

Hocking G & Cousins MJ (2003). Ketamine in chronic pain management: an evidence-based review. *Anesth Analg* **97**, 1730-1739.

Iadarola JM & Caudle RM (1997). Good pain, bad pain. *Science* **278**, 239-240.

Ikeda O, Murakami M, Ino H, Yamazaki M, Nemoto T, Koda M, Nakayama C, & Moriya H (2001). Acute up-regulation of brain-derived neurotrophic factor expression resulting from experimentally induced injury in the rat spinal cord. *Acta Neuropathol* **102**, 239-245.

Inoue K (2006). The function of microglia through purinergic receptors: neuropathic pain and cytokine release. *Pharmacol Ther* **109**, 210-226.

International Association for the Study of Pain (IASP)

Jensen TS, Madsen CS, & Finnerup NB (2009). Pharmacology and treatment of neuropathic pains. *Curr Opin Neurol* **22**, 467-474.

Ji RR, Kohno T, Moore KA, & Woolf CJ (2003). Central sensitization and LTP: do pain and memory share similar mechanisms? *Trends Neurosci* **26**, 696-705.

Ji RR & Woolf CJ (2001). Neuronal plasticity and signal transduction in nociceptive neurons: implications for the initiation and maintenance of pathological pain. *Neurobiol Dis* **8**, 1-10.

Jin SX, Zhuang ZY, Woolf CJ, & Ji RR (2003). p38 mitogen-activated protein kinase is activated after a spinal nerve ligation in spinal cord microglia and dorsal root ganglion neurons and contributes to the generation of neuropathic pain. *J Neurosci* **23**, 4017-4022.

Kanai Y & Hediger MA (1992). Primary structure and functional characterization of a high-affinity glutamate transporter. *Nature* **360**, 467-471.

Kerr BJ, Bradbury EJ, Bennett DL, Trivedi PM, Dassan P, French J, Shelton DB, McMahon SB, & Thompson SW (1999). Brain-derived neurotrophic factor modulates nociceptive sensory inputs and NMDA-evoked responses in the rat spinal cord. *J Neurosci* **19**, 5138-5148.

Kew JN & Kemp JA (2005). Ionotropic and metabotropic glutamate receptor structure and pharmacology. *Psychopharmacology (Berl)* **179**, 4-29.

Khasabov SG, Rogers SD, Ghilardi JR, Peters CM, Mantyh PW, & Simone DA (2002). Spinal neurons that possess the substance P receptor are required for the development of central sensitization. *J Neurosci* **22**, 9086-9098.

Kim KJ, Yoon YW, & Chung JM (1997). Comparison of three rodent neuropathic pain models. *Exp Brain Res* **113**, 200-206.

Koerber HR, Mirnics K, Brown PB, & Mendell LM (1994). Central sprouting and functional plasticity of regenerated primary afferents. *J Neurosci* **14**, 3655-3671.

Kontinen VK & Meert TF (2002). Vocalization responses after intrathecal administration of ionotropic glutamate receptor agonists in rats. *Anesth Analg* **95**, 997-1001, table.

Kostyuk E, Voitenko N, Kruglikov I, Shmigol A, Shishkin V, Efimov A, & Kostyuk P (2001). Diabetes-induced changes in calcium homeostasis and the effects of calcium channel blockers in rat and mice nociceptive neurons. *Diabetologia* **44**, 1302-1309.

Kreutzberg GW (1996). Microglia: a sensor for pathological events in the CNS. *Trends Neurosci* **19**, 312-318.

Kugler P & Schmitt A (1999). Glutamate transporter EAAC1 is expressed in neurons and glial cells in the rat nervous system. *Glia* **27**, 129-142.

Latremoliere A & Woolf CJ (2009). Central sensitization: a generator of pain hypersensitivity by central neural plasticity. *J Pain* **10**, 895-926.

Lever IJ, Bradbury EJ, Cunningham JR, Adelson DW, Jones MG, McMahon SB, Marvizon JC, & Malcangio M (2001). Brain-derived neurotrophic factor is released in the dorsal horn by distinctive patterns of afferent fiber stimulation. *J Neurosci* **21**, 4469-4477.

Liaw WJ, Stephens RL, Jr., Binns BC, Chu Y, Sepkuty JP, Johns RA, Rothstein JD, & Tao YX (2005). Spinal glutamate uptake is critical for maintaining normal sensory transmission in rat spinal cord. *Pain* **115**, 60-70.

Lu VB, Ballanyi K, Colmers WF, & Smith PA (2007). Neuron type-specific effects of brain-derived neurotrophic factor in rat superficial dorsal horn and their relevance to 'central sensitization'. *J Physiol* **584**, 543-563.

Lu VB, Biggs JE, Stebbing MJ, Balasubramanyan S, Todd KG, Lai AY, Colmers WF, Dawbarn D, Ballanyi K, & Smith PA (2009). Brain-derived neurotrophic factor drives the changes in excitatory synaptic transmission in the rat superficial dorsal horn that follow sciatic nerve injury. *J Physiol* **587**, 1013-1032.

Lu VB, Moran TD, Balasubramanyan S, Alier KA, Dryden WF, Colmers WF, & Smith PA (2006). Substantia Gelatinosa neurons in defined-medium organotypic slice culture are similar to those in acute slices from young adult rats. *Pain* **121**, 261-275.

Lu Y & Perl ER (2003). A specific inhibitory pathway between substantia gelatinosa neurons receiving direct C-fiber input. *J Neurosci* **23**, 8752-8758.

Lu Y & Perl ER (2005). Modular organization of excitatory circuits between neurons of the spinal superficial dorsal horn (laminae I and II). *J Neurosci* **25**, 3900-3907.

Maeda S, Kawamoto A, Yatani Y, Shirakawa H, Nakagawa T, & Kaneko S (2008). Gene transfer of GLT-1, a glial glutamate transporter, into the spinal cord by recombinant adenovirus attenuates inflammatory and neuropathic pain in rats. *Mol Pain* **4**, 65.

Mannion RJ, Costigan M, Decosterd I, Amaya F, Ma QP, Holstege JC, Ji RR, Acheson A, Lindsay RM, Wilkinson GA, & Woolf CJ (1999). Neurotrophins: peripherally and centrally acting modulators of tactile stimulus-induced inflammatory pain hypersensitivity. *Proc Natl Acad Sci U S A* **96**, 9385-9390.

Mao J, Coghill RC, Kellstein DE, Frenk H, & Mayer DJ (1992). Calcitonin gene-related peptide enhances substance P-induced behaviors via metabolic inhibition: in vivo evidence for a new mechanism of neuromodulation. *Brain Res* **574**, 157-163.

Marshall GE, Shehab SA, Spike RC, & Todd AJ (1996). Neurokinin-1 receptors on lumbar spinothalamic neurons in the rat. *Neuroscience* **72**, 255-263.

Matayoshi S, Jiang N, Katafuchi T, Koga K, Furue H, Yasaka T, Nakatsuka T, Zhou XF, Kawasaki Y, Tanaka N, & Yoshimura M (2005). Actions of brain-derived neurotrophic factor on spinal nociceptive transmission during inflammation in the rat. *J Physiol* **569**, 685-695.

Max MB, Schafer SC, Culnane M, Dubner R, & Gracely RH (1988). Association of pain relief with drug side effects in postherpetic neuralgia: a single-dose study of clonidine, codeine, ibuprofen, and placebo. *Clin Pharmacol Ther* **43**, 363-371.

Mayer ML & Westbrook GL (1987). The physiology of excitatory amino acids in the vertebrate central nervous system. *Prog Neurobiol* **28**, 197-276.

McAllister AK, Katz LC, & Lo DC (1999). Neurotrophins and synaptic plasticity. *Annu Rev Neurosci* **22**, 295-318.

McCleane G (2004). Pharmacological strategies in relieving neuropathic pain. *Expert Opin Pharmacother* **5**, 1299-1312.

Merskey H & Spear FG (1967). The concept of pain. *J Psychosom Res* **11**, 59-67.

Michael GJ, Averill S, Nitkunan A, Rattray M, Bennett DL, Yan Q, & Priestley JV (1997). Nerve growth factor treatment increases brain-derived neurotrophic factor selectively in TrkA-expressing dorsal root ganglion cells and in their central terminations within the spinal cord. *J Neurosci* **17**, 8476-8490.

Miletic G & Miletic V (2002). Increases in the concentration of brain derived neurotrophic factor in the lumbar spinal dorsal horn are associated with pain behavior following chronic constriction injury in rats. *Neurosci Lett* **319**, 137-140.

Millan MJ (1999). The induction of pain: an integrative review. *Prog Neurobiol* **57**, 1-164.

Moulin DE, Clark AJ, Gilron I, Ware MA, Watson CP, Sessle BJ, Coderre T, Morley-Forster PK, Stinson J, Boulanger A, Peng P, Finley GA, Taenzer P, Squire P, Dion D, Cholkan A, Gilani A, Gordon A, Henry J, Jovey R, Lynch M, Mailis-Gagnon A, Panju A, Rollman GB, & Velly A (2007). Pharmacological management of chronic neuropathic pain - consensus statement and guidelines from the Canadian Pain Society. *Pain Res Manag* **12**, 13-21.

Nakajima Y, Iwakabe H, Akazawa C, Nawa H, Shigemoto R, Mizuno N, & Nakanishi S (1993). Molecular characterization of a novel retinal

metabotropic glutamate receptor mGluR6 with a high agonist selectivity for L-2-amino-4-phosphonobutyrate. *J Biol Chem* **268**, 11868-11873.

Neugebauer V, Chen PS, & Willis WD (1999). Role of metabotropic glutamate receptor subtype mGluR1 in brief nociception and central sensitization of primate STT cells. *J Neurophysiol* **82**, 272-282.

Nicholls D & Attwell D (1990). The release and uptake of excitatory amino acids. *Trends Pharmacol Sci* **11**, 462-468.

Nie H & Weng HR (2009). Glutamate transporters prevent excessive activation of NMDA receptors and extrasynaptic glutamate spillover in the spinal dorsal horn. *J Neurophysiol* **101**, 2041-2051.

Nishiyama T, Gyermek L, Lee C, Kawasaki-Yatsugi S, & Yamaguchi T (1999). The systemically administered competitive AMPA receptor antagonist, YM872, has analgesic effects on thermal or formalin-induced pain in rats. *Anesth Analg* **89**, 1534-1537.

Obata K & Noguchi K (2006). BDNF in sensory neurons and chronic pain. *Neurosci Res* **55**, 1-10.

Patapoutian A & Reichardt LF (2001). Trk receptors: mediators of neurotrophin action. *Curr Opin Neurobiol* **11**, 272-280.

PEARSON AA (1952). Role of gelatinous substance of spinal cord in conduction of pain. *AMA Arch Neurol Psychiatry* **68**, 515-529.

Pin JP & Duvoisin R (1995). The metabotropic glutamate receptors: structure and functions. *Neuropharmacology* **34**, 1-26.

Pines G, Danbolt NC, Bjoras M, Zhang Y, Bendahan A, Eide L, Koepsell H, Storm-Mathisen J, Seeberg E, & Kanner BI (1992). Cloning and expression of a rat brain L-glutamate transporter. *Nature* **360**, 464-467.

Pitcher GM & Henry JL (2008). Governing role of primary afferent drive in increased excitation of spinal nociceptive neurons in a model of sciatic neuropathy. *Exp Neurol* **214**, 219-228.

Pow DV & Barnett NL (2000). Developmental expression of excitatory amino acid transporter 5: a photoreceptor and bipolar cell glutamate transporter in rat retina. *Neurosci Lett* **280**, 21-24.

Price TJ, Cervero F, & de KY (2005). Role of cation-chloride-cotransporters (CCC) in pain and hyperalgesia. *Curr Top Med Chem* **5**, 547-555.

Ren K & Dubner R (2007). Pain facilitation and activity-dependent plasticity in pain modulatory circuitry: role of BDNF-TrkB signaling and NMDA receptors. *Mol Neurobiol* **35**, 224-235.

REXED B (1952). The cytoarchitectonic organization of the spinal cord in the cat. *J Comp Neurol* **96**, 414-495.

Robinson MB (1998). The family of sodium-dependent glutamate transporters: a focus on the GLT-1/EAAT2 subtype. *Neurochem Int* **33**, 479-491.

Robinson MB & Dowd LA (1997). Heterogeneity and functional properties of subtypes of sodium-dependent glutamate transporters in the mammalian central nervous system. *Adv Pharmacol* **37**, 69-115.

Rothstein JD, Dykes-Hoberg M, Pardo CA, Bristol LA, Jin L, Kuncl RW, Kanai Y, Hediger MA, Wang Y, Schielke JP, & Welty DF (1996). Knockout of glutamate transporters reveals a major role for astroglial transport in excitotoxicity and clearance of glutamate. *Neuron* **16**, 675-686.

Rothstein JD, Martin L, Levey AI, Dykes-Hoberg M, Jin L, Wu D, Nash N, & Kuncl RW (1994). Localization of neuronal and glial glutamate transporters. *Neuron* **13**, 713-725.

Salio C, Averill S, Priestley JV, & Merighi A (2007). Costorage of BDNF and neuropeptides within individual dense-core vesicles in central and peripheral neurons. *Dev Neurobiol* **67**, 326-338.

Santos SF, Rebelo S, Derkach VA, & Safronov BV (2007). Excitatory interneurons dominate sensory processing in the spinal substantia gelatinosa of rat. *J Physiol* **581**, 241-254.

Scholz J & Woolf CJ (2002). Can we conquer pain? *Nat Neurosci* **5 Suppl**, 1062-1067.

Scholz J & Woolf CJ (2007). The neuropathic pain triad: neurons, immune cells and glia. *Nat Neurosci* **10**, 1361-1368.

Sheldon AL & Robinson MB (2007). The role of glutamate transporters in neurodegenerative diseases and potential opportunities for intervention. *Neurochem Int* **51**, 333-355.

Slack SE, Pezet S, McMahon SB, Thompson SW, & Malcangio M (2004). Brain-derived neurotrophic factor induces NMDA receptor subunit one phosphorylation via ERK and PKC in the rat spinal cord. *Eur J Neurosci* **20**, 1769-1778.

Slack SE & Thompson SW (2002). Brain-derived neurotrophic factor induces NMDA receptor 1 phosphorylation in rat spinal cord. *Neuroreport* **13**, 1967-1970.

Snider WD & McMahon SB (1998). Tackling pain at the source: new ideas about nociceptors. *Neuron* **20**, 629-632.

Sonnewald U, Westergaard N, & Schousboe A (1997). Glutamate transport and metabolism in astrocytes. *Glia* **21**, 56-63.

Spike RC, Puskar Z, Andrew D, & Todd AJ (2003). A quantitative and morphological study of projection neurons in lamina I of the rat lumbar spinal cord. *Eur J Neurosci* **18**, 2433-2448.

Stewart WF, Ricci JA, Chee E, Morganstein D, & Lipton R (2003). Lost productive time and cost due to common pain conditions in the US workforce. *JAMA* **290**, 2443-2454.

Stoppini L, Buchs PA, & Muller D (1991). A simple method for organotypic cultures of nervous tissue. *J Neurosci Methods* **37**, 173-182.

Storck T, Schulte S, Hofmann K, & Stoffel W (1992). Structure, expression, and functional analysis of a Na(+)-dependent glutamate/aspartate transporter from rat brain. *Proc Natl Acad Sci U S A* **89**, 10955-10959.

Sun RQ, Lawand NB, & Willis WD (2003). The role of calcitonin gene-related peptide (CGRP) in the generation and maintenance of mechanical

allodynia and hyperalgesia in rats after intradermal injection of capsaicin. *Pain* **104**, 201-208.

Sun RQ, Tu YJ, Lawand NB, Yan JY, Lin Q, & Willis WD (2004). Calcitonin gene-related peptide receptor activation produces PKA- and PKC-dependent mechanical hyperalgesia and central sensitization. *J Neurophysiol* **92**, 2859-2866.

Sung B, Lim G, & Mao J (2003). Altered expression and uptake activity of spinal glutamate transporters after nerve injury contribute to the pathogenesis of neuropathic pain in rats. *J Neurosci* **23**, 2899-2910.

Tanaka K (1993). Expression cloning of a rat glutamate transporter. *Neurosci Res* **16**, 149-153.

Tao YX, Gu J, & Stephens RL, Jr. (2005). Role of spinal cord glutamate transporter during normal sensory transmission and pathological pain states. *Mol Pain* **1**, 30.

Thompson SW, Bennett DL, Kerr BJ, Bradbury EJ, & McMahon SB (1999). Brain-derived neurotrophic factor is an endogenous modulator of nociceptive responses in the spinal cord. *Proc Natl Acad Sci U S A* **96**, 7714-7718.

Todd AJ, McGill MM, & Shehab SA (2000). Neurokinin 1 receptor expression by neurons in laminae I, III and IV of the rat spinal dorsal horn that project to the brainstem. *Eur J Neurosci* **12**, 689-700.

Tonra JR, Curtis R, Wong V, Cliffer KD, Park JS, Timmes A, Nguyen T, Lindsay RM, Acheson A, & DiStefano PS (1998). Axotomy upregulates the anterograde transport and expression of brain-derived neurotrophic factor by sensory neurons. *J Neurosci* **18**, 4374-4383.

Turk DC (2002). Clinical effectiveness and cost-effectiveness of treatments for patients with chronic pain. *Clin J Pain* **18**, 355-365.

Tzingounis AV & Wadiche JI (2007). Glutamate transporters: confining runaway excitation by shaping synaptic transmission. *Nat Rev Neurosci* **8**, 935-947.

US Census Bureau (2007)

Valerio A, Rizzonelli P, Paterlini M, Moretto G, Knopfel T, Kuhn R, Memo M, & Spano P (1997). mGluR5 metabotropic glutamate receptor distribution in rat and human spinal cord: a developmental study. *Neurosci Res* **28**, 49-57.

Vanegas H & Schaible HG (2004). Descending control of persistent pain: inhibitory or facilitatory? *Brain Res Brain Res Rev* **46**, 295-309.

Vidnyanszky Z, Hamori J, Negyessy L, Ruegg D, Knopfel T, Kuhn R, & Gorcs TJ (1994). Cellular and subcellular localization of the mGluR5a metabotropic glutamate receptor in rat spinal cord. *Neuroreport* **6**, 209-213.

Vo T, Rice AS, & Dworkin RH (2009). Non-steroidal anti-inflammatory drugs for neuropathic pain: how do we explain continued widespread use? *Pain* **143**, 169-171.

Wall PD & Gutnick M (1974). Ongoing activity in peripheral nerves: the physiology and pharmacology of impulses originating from a neuroma. *Exp Neurol* **43**, 580-593.

Weinberger DR (2007). Schizophrenia drug says goodbye to dopamine. *Nat Med* **13**, 1018-1019.

Weng HR, Aravindan N, Cata JP, Chen JH, Shaw AD, & Dougherty PM (2005). Spinal glial glutamate transporters downregulate in rats with taxol-induced hyperalgesia. *Neurosci Lett* **386**, 18-22.

Weng HR, Chen JH, & Cata JP (2006). Inhibition of glutamate uptake in the spinal cord induces hyperalgesia and increased responses of spinal dorsal horn neurons to peripheral afferent stimulation. *Neuroscience* **138**, 1351-1360.

Weng HR, Chen JH, Pan ZZ, & Nie H (2007). Glial glutamate transporter 1 regulates the spatial and temporal coding of glutamatergic synaptic transmission in spinal lamina II neurons. *Neuroscience* **149**, 898-907.

Willis WD (1985). Nociceptive pathways: anatomy and physiology of nociceptive ascending pathways. *Philos Trans R Soc Lond B Biol Sci* **308**, 253-270.

Willis WD & Westlund KN (1997). Neuroanatomy of the pain system and of the pathways that modulate pain. *J Clin Neurophysiol* **14**, 2-31.

Woolf CJ (1983). Evidence for a central component of post-injury pain hypersensitivity. *Nature* **306**, 686-688.

Woolf CJ (1991). Generation of acute pain: central mechanisms. *Br Med Bull* **47**, 523-533.

Woolf CJ & Chong MS (1993). Preemptive analgesia--treating postoperative pain by preventing the establishment of central sensitization. *Anesth Analg* **77**, 362-379.

Woolf CJ & Doubell TP (1994). The pathophysiology of chronic pain--increased sensitivity to low threshold A beta-fibre inputs. *Curr Opin Neurobiol* **4**, 525-534.

Woolf CJ & Salter MW (2000). Neuronal plasticity: increasing the gain in pain. *Science* **288**, 1765-1769.

Xin WJ, Weng HR, & Dougherty PM (2009). Plasticity in expression of the glutamate transporters GLT-1 and GLAST in spinal dorsal horn glial cells following partial sciatic nerve ligation. *Mol Pain* **5**, 15.

Yajima Y, Narita M, Usui A, Kaneko C, Miyatake M, Narita M, Yamaguchi T, Tamaki H, Wachi H, Seyama Y, & Suzuki T (2005). Direct evidence for the involvement of brain-derived neurotrophic factor in the development of a neuropathic pain-like state in mice. *J Neurochem* **93**, 584-594.

Yernool D, Boudker O, Jin Y, & Gouaux E (2004). Structure of a glutamate transporter homologue from Pyrococcus horikoshii. *Nature* **431**, 811-818.

Zerangue N & Kavanaugh MP (1996). Flux coupling in a neuronal glutamate transporter. *Nature* **383**, 634-637.

Zheng J, Lu Y, & Perl ER (2010). Inhibitory neurones of the spinal substantia gelatinosa mediate interaction of signals from primary afferents. *J Physiol* **588**, 2065-2075.

Zhou S, Bonasera L, & Carlton SM (1996). Peripheral administration of NMDA, AMPA or KA results in pain behaviors in rats. *Neuroreport* **7**, 895-900.

Zhou XF, Parada LF, Soppet D, & Rush RA (1993). Distribution of trkB tyrosine kinase immunoreactivity in the rat central nervous system. *Brain Res* **622**, 63-70.

Zhou XF & Rush RA (1996). Endogenous brain-derived neurotrophic factor is anterogradely transported in primary sensory neurons. *Neuroscience* **74**, 945-953.

Zou X, Lin Q, & Willis WD (2000). Enhanced phosphorylation of NMDA receptor 1 subunits in spinal cord dorsal horn and spinothalamic tract neurons after intradermal injection of capsaicin in rats. *J Neurosci* **20**, 6989-6997.

CHAPTER 2 METHODOLOGY

All experimental procedures have been approved by the University of Alberta Health Sciences Laboratory Animal Services Welfare Committee and complied with the guidelines of Canadian Council for Animal care.

2.1 Defined-medium Organotypic Cultures

The DMOTC technique was adapted and modified from previously published methods (Braschler et al., 1989, Gahwiler, 1981; Ballerini and Galante, 1998; Gahwiler, 1997). Furthermore, the DMOTC technique used in this project was identical with that used by Lu et al. (2006). Embryonic day 13-14 rat fetuses were isolated by caesarean section from time-pregnant Sprague-Dawley rats (Charles River, Saint-Constant, PQ, Canada) under 2-5% isoflurane anaesthesia. Euthanasia was subsequently performed on the female rats by cervical dislocation under the isoflurane anaesthesia. The embryonic sac was placed in chilled Hanks' Balanced Salt Solution (HBSS) containing (in mM): 138 NaCl, 5.33 KCl, 0.44 KH_2PO_4, 0.5 $MgCl_2$-$6H_2O$, 0.41 $MgSO_4$-$7H_2O$, 4 $NaHCO_3$, 0.3 Na_2HPO_4, 5.6 d-glucose, and 1.26 $CaCl_2$. Sterile and aseptic conditions were applied throughout the rest of the procedure. Each fetus was removed from the embryonic sac and placed in a new dish of chilled HBSS. Individual fetuses were decapitated and their backs were isolated by cutting away hind limbs and tissues ventral to the spinal cord. Transverse spinal cord slices (275–325 μm) were obtained using a tissue chopper (McIlwain, St. Louis, MO, USA). Only lumbar slices with an intact spinal cord and two attached

DRGs were selected and excess ventral tissue was trimmed. Then the slices were kept for 1 h at 4°C in a new dish of HBSS.

The slices were plated onto clean glass coverslips (Karl Hecht, Sondheim, Germany) with a clot of reconstituted chicken plasma (lyophilized, 0.2 mg/L heparin; Cocalico Biologicals Inc., Stevens, PA, USA) and thrombin (200 units/ml; Sigma, St. Louis, MO, USA) and were allowed to dry for 1 h at 20-22°C (Figure 2-1). Coverslips were inserted into flat-bottomed tissue culture tubes (Nunc-Nalgene International, Mississauga, Ont., Canada) filled with 1 ml of culture medium and then placed into a roller drum (Model # TC-8, New Brunswick Scientific, Edison, NJ, USA) rotating at 120 rotations per hour in a dry heat incubator at 36 °C (regular air-no CO_2; Figure 2-2). The medium in the tubes was composed of 82% Dulbecco's modified Eagle's medium (DMEM), 10% fetal bovine serum, and 8% sterile water to adjust osmolarity (all from Gibco, Grand Island, NY, USA). This medium was supplemented with 20 ng/ml NGF (Alomone Laboratories, Jerusalem, Israel) for the first 4 d. Antibiotic and antimycotic drugs (5 units/ml penicillin G, 5 units /ml streptomycin, and 12.5 ng/ml amphotericin B; Gibco) were also included in the medium during the first 4 d of culture. After the 4 d period, the slices were treated with a 10 μM antimitotic drug cocktail consisting of uridine, cytosine-β-d-arabino-furanoside (AraC), and 5-fluorodeoxyuridine (all from SIGMA) for 24 h to prevent the overgrowth of glial cells. During this treatment, the serum medium was halved with a serum-free, defined medium consisting of Neurobasal medium, 5 mM Glutamax-1, and N-2 supplement (all from Gibco). At the end of day 5, the

medium was completely exchanged to the serum-free, defined medium. The medium within these tubes was exchanged with freshly prepared serum-free medium every 4-5 d and the DMOTC slices in the culture tubes were maintained in the roller drum until the recordings were performed.

2.2 Dihydrokainate (DHK) and BDNF Treatments

DMOTC slices were maintained *in vitro* 3-4 weeks before experiments to allow cultures to stabilize. The DHK and BDNF treatment schedules paralleled previous studies (Lu et al., 2007; Lu et al., 2009) in order for the time at which DHK or BDNF introduced to the dorsal horn neurons would correlate with the time-course of BDNF elevation following nerve injury. DHK (16μM, twice the K_d; Tocris, Missouri, USA) or BDNF (200ng/ml; Alamone Laboratories, Jerusalem, Israel) was added to DMOTC medium and the medium was administered to DMOTC slices after 15-21 days *in vitro* for a period of 5-6 days. The recordings were performed on the 5^{th} or 6^{th} treatment day. The DHK or BDNF medium was exchanged on the 3^{rd} treatment day (Figure 2-3). Untreated DMOTC slices were served as controls.

2.3 Confocal Calcium Imaging

The membrane permeable acetoxymethyl (AM) ester of the Ca^{2+}-sensitive dyes Fluo-4 (TEF Labs Inc. Austin, Texas, USA) or Fluo-8L (Cedarlane, Burlington, Ontario, Canada) were used on DMOTC slices. Fluo-4-AM or Fluo-8L-AM dye was dissolved in a mixture of dimethyl sulfoxide

(DMSO) and 20% pluronic acid (Invitrogen, Burlington, Ontario, Canada) and made into 5 μM solution. 12 μL of 5 μM Fluo-4-AM or Fluo-8L-AM dye was added to a flat-bottomed tissue culture tube containing 1ml DMOTC medium then incubated in the roller drum for 60 min. Following the 60min incubation period, the DMOTC slice was placed in a recording chamber and perfused with external recording solution containing (in mM): 127 NaCl, 2.5 KCl, 1.2 NaH_2PO_4, 1.3 $MgSO_4$, 26 $NaHCO_3$, 25 D-glucose, 2.5 $CaCl_2$, at a flow rate of 4 ml/min. A confocal microscope with an argon (488 nm) laser and filters (20X XLUMPlanF1-NA-0.95 objective; Olympus FV300, Markham, Ontario, Canada) was used to measure Ca^{2+}-fluorescence signals. Fluorescently labelled dorsal horn neurons and glia were recorded at a depth of 30-60 μm. Full frame images (512 x 512 pixels) were recorded in a fixed x-y image plane at a scanning rate of 0.7-0.8 s/frame. Cell bodies of individual neurons were selected and fluorescence signals were produced with FluoView v. 4.3 software (Olympus). The neurons were selected according to the size of the cell body, presence of basal oscillations and responses to 35 mM K^+, electrical stimulations and drugs. Two different methods were used to evoke Ca^{2+} signals in the DMOTC. The first method involved depolarizing neurons with a high K^+ solution (35 mM, 90 s application), whereas the other method involved recording Ca^{2+} signals evoked by stimulation of the dorsal root entry zone or DRG.

2.4 Electrical Stimulation

I have developed a multi-pulse electrical stimulation protocol to produce a suitable and more physiological method to evoke Ca^{2+} signals of neurons. A bipolar tungsten electrode (model number: TST33A05KT, World Precision Instruments, Inc., Sarasota, FL, USA) was shielded by a glass electrode tubing, exposing only the tip and the connector located at the end of the electrode. The tip of electrode was positioned on dorsal root entry zone or DRG of the DMOTC to evoke Ca^{2+} signals upon stimulations. The dorsal root entry zone or DRG was stimulated at 50 Hz for 5 s with a pulse width of 100 μs for all experiments. Stimulations were applied at twice the threshold intensity required to produce a detectable response and each stimulus was applied at an interval of 5 min. A repeated stimulus protocol was used as the responses to stimulation varied in the first few stimulations (Figure 2-4). The stimulations were applied up to 8 times and it was found that the responses were more consistent between 5^{th} to 8^{th} stimulations (Figure 2-4). Therefore the responses to 5^{th} and 6^{th} stimulations were analyzed in chronic treatment experiments.

When the 50 Hz, 5 s stimulus protocol was compared with a 50 Hz, 1 s stimulus protocol (Figure 2-5) it was found that the latter produced consistent responses throughout the entire series of stimulations. However, the area under the curve and peak amplitude of the responses to 5^{th} and 6^{th} stimulations using the 50Hz, 5s protocol were similar to the responses produced by the 50Hz, 1s protocol. Therefore, the results suggest that although the 50Hz, 1s protocol may

have been a suitable protocol, the 50Hz, 5s protocol was also an appropriate method to evoke Ca^{2+} signals.

2.4.1 Electrical Stimulation protocol in acute and chronic treatments

DHK was applied acutely during a series of 4 electrical stimuli (S1-S4). At the end of S2, DHK (0.1 mM) dissolved in the external solution was perfused to the DMOTC slice for 5 min and the next 2 evoked Ca^{2+} signals (S3 and S4) were recorded. In contrast, chronic DHK and BDNF protocols involved a series of 8 stimuli (S1-S8) recorded and responses to S5 and S6 were analyzed. For chronic DHK treatment, the concentration of DHK (16 μM, twice the K_d) was lower than the concentration used in acute treatments (0.1 mM) to avoid excitotoxicity.

To analyze the effects of DHK on properties of NMDA receptors, D-(-)-2-Amino-5-phosphonopentanoic acid (D-AP5; Tocris, Missouri , USA) and 6-Cyano-7-nitroquinoxaline-2,3-dione (CNQX; Tocris, Missouri , USA) were used in DHK treated (5-6d) and control DMOTC slices to block NMDA and AMPA/Kainate receptors, respectively. External solution containing D-AP5 (50μM) was administered at the end of 4^{th} stimulus (S4) for 5 min and responses to 5^{th} and 6^{th} stimulations (S5 and S6, respectively) were observed. Then the external solution containing D-AP5 (50 μM) and CNQX (10 μM) was applied at the end of S6 for 5 min and the responses were recorded at 7^{th} and 8^{th} stimulations (S7 and S8, respectively).

To analyze the effects of DHK on properties of Ca^{2+}-permeable AMPA receptors, N,N,N,-Trimethyl-5-[(tricyclo[3.3.1.13,7]dec-1-ylmethyl)amino]-1-pentanaminiumbromide hydrobromide (IEM1460; Tocris, Missouri , USA) was administered at (50 μM). D-AP5 (50 μM) was administered to the external solution at the end of S1 to the end of the experiment to block NMDA receptors. External solution containing IEM1460 (50 μM) was introduced to the slices at the end of S4 for 5min. Then external solution with D-AP5 (50 μM) and CNQX (10 μM) was administered at the end of S6 for 5minutes.

To observe the effects of DHK on mGluR subtype 1 and 5 ($mGluR_1$ and $mGluR_5$, respectively), the corresponding antagonists were used. 50 μM of $mGluR_1$ antagonist, (S)-(+)-a-Amino-4-carboxy-2-methylbenzeneacetic acid (LY 367385) or 10 μM of $mGluR_5$ antagonist, 2-Methyl-6-(phenylethynyl)pyridine hydrochloride (MPEP) was dissolved in the external solution and perfused to the DMOTC (untreated control or DHK treated) at the end of S4 for 5 min. To block NMDA and AMPA/kaniate receptors, D-AP5 (50 μM) and CNQX (10μM) were administered to the external solution after S1 until the end of the experiment.

To investigate the effects of long-term exposure to DHK and BDNF on activation of glutamate receptors, a series of ionotropic and metabotropic receptor agonists were applied in the same order in all experiments.

2.5 Statistical Analysis

Figures were produced with Origin 5.0 (OriginLab, Northamton, MA, USA) and graphs were produced with GraphPad Prisim 5.0 (San Diego, California, USA). Statistical comparisons were made using Student's paired and unpaired t-tests and one-way analysis of variance (ANOVA) with Dunnett post hoc test (GraphPad Prisim, San Diego, California, USA). Statistical significance was taken as $p<0.05$.

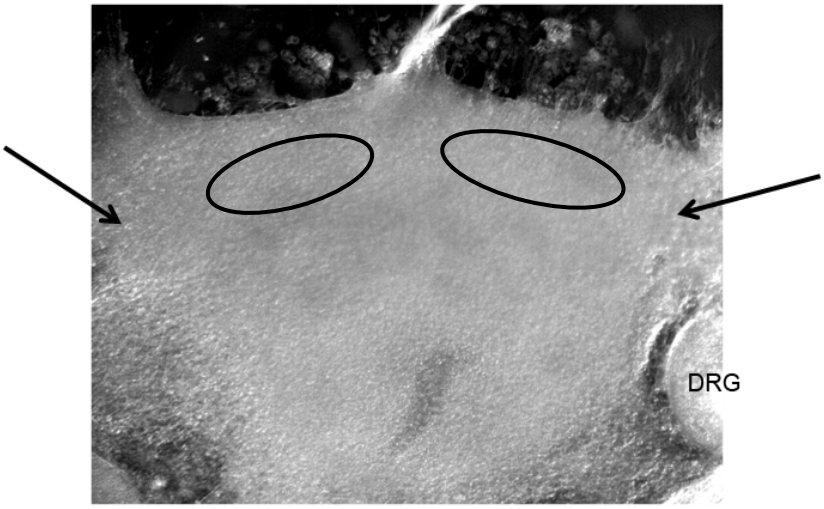

Figure 2-1. Organotypic spinal cord slice maintained 10 d *in vitro*. Arrows indicate stimulated regions and the circles indicate region where the recordings were obtained (modified from Lu et al., 2006).

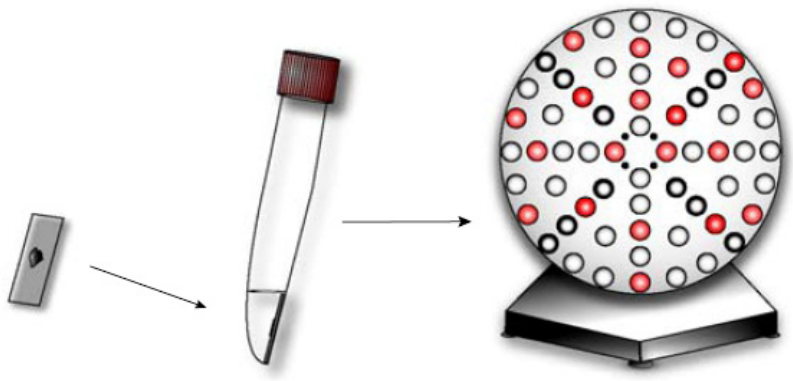

Figure 2-2. Diagram of organotypic culture preparation. Flat-bottomed tubes with coverslips were incubated in a roller drum (Lu et al., 2006).

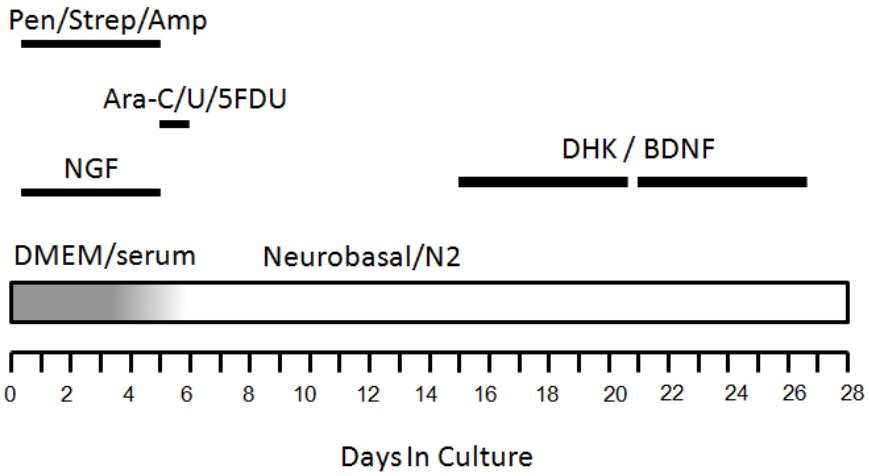

Figure 2-3. Time course of media changes in DMOTCs and DHK and BDNF treatments. Pen/Strep/Amp: Antibiotic and antimycotic drugs. Ara-C/U/5FDU: antimitotic drug cocktail. Two DHK/BDNF treatment periods are indicated.

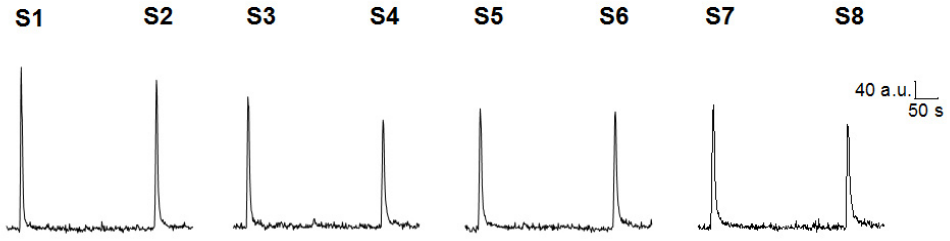

Figure 2-4. Ca^{2+} signals evoked in response to a series of stimuli (S1-S8) given to an untreated control dorsal horn neuron (50 Hz, 5 s stimulus protocol).

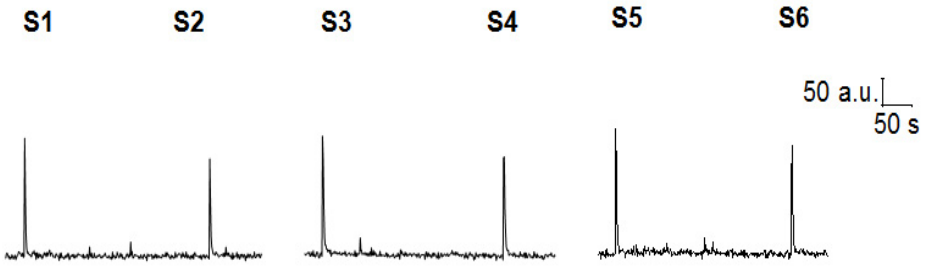

Figure 2-5. Ca^{2+} signals evoked in response to a series of stimuli (S1-S6) given to an untreated control dorsal horn neuron (50 Hz, 1 s stimulus protocol).

2.6 References

Ballerini L & Galante M (1998). Network bursting by organotypic spinal slice cultures in the presence of bicuculline and/or strychnine is developmentally regulated. *Eur J Neurosci* **10**, 2871-2879.

Braschler UF, Iannone A, Spenger C, Streit J, & Luscher HR (1989). A modified roller tube technique for organotypic cocultures of embryonic rat spinal cord, sensory ganglia and skeletal muscle. *J Neurosci Methods* **29**, 121-129.

Gahwiler BH (1981). Organotypic monolayer cultures of nervous tissue. *J Neurosci Methods* **4**, 329-342.

Gahwiler BH, Capogna M, Debanne D, McKinney RA, & Thompson SM (1997). Organotypic slice cultures: a technique has come of age. *Trends Neurosci* **20**, 471-477.

Lu VB, Ballanyi K, Colmers WF, & Smith PA (2007). Neuron type-specific effects of brain-derived neurotrophic factor in rat superficial dorsal horn and their relevance to 'central sensitization'. *J Physiol* **584**, 543-563.

Lu VB, Biggs JE, Stebbing MJ, Balasubramanyan S, Todd KG, Lai AY, Colmers WF, Dawbarn D, Ballanyi K, & Smith PA (2009). Brain-derived neurotrophic factor drives the changes in excitatory synaptic transmission

in the rat superficial dorsal horn that follow sciatic nerve injury. *J Physiol* **587**, 1013-1032.

Lu VB, Moran TD, Balasubramanyan S, Alier KA, Dryden WF, Colmers WF, & Smith PA (2006). Substantia Gelatinosa neurons in defined-medium organotypic slice culture are similar to those in acute slices from young adult rats. *Pain* **121**, 261-275.

CHAPTER 3 EFFECTS OF ACUTE AND LONG-TERM TREATMENTS WITH DHK ON EXCITABILITY OF SPINAL DORSAL HORN NEURONS IN DMOTC

3.1 Acute application of DHK

Two methods were used to examine the effects of acute application of DHK on the excitability of dorsal horn neurons. The first method involved using a high potassium challenge (35 mM K^+ solution) to evoke Ca^{2+} signals. Dorsal horn neurons were first stimulated with 35 mM K^+ solution for 90 s (Figure 3-1A). After a 15min K^+ solution washout period, DHK (0.1 mM), dissolved in the 35 mM K^+ solution, was perfused for 90s (Figure 3-1B). The control area under the Ca^{2+} signal was 97518.8 ± 23535.9 arbitrary fluorescence units (a.u.), that in DHK was 93441.8 ± 23092.7 a.u.. The control peak amplitude was 555.6 ± 110.6 a.u. and that in DHK was 423.1 ± 90.5 a.u.. The control time constant of decay of Ca^{2+} signal was 235.1 ± 52.6 s and that in DHK was 192.8 ± 32.5 s. Figure 3-1C and E indicated that the area under the Ca^{2+} signal (paired t-test, $p>0.05$), and rate of decay of Ca^{2+} signal (paired t-test, $p>0.05$) evoked by K^+ in presence of DHK were not significantly different compared to K^+ solution alone (n=20, 5 DMOTCs). However, the peak amplitude of Ca^{2+} signal (paired t-test, $p= 0.022$).

The second method involved using electrical stimuli to evoke Ca^{2+} signals. As described in Chapter 2, there was a series of 4 stimuli (S1-S4). To investigate the effects of acute application of DHK on the dorsal horn neurons, DHK (0.1 mM), dissolved in the external solution, was administered after S2 for 5min (Figure 3-2A). The S1 through S4 areas under the Ca^{2+} signal were 7053.0 ± 909.5 a.u., 5968.5 ± 685.2 a.u., 8460.9 a.u. ± 1010.2 a.u. and 6927.8 ± 736.4 a.u., respectively. The S1 through S4 peak amplitudes were 743.4 ± 60.3 a.u.,

636.9 ± 51.6 a.u., 687.1 ± 57.9 a.u., 552.4 ± 49.2 a.u., respectively. The S1-S4 time constant of decay were 5.9 ± 0.4 s, 5.6 ± 0.2 s, 7.8 ± 0.5 s, 7.4 ± 0.6 s, respectively. There was no significant change in the area under the Ca^{2+} signal (Figure 3-2F) and its peak amplitude of Ca^{2+} signal (Figure 3-2G) in the presence of DHK (n=54, 5 DMOTCs, paired t-test, $p>0.05$ for both area and peak amplitude). However, Figure 3-2H indicated that the rate of decay of the Ca^{2+} signals significantly decreased following the acute application of DHK (paired t-test, $p= 0.0004$ between S1 and S3, $p= 0.0002$ between S2 and S4). It is evident that the results obtained from the two methods are generally similar, as DHK fails to change the amplitude or area under the curve of K^+ evoked or stimulus evoked Ca^{2+} responses. DHK did however slow the rate of decay of stimulus evoked responses but not that of K^+ evoked responses. One possible explanation for this is that the Ca^{2+} response evoked by 35mM K^+ reflects both opening of voltage gated Ca^{2+} channels and the release of excitatory neurotransmitters whereas, the stimulus evoked response reflects the actions of excitatory neurotransmitters only. The DHK induced reduction in glutamate uptake may therefore have a larger effect under these circumstances. It is also possible that the DHK had more time to equilibrate with the slice in the stimulation experiments when it was administered for 5min prior to the test stimulus. By contrast, the concurrent application of DHK and 35mM K^+ may have not provided enough time for the drug to fully equilibrate with the tissue.

3.2 Chronic application of DHK

As discussed in Chapter 2, the amplitudes of S5 to S8 displayed much less variability than the amplitudes of S1 to S4 therefore only S5 and S6 were compared and analyzed. Figure 3-3A and B illustrate three individual S5 and S6 Ca^{2+} responses from untreated control (n=40, 6 DMOTCs) and DHK treated (5-6d; n=24, 5 DMOTCs) neurons. Sample fluorescent images of dorsal horn neurons of control (Figure 3-3C) and DHK treated (Figure 3-3D) neurons at S5 are shown. After chronic application of DHK, there was a significant increase in the area under the stimulation evoked Ca^{2+} signal compared to that in control neurons (Figure 3-3E, unpaired t-test, p=0.0016 for S5 and p=0.0029 for S6). The S5 control area under the Ca^{2+} signal was 2259.5 ± 234.6 a.u. and that in DHK was 5313.6 ± 1135.6 a.u.. The S6 control area was 2082.9 ± 226.7 a.u. and that in DHK was 3715.0.1± 566.6 a.u.. No significant changes in peak amplitude of Ca^{2+} signal were observed between untreated control and DHK treated neurons (Figure 3-3F, unpaired t-test, p>0.05 for both S5 and S6). The S5 control peak amplitude was 215.0 ± 20.5 a.u. and that in DHK was 316.2 ± 72.3 a.u.. The S6 control peak amplitude was 189.8 ± 18.2 a.u. and that in DHK was 242.8 ± 34.4 a.u.. Chronic application of DHK resulted in a significant decrease the in rate of decay Ca^{2+} signal compared to the control neurons (Figure 3-3G, unpaired t-test, p=0.0015 for S5 and p=0.0074 for S6). For S5 control, the time constant of decay was 6.5 ± 0.5 s and that in DHK was 10.5 ± 1.4 s. For S6, the control, the time constant of decay was 6.5 ± 0.5 s and that in DHK was 14.4 ± 3.6 s.

Figure 3-1. Acute application of DHK (35mM K^+ challenge).

A and B: Sample fluorescent Ca^{2+} intensity traces during 35mM K^+ challenge (90s; A) and DHK (0.1mM) + 35mM K^+ challenge (90s) which was applied after 15min following the K^+ challenge (B). C, D and E: area under the fluorescence Ca^{2+} signal (C) evoked by the 35 mM K^+ and DHK solution was not significantly different compared to K^+ solution alone (n=20, 5 DMOTCs, paired t-test, $p>0.05$). Peak amplitude of fluorescence Ca^{2+} signal (D) was significantly increased following the application of 35 mM K^+ and DHK solution (paired t-test, $p=0.022$). Time constant of decay of Ca^{2+} fluorescence signal (E) was not significantly different compared to K^+ solution alone (paired t-test, $p>0.05$). Scaling is in arbitrary units (A.U.) for area under the fluorescence signal and peak amplitude of fluorescence signal. Scaling is in seconds (s) for time constant of decay. Error bars indicate S.E.M..

Figure 3-1

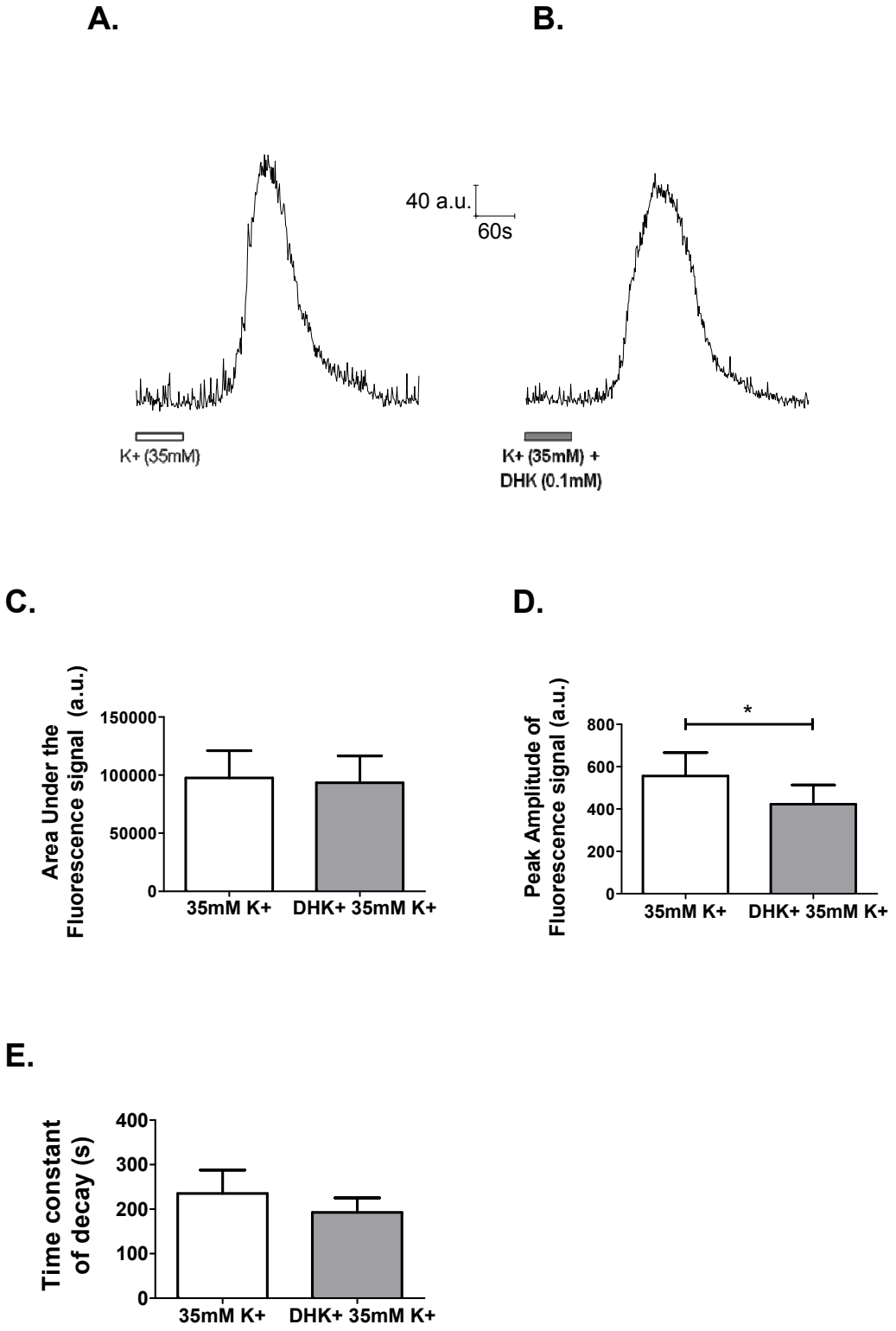
A.
B.
40 a.u.
60s
K+ (35mM)
K+ (35mM) +
DHK (0.1mM)
C.
Area Under the Fluorescence signal (a.u.)
150000
100000
50000
0
35mM K+
DHK+ 35mM K+
D.
Peak Amplitude of Fluorescence signal (a.u.)
800
600
400
200
0
*
35mM K+
DHK+ 35mM K+
E.
Time constant of decay (s)
400
300
200
100
0
35mM K+
DHK+ 35mM K+

Figure 3-2. Acute application of DHK (Electrical stimuli).

A: Electrical stimulation protocol of acute application of DHK (0.1mM). B and C: Staggered fluorescent Ca^{2+} intensity traces from three cells in the same DMOTC slice before application of DHK (B) and after 5min application of DHK (C). D and E: Sample fluorescent images of dorsal horn neurons stimulated before (D) and after the application of DHK (E). White scale bar is 50μm. F,G and H: Area under the Ca^{2+} signals (F), peak amplitude (G) and time constant of decay of Ca^{2+} signals (H) evoked by electrical stimulations are illustrated (n=54, 5 DMOTCs, paired t-test, ***$p<0.001$). Scaling is in arbitrary units (A.U.) for area under the fluorescence signal and peak amplitude of fluorescence signal. Scaling is in seconds (s) for time constant of decay. Error bars indicate S.E.M..

Figure 3-2

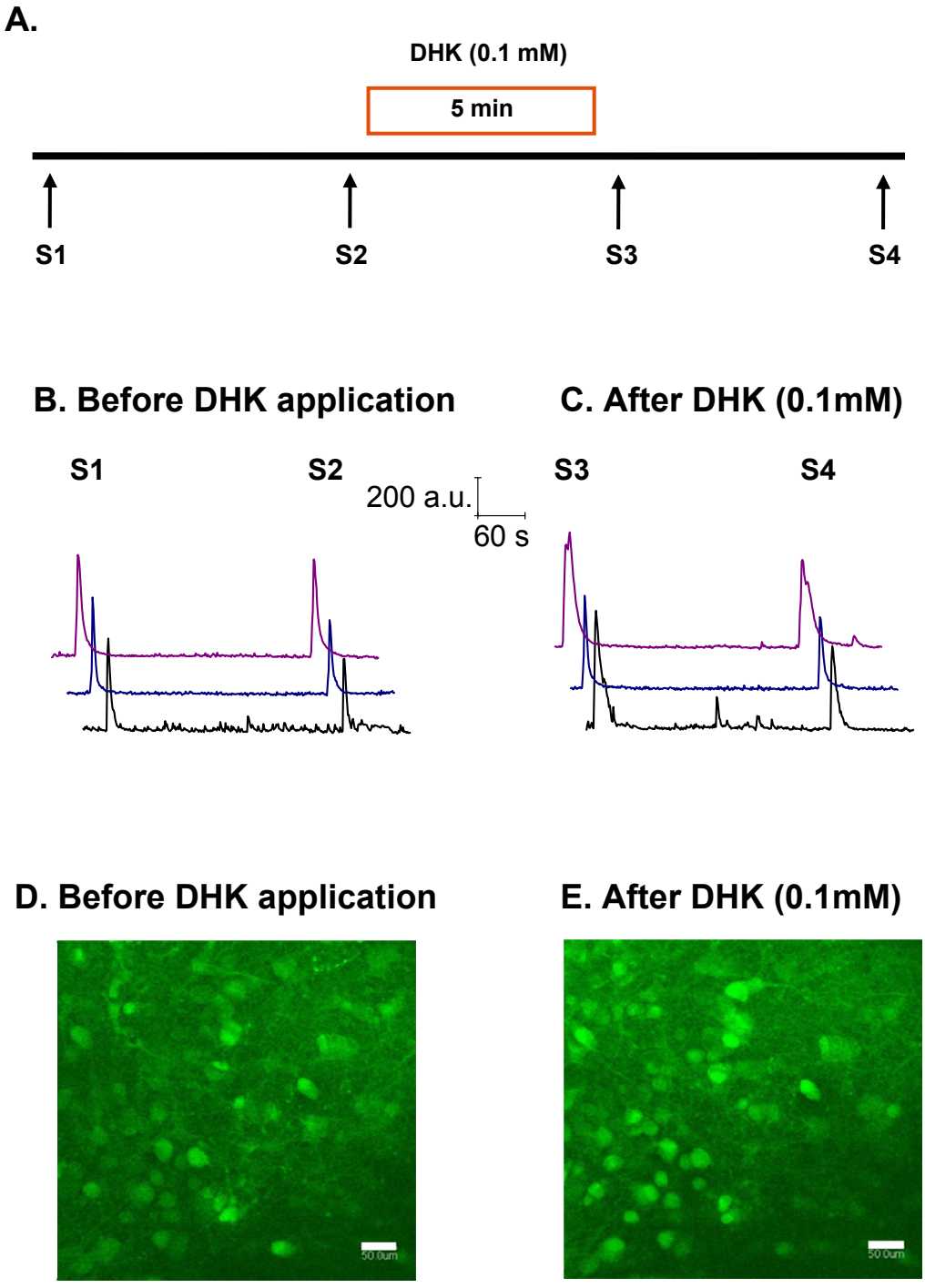
A.
DHK (0.1 mM)
5 min
S1
S2
S3
S4
B. Before DHK application
C. After DHK (0.1mM)
S1
S2
200 a.u.
60 s
S3
S4
D. Before DHK application
E. After DHK (0.1mM)

F.

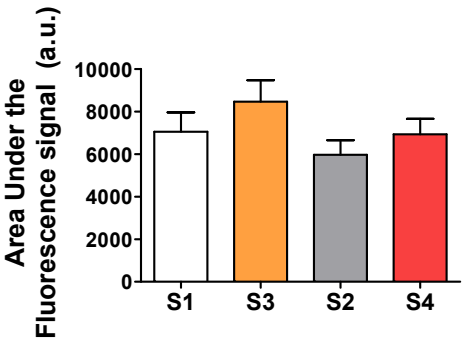
Area Under the Fluorescence signal (a.u.)
10000
8000
6000
4000
2000
0
S1
S3
S2
S4

G.

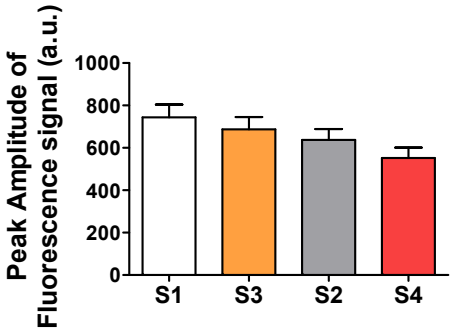
Peak Amplitude of Fluorescence signal (a.u.)
1000
800
600
400
200
0
S1
S3
S2
S4

H.

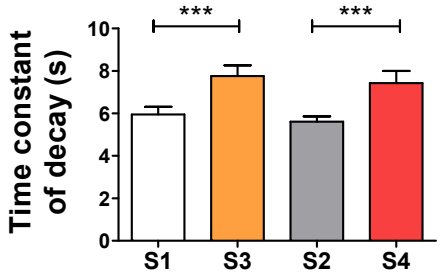
Time constant of decay (s)
***
***
10
8
6
4
2
0
S1
S3
S2
S4

Figure 3-3. Chronic application of DHK.

A and B: Staggered fluorescent Ca^{2+} intensity traces from three cells in the same DMOTC slice of untreated control (A) and DHK treated (5-6d) dorsal horn neurons (B). C and D: Sample fluorescent images of dorsal horn neurons of control (C; n=40, 6 DMOTCs) and DHK treated (D; n=24, 5 DMOTCs) neurons. White scale bar is 50μm. E, F and G: Area under the Ca^{2+} signal (E), peak amplitude (F) and time constant of decay of Ca^{2+} signals (G) evoked by electrical stimulations are indicated (unpaired t-test, **$p<0.01$). Scaling is in arbitrary units (A.U.) for area under the fluorescence signal and peak amplitude of fluorescence signal. Scaling is in seconds (s) for time constant of decay. Error bars indicate S.E.M..

Figure 3-3

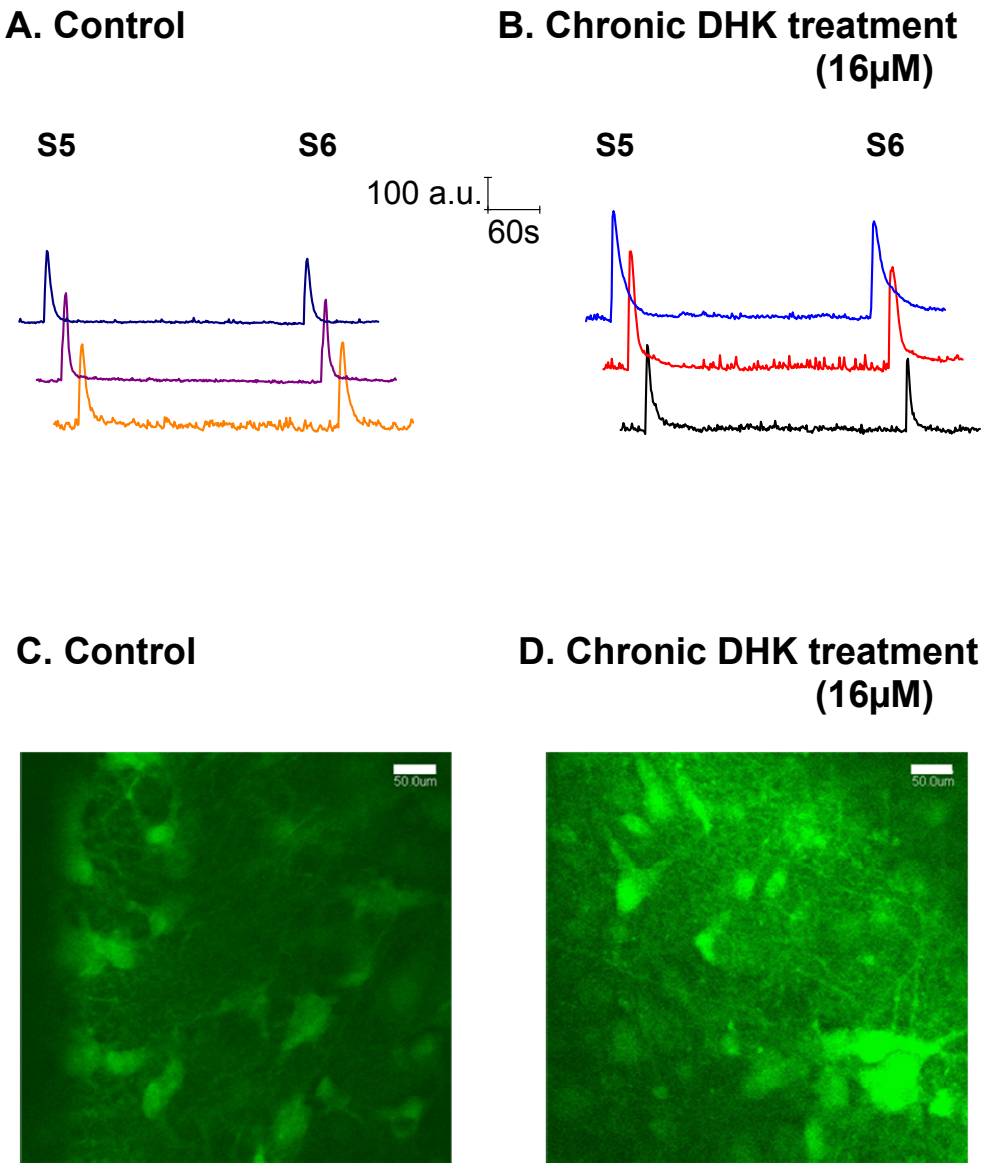
A. Control
B. Chronic DHK treatment (16μM)
S5
S6
100 a.u.
60s
S5
S6
C. Control
D. Chronic DHK treatment (16μM)
50.0um
50.0um

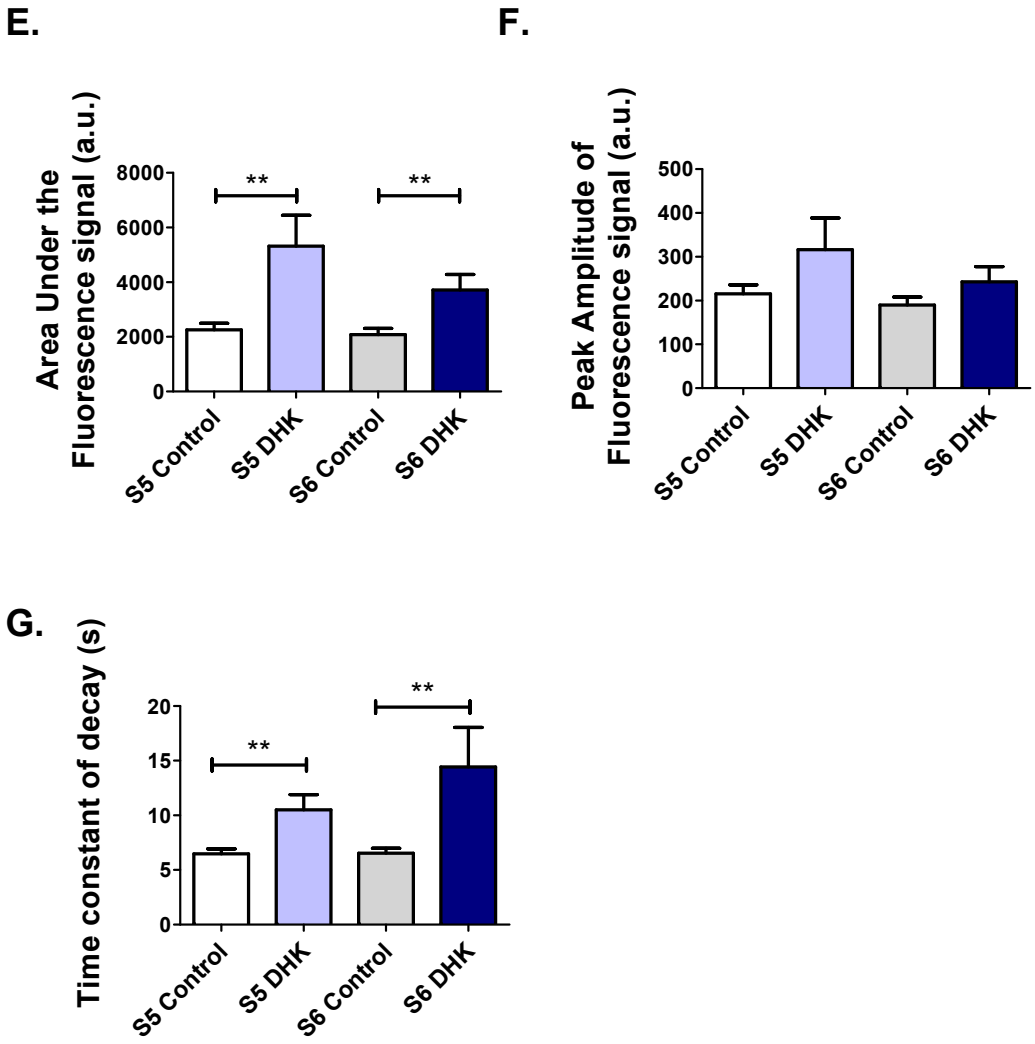
E.
F.
G.
Area Under the Fluorescence signal (a.u.)
8000
6000
4000
2000
0
**
**
S5 Control
S5 DHK
S6 Control
S6 DHK
Peak Amplitude of Fluorescence signal (a.u.)
500
400
300
200
100
0
Time constant of decay (s)
20
15
10
5
0
**
**

CHAPTER 4 EFFECTS OF LONG-TERM INHIBITION OF EAAT2 ON PHARMACOLOGY OF GLUTAMATE RECEPTORS

4.1 Effects of DHK on properties of NMDA receptors

In general, the kinetics of NMDA receptor responses are slower than those involving AMPA or kainate receptors. This raised the possibility that the increase in duration and slowed rate of decay of Ca^{2+} responses seen in the presence of chronic DHK treatment reflected access of synaptically released glutamate to NMDA receptors. To test this possibility, the NMDA receptor antagonist, AP5 (50μM) was administered to untreated control (n=30, 8 DMOTCs) and DHK treated (5-6d, n=37, 5 DMOTCs) neurons (Figure 4-1A). Fluorescent Ca^{2+} intensity traces from three neurons in the same DMOTC slice of untreated control and DHK treated dorsal horn neurons are illustrated (Figure 4-1B and C). The S5-S8 responses of untreated control neurons following the application of AP5 followed by a combination of AP5 and the AMPA/kainate blocker, CNQX (10μM) were compared with another set of untreated control neurons that had not been treated with the antagonists (n=40, 6 DMOTCs, Figure 4-1D-F). Furthermore, the responses of DHK treated neurons following the application of AP5 + CNQX were compared with the responses of DHK treated neurons without the antagonists (n=24, 5 DMOTCs, Figure 4-1D-F).

No significant differences in the area under the Ca^{2+} signal were observed between the untreated control and AP5 treated groups for both S5 and S6 (unpaired t-test, $p>0.05$ for both). By contrast, AP5 significantly decreased the area under the Ca^{2+} signal responses to stimulation in DHK treated neurons (unpaired t-test, $p=0.0067$ for S5, $p=0.0159$ for S6). The S5 untreated control area under the Ca^{2+} signal was 2259.5 ± 234.6 a.u. and the S5 control following

the administration of AP5 was 1553.2 ± 325.3 a.u.. The S5 area under the Ca^{2+} signal of DHK treated neurons was 5313.6 ± 1135.6 a.u. and the DHK S5 following the administration of AP5 was 2362.7 ± 420.6 a.u.. The S6 untreated control area under the Ca^{2+} signal was 2082.9 ± 226.7 a.u. and the S6 control following the administration of AP5 was 1481.4 ± 312.2 a.u.. The S6 area of DHK treated neurons was 3715.0 ± 566.6 a.u. and the DHK S6 following the administration of AP5 was 2068.4 ± 387.8 a.u. (Figure 4-1D).

Figure 4-1E shows that peak amplitude of the stimulation evoked Ca^{2+} signal significantly decreased following the application of AP5 in both control (unpaired t-test, $p<0.0001$) and DHK treated neurons (unpaired t-test, $p<0.0001$). The S5 untreated control peak amplitude was 215.0 ± 20.5 a.u. and the S5 control following the administration of AP5 was 126.4 ± 29.3 a.u.. The S5 peak amplitude of DHK treated neurons was 316.2 ± 71.3 a.u. and the DHK S5 following the administration of AP5 was 136.9 ± 16.8 a.u.. The S6 untreated control peak amplitude of the Ca^{2+} signal was 189.8 ± 18.2 a.u. and the S6 control following the administration of AP5 was 113.6 ± 20.9 a.u.. The S6 peak amplitude of DHK treated neurons was 242.8 ± 34.4 a.u. and the DHK S6 following the administration of AP5 was 124.0± 13.1 a.u..

In terms of the rate of decay, no significant differences were found between the two control groups (unpaired t-test, $p>0.05$) and the two DHK treated groups (Figure 4-1F, unpaired t-test, $p>0.05$). The S5 untreated time constant for decay was 6.5 ± 0.5 s and the S5 control following the

administration of AP5 was 7.0 ± 0.8 s. The S5 time constant for decay of DHK treated neurons was 10.1 ± 1.4 s and the DHK S5 following the administration of AP5 was 10.8 ± 1.5 s. The S6 untreated control time constant for decay of the Ca^{2+} signal was 6.5 ± 0.5 s and the S6 control following the administration of AP5 was 7.7 ± 1.0 s. The S6 time constant for decay of DHK treated neurons was 14.0 ± 3.5 s and the DHK S6 following the administration of AP5 was 11.6 ± 1.5 s. These results indicated that there were no significant differences in the peak amplitude and rate of decay of the Ca^{2+} signals between the control and DHK treated dorsal horn neurons following application of AP5 (Figure 4-1E and F).

Application of CNQX and AP5 at the end of S6 significantly reduced the area under the stimulation evoked Ca^{2+} signal in both control (unpaired t-test, $p<0.001$ for S7 and $p<0.001$ for S8) and DHK treated neurons (Figure 4-1D, unpaired t-test, $p<0.001$ for S7 and $p<0.001$ for S8). The S7 untreated control area under the Ca^{2+} signal was 1920.1 ± 225.9 a.u. and the S7 control following the administration of CNQX and AP5 was 608.6 ± 125.1 a.u.. The S8 untreated control area was 1854.5 ± 233.4 a.u. and the S8 control following the administration of CNQX and AP5 was 623.0 ± 118.6 a.u.. The S7 area of DHK treated neurons was 3896.2 ± 752.0 a.u. and the DHK S7 following the administration of AP5 was 898.6 ± 131.6 a.u.. The S8 area of DHK treated neurons was 2823.6 ± 515.1 a.u. and the DHK S8 following the administration of CNQX and AP5 was 971.8 ± 139.8 a.u..

Moreover, application of CNQX and AP5 significantly reduced the peak amplitude of Ca^{2+} signal in both control (unpaired t-test, $p<0.001$ for S7 and $p<0.001$ for S8) and DHK treated neurons (Figure 4-1E, unpaired t-test, $p<0.001$ for S7 and $p<0.001$ for S8). The S7 untreated control peak amplitude of Ca^{2+} signal was 177.1 ± 18.2 a.u. and the S7 control following the administration of CNQX and AP5 was 47.7 ± 6.5 a.u.. The S8 untreated control peak amplitude was 166.1 ± 17.2 a.u. and the S8 control following the administration of CNQX and AP5 was 50.5 ± 8.0 a.u.. The S7 peak amplitude of DHK treated neurons was 224.8 ± 30.8 a.u. and the DHK S7 following the administration of AP5 was 67.9 ± 9.2 a.u.. The S8 peak amplitude of DHK treated neurons was 180.9 ± 24.8 a.u. and the DHK S8 following the administration of CNQX and AP5 was 69.7 ± 8.2 a.u..

No significant differences in the time constant for decay were found following the application of CNQX and AP5 in both control (unpaired t-test, $p>0.05$ for S7 and S8) and DHK treated neurons (Figure 4-1F, unpaired t-test, $p>0.05$ for S7 and S8). The S7 untreated control time constant for decay of Ca^{2+} signal was 6.9 ± 0.5 s and the S7 control following the administration of CNQX and AP5 was 6.6 ± 0.8 s. The S8 untreated control time constant was 7.3 ± 0.7 s and the S8 control following the administration of CNQX and AP5 was 6.8 ± 1.0 s. The S7 time constant for decay of DHK treated neurons was 12.0 ± 2.2 s and the DHK S7 following the administration of AP5 was 9.9 ± 1.6 s. The S8 time

constant for decay for DHK treated neurons was 16.4 ± 4.0 s and the DHK S8 following the administration of AP5 was 10.6 ± 1.9 s.

Therefore, the results suggested that the application of AP5 was more effective in DHK treated neurons. Moreover, it was observed that in both control and DHK treated neurons, the responses to stimulations were not completely eliminated by AP5 and CNQX (Figure 4-1D-F).

4.2 Effects of DHK on Ca^{2+}-permeable AMPA receptors

It has been reported that Ca^{2+}-permeable AMPA receptors which are highly expressed in lamina I and II of the dorsal horn of the spinal cord, are likely involved in nociceptive transmission (Bleakman et al., 2006). Therefore a selective blocker of Ca^{2+} permeable AMPA receptors, IEM1460 (50μM; Santos et al., 2009) was used to investigate if the expression of Ca^{2+}-permeable AMPA receptors is altered following long-term inhibition of EAAT2 in dorsal horn neurons.

To ensure that NMDA receptors were not activated, AP5 (50μM) was applied after S1 and all subsequent recordings were made in the presence of NMDA receptor blockade. The S5-S8 responses of untreated control neurons (n=29, 6 DMOTCs) following the application of IEM1460 at the end of S4 and CNQX (10μM) at the end of S6 were compared with another set of untreated control neurons that had only been treated with AP5 (n=33, 3 DMOTCs, Figure 4-2A). Furthermore, the S5-S8 responses of DHK treated neurons (n=33, 6 DMOTCs) following the application of the antagonists were compared with the

responses of DHK treated neurons with only AP5 (n=34, 4 DMOTCs, Figure 4-2A). Typical recordings from 3 control and DHK treated (5-6d) neurons are illustrated (Figure 4-2B and C).

The S5 untreated control area under the stimulation evoked Ca^{2+} signal was 872.8 ± 216.0 a.u. and the S5 control following the administration of IEM1460 was 1332.7 ± 337.3 a.u.. The S5 area under the Ca^{2+} signal of DHK treated neurons was 2286.0 ± 605.8 a.u. and the DHK S5 following the administration of IEM1460 was 855.4 ± 112.9 a.u.. Thus for S5, administration of IEM1460 did not significantly alter the area under the Ca^{2+} signal in the control neurons but significantly reduced the area under the Ca^{2+} signal in DHK treated neurons (Figure 4-2D, unpaired t-test, p= 0.0253). The S6 untreated control area under the Ca^{2+} signal was 729.7 ± 193.6 a.u. and the S6 control following the administration of IEM1460 was 997.7 ± 221.7 a.u.. The S6 area of DHK treated neurons was 1653.2 ± 466.4 a.u. and the DHK S6 following the administration of IEM1460 was 988.1 ± 137.2 a.u. (Figure 4-2D). None of these changes were significant. Thus, for S6 the presence of DHK failed to alter the effectiveness of IEM 1469.

The S5 untreated control peak amplitude of stimulation evoked Ca^{2+} signal was 73.6 ± 15.8 a.u. and the S5 control following the administration of IEM1460was 75.3 ± 13.2 a.u.. The S5 peak amplitude of DHK treated neurons was 95.8 ± 18.9 a.u. and the DHK S5 following the administration of IEM1460 was 83.8 ± 11.3 a.u.. The S6 untreated control peak amplitude of Ca^{2+} signal was

58.2 ± 8.0 a.u. and the S6 control following the administration of IEM1460 was 73.3 ± 12.4 a.u.. The S6 peak amplitude of DHK treated neurons was 77.7 ± 12.5 a.u. and the DHK S6 following the administration of IEM1460 was 76.0 ± 9.6 a.u. (Figure 4-2E). Thus for both S5 and S6, no significant changes in the amplitude of stimulus-evoked Ca^{2+} responses were observed following the application of IEM1460 in both control (unpaired t-test, $p>0.05$) and DHK treated neurons (Figure 4-2E, unpaired t-test, $p>0.05$).

The S5 untreated control time constant of decay of Ca^{2+} signal was 8.3 ± 0.9 s and the S5 control following the administration of IEM1460 was 11.3 ± 2.9 s. The S5 time constant of DHK treated neurons was 11.1 ± 1.2 s and the DHK S5 following the administration of IEM1460 was 6.5 ± 0.4 s. The S6 untreated control time constant of decay was 8.1 ± 0.9 s and the S6 control following the administration of IEM1460 was 10.3 ± 1.8 s. The S6 time constant DHK treated neurons was 12.4 ± 1.8 s and the DHK S6 following the administration of IEM1460 was 8.0 ± 1.6 s (Figure 4-2F). Time constant of decay of S5 of DHK treated neurons significantly decreased after the application of IEM1460 (unpaired t-test, $p= 0.0008$) but no significant differences were found in the control neurons (Figure 4-2F, unpaired t-test, $p>0.05$). No significant changes in time constant were seen for S6 (Figure 4-2F, unpaired t-test, $p>0.05$).

Application of CNQX and AP5 at the end of S6 significantly decreased the area under the Ca^{2+} signal in both untreated control ($p< 0.001$ for both S7 and S8) and DHK treated neurons (Figure 4-2D, $p< 0.001$ for both S7 and S8).

S7 untreated control area under the Ca^{2+} signal was 1920.1 ± 225.9 a.u. and the S7 control following the administration of CNQX was 428.7 ± 109.8 a.u.. The S7 area under the Ca^{2+} signal of DHK treated neurons was 3896.2 ± 752.1 a.u. and the DHK S7 following the administration of CNQX was 734.7 ± 167.3 a.u.. The S8 untreated control area under the Ca^{2+} signal was 1854.5 ± 233.4 a.u. and the S8 control following the administration of CNQX was 621.3 ± 131.8 a.u.. The S8 area of DHK treated neurons was 2823.6 ± 515.1 a.u. and the DHK S8 following the administration of CNQX was 637.7 ± 119.5 a.u..

The S7 untreated control peak amplitude of Ca^{2+} signal was 177.1 ± 18.2 a.u. and the S7 control following the administration of CNQX was 40.0 ± 8.2 a.u.. The S7 peak amplitude of DHK treated neurons was 224.8 ± 30.8 a.u. and the DHK S7 following the administration of CNQX was 50.2 ± 7.5 a.u.. The S8 untreated control peak amplitude of Ca^{2+} signal was 166.1 ± 17.2 a.u. and the S8 control following the administration of CNQX was 47.8 ± 8.8 a.u.. The S8 peak amplitude of DHK treated neurons was 180.9 ± 24.8 a.u. and the DHK S8 following the administration of CNQX was 50.8 ± 7.1 a.u..

The S7 untreated control time constant of decay of Ca^{2+} signal was 6.9 ± 0.5 s and the S7 control following the administration of CNQX was 5.5 ± 0.8 s. The S7 time constant of decay of DHK treated neurons was 12.0 ± 2.2 s and the DHK S7 following the administration of CNQX was 9.2 ± 2.3 s. The S8 untreated control time constant of decay of Ca^{2+} signal was 7.3 ± 0.7 s and the S8 control following the administration of CNQX was 7.5 ± 1.0 s. The S8 time

constant of decay of DHK treated neurons was 16.4 ± 4.0 s and the DHK S8 following the administration of CNQX was 5.4 ± 0.3 s.

Thus application of CNQX and AP5 at the end of S6 significantly decreased the peak amplitude of Ca^{2+} signal (Figure 4-2E) in both control (unpaired t-test, $p<0.001$ for both S7 and S8) and DHK treated neurons (unpaired t-test, $p<0.001$ for both S7 and S8). In DHK treated neurons, the S8 rate of decay of Ca^{2+} signal was significantly decreased (unpaired t-test, $p=0.0021$) but not in control neurons (Figure 4-2F, unpaired t-test, $p>0.05$) nor in either situation for S7 (Figure 4-2F, unpaired t-test, $p>0.05$).

Again, the responses to electrical stimuli were not completely eliminated by AP5 and CNQX (Figure 4-2D-F). Overall, these results are consistent with the possibility that there may be a change in the pharmacological properties of AMPA receptors following chronic inhibition of EAAT2. Specifically, there might be a slight increase in the ratio of IEM1460 sensitive (Ca^{2+} permeable) to IEM1460 insensitive (Ca^{2+} impermeable) AMPA receptors.

4.3 Effects of DHK on $mGluR_1$ and $mGluR_5$

The previous data indicate that AP5 and CNQX failed to completely abolish the responses to electrical stimuli. Thus these data suggest the possibility of involvement of other receptor types. One possibility is that some of the Ca^{2+} responses reflect activation of mGluRs, in particular $mGluR_1$ and $mGluR_5$ which signal through G_q (Fagni et al., 2004). To test this possibility, antagonists of $mGluR_1$ and $mGluR_5$ were used. LY 367385 (50μM) and MPEP (10μM)

dissolved in the external solution were perfused to untreated control and DHK treated DMOTCs to block $mGluR_1$ and $mGluR_5$, respectively (Salt and Turner, 1998; Salt et al., 1999). The antagonists were administered to the DMOTCs between S4 and S5 for 5min (Figure 4-3A and 4-4A). AP5 (50μM) and CNQX (10μM) were administered to the DMOTCs after S1 to ensure the ionotropic receptors were blocked (Figure 4-3A and 4-4A).

The S5-S8 responses of untreated control neurons following the application of LY 367385 or MPEP were compared with another set of untreated control neurons that had been treated with CNQX and AP5 (n=30, 7 DMOTCs, Figure 4-5A-C). The responses of DHK treated neurons following the application of either antagonist were compared with the responses of DHK treated neurons with CNQX and AP5 (n=37, 5 DMOTCs, Figure 4-5A-C). All of the control and DHK treated S5 responses were normalized to control and DHK treated CNQX+AP5 responses, respectively (Figure 4-5A-C).

Administration of the $mGluR_1$ antagonist, LY 367385 did not significantly decrease the area under the Ca^{2+} signal, peak amplitude and time constant of decay of Ca^{2+} signals in untreated control neurons (Figure 4-5A-C, n=40, 3 DMOTCs, ANOVA, $p>0.05$ for all). By contrast, LY 367385 significantly decreased the area under the Ca^{2+} signal (ANOVA, $p<0.05$) in DHK treated neurons (n=45, 4 DMOTCs, Figure 4-5A). LY 367385 did not significantly change the peak amplitude of Ca^{2+} signal (ANOVA, $p>0.05$) but significantly decreased the time constant of decay of the stimulation evoked Ca^{2+} signal (ANOVA, $p<0.05$) in DHK treated neurons (Figure 4-5B and C).

In both untreated control (n=37, 5 DMOTCs) and DHK treated (n=33, 3 DMOTCs) neurons, administration of the $mGluR_5$ receptor antagonist, MPEP, significantly decreased the area under the Ca^{2+} signal (Figure 4-5A, ANOVA, $p<0.05$ for control and $p<0.001$ for DHK treated). Although MPEP did not significantly change the peak amplitude of Ca^{2+} signal of control neurons (ANOVA, $p>0.05$), it significantly decreased the peak amplitude of DHK treated neurons (Figure 4-5B, ANOVA, $p<0.01$). MPEP significantly decreased the time constant of decay in both control (ANOVA, $p<0.01$) and DHK treated neurons (Figure 4-5C, ANOVA, $p<0.05$). Therefore, the results suggest that contribution of $mGluR_5$ does not appear to change after the DHK treatment and $mGluR_1$ may be involved in generating the Ca^{2+} signal in DHK treated neurons.

4.4 Effects of DHK and BDNF on activation of ionotropic and metabotropic glutamate receptors

To examine further the changes in various types of receptors induced by chronic EAAT2 inhibition and treatment with BDNF, a series of ionotropic and metabotropic receptor agonists were administered to untreated control (n=38, 4 DMOTCs), DHK (n=32, 4 DMOTCs) and BDNF (n=37, 5 DMOTCs) treated dorsal horn neurons First, 35mM K^+ solution was administered to confirm viability of neurons. Then, a series of agonists (90s application each), AMPA (10μM), NMDA (50μM), (RS)-3,5-Dihydroxyphenylglycine (DHPG; 50μM; Schoepp et al., 1994) and DHPG (50μM) and MPEP (10μM; Gasparini et al., 1999), were administered to activate AMPA receptors, NMDA receptors,

$mGluR_1$ and $mGluR_5$ and only $mGluR_1$, respectively (Figure 4-6A). Furthermore, each agonist was washed out for 15min prior to the subsequent agonist application. The mGluR agonists did not change the baseline of Ca^{2+} signals in all control, DHK and BDNF treated neurons, therefore the responses following the administration of those agonists were not analyzed (Figure 4-6B-D).

The area under the Ca^{2+} signals of untreated control, DHK and BDNF treated neurons following the administration of K^+ were 32023.8 ± 3733.3 a.u., 48432.7 ± 6142.6 a.u. and 71052.7 ± 8328.1 a.u., respectively. The area under the Ca^{2+} signals of untreated control, DHK and BDNF treated neurons following the application of AMPA were 60604.7 a.u. ± 7122.2 a.u., 107577.4 ± 17666.5 a.u. and 169440.5 ± 16236.3 a.u., respectively. The area under the Ca^{2+} signals of untreated control, DHK and BDNF treated neurons following the application of NMDA were 14904.5 ± 2257.1 a.u., 26947.7 ± 4198.5 a.u. and 24234.3 ± 3233.9 a.u., respectively. Application of the K^+ solution significantly increased the area under the Ca^{2+} signal (ANOVA, $p<0.01$) and peak amplitude of Ca^{2+} signal in BDNF treated neurons compared to the control neurons (Figure 4-6E and F, ANOVA, $p<0.01$). Following the administration of AMPA, the area under the Ca^{2+} signals significantly increased in DHK (ANOVA, $p<0.05$) and BDNF (ANOVA, $p<0.01$) treated neurons compared to the control neurons (Figure 4-6E). BDNF treated neurons also had significantly greater area under the Ca^{2+} signal than the DHK treated neurons (Figure 4-6E, ANOVA, $p<0.01$).

The peak amplitude of Ca^{2+} signals of untreated control, DHK and BDNF treated neurons following the administration of K^+ were 264.5 ± 32.5 a.u., 416.5 ± 51.9 a.u. and 582.2 ± 64.9 a.u., respectively. The peak amplitude of Ca^{2+} signals of untreated control, DHK and BDNF treated neurons following the administration of AMPA were 289.0 ± 35.7 a.u., 519.6 ± 84.6 a.u. and 636.6 ± 62.6 a.u., respectively. The peak amplitude of Ca^{2+} signals of control, DHK and BDNF treated neurons following the administration of NMDA were 116.3 ± 16.2 a.u., 205.0 ± 26.2 a.u. and 168.1 ± 18.7 a.u., respectively. AMPA significantly increased the peak amplitude of Ca^{2+} signal in both DHK (ANOVA, $p<0.05$) and BDNF (ANOVA, $p<0.01$) treated neurons compared to the control neurons (Figure 4-6F). NMDA significantly increased the area under the Ca^{2+} signal (ANOVA, $p<0.01$) and peak amplitude of Ca^{2+} signals (ANOVA, $p<0.01$) in DHK treated neurons but not in BDNF treated neurons (ANOVA, $p>0.05$) compared to the control neurons (Figure 4-6E and F).

The time constant of decay of Ca^{2+} signals of untreated control, DHK and BDNF treated neurons following the application of K^+ were 62.8 ± 7.7 s, 53.1 ± 2.7 s and 75.5 ± 20.1 s, respectively. The time constant of decay of Ca^{2+} signals of untreated control, DHK and BDNF treated neurons following the administration of AMPA were 274.6 ± 49.7 s, 247.7 ± 50.1 s and 251.3 ± 62.9 s, respectively. The time constant of decay of Ca^{2+} signals of untreated control, DHK and BDNF treated neurons following the application of NMDA were 75.0 ± 15.0 s, 64.4 ± 7.7 s and 111.1 ± 20.7 s, respectively. No significant differences were found in terms of the rate of decay of Ca^{2+} signals in both DHK and BDNF

treated neurons following the application of K^+ , AMPA and NMDA (Figure 4-6G, ANOVA, $p>0.05$ for all).

Although both DHK and BDNF increased Ca^{2+} signals in response to AMPA, the effects of DHK and BDNF were different as only BDNF significantly increased Ca^{2+} signals following administration of K^+ and only DHK significantly increased Ca^{2+} signals following administration of NMDA.

Figure 4-1. Effects of DHK on properties of NMDA receptors.

A: Electrical stimulation protocol of application of AP5 (50μM) and CNQX (10μM) and AP5. AP5 was administered after S4 for 5min and CNQX and AP5 were administered after S6 for 5min. B and C: Staggered fluorescent Ca^{2+} intensity traces from three dorsal horn neurons in the same untreated control (B) and DHK treated (C, 5-6d) DMOTC slice. D-F: S5 to S8 of area under the Ca^{2+} signals (D), peak amplitude (E) and time constant of decay of Ca^{2+} signals (F) evoked by electrical stimulations are indicated (unpaired t-test, *$p<0.05$, **$p<0.01$, ***$p<0.001$). S5-S8 of untreated control neurons (n=30, 8 DMOTCs) following the application of AP5 and a combination of AP5 and CNQX were compared with another set of untreated control neurons that had not been treated with the antagonists (n=40, 6 DMOTCs) which are indicated as the "Control" bars in D-F. S5-S8 of DHK treated neurons (n=37, 5 DMOTCs) following the application of the antagonists were compared with the responses of DHK treated neurons without the antagonists (n=24, 5 DMOTCs) which are indicated as the "DHK" bars in D-F. Scaling is in arbitrary units (A.U.) for area under the fluorescence signal and peak amplitude of fluorescence signal. Scaling is in seconds (s) for time constant of decay. Error bars indicate S.E.M..

Figure 4-1

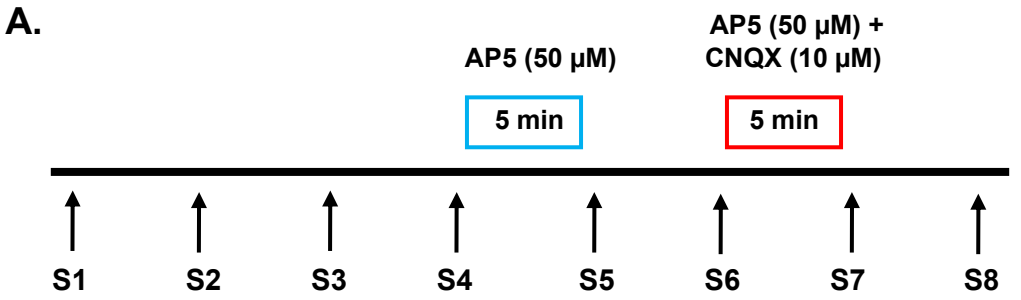
A.
AP5 (50 μM)
5 min
AP5 (50 μM) +
CNQX (10 μM)
5 min
S1
S2
S3
S4
S5
S6
S7
S8

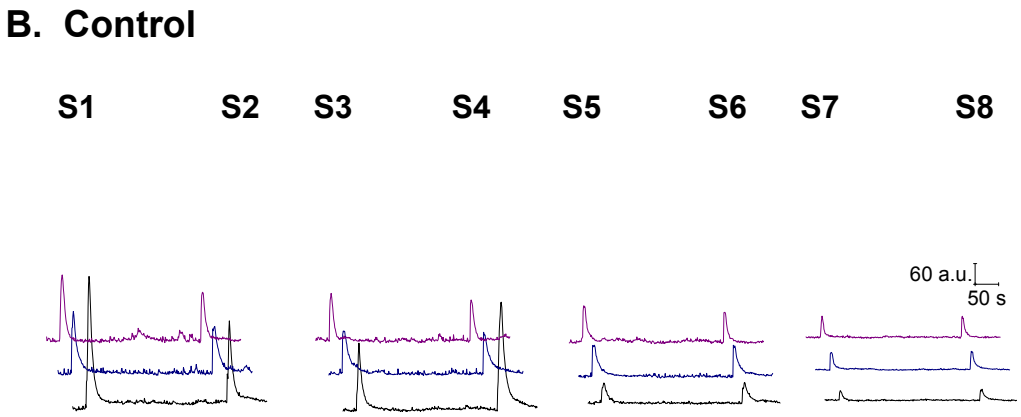
B. Control
S1
S2
S3
S4
S5
S6
S7
S8
60 a.u.
50 s

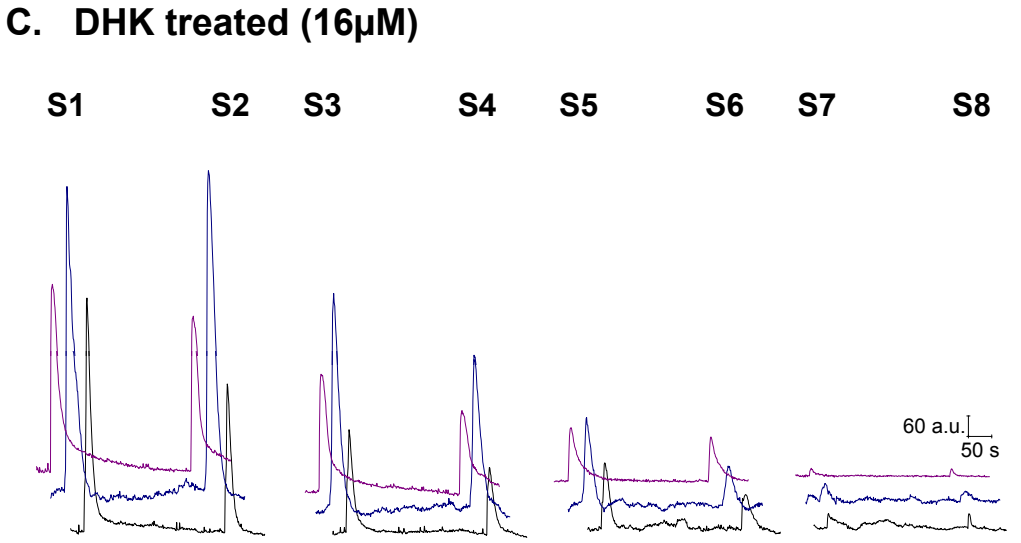
C. DHK treated (16μM)
S1
S2
S3
S4
S5
S6
S7
S8
60 a.u.
50 s

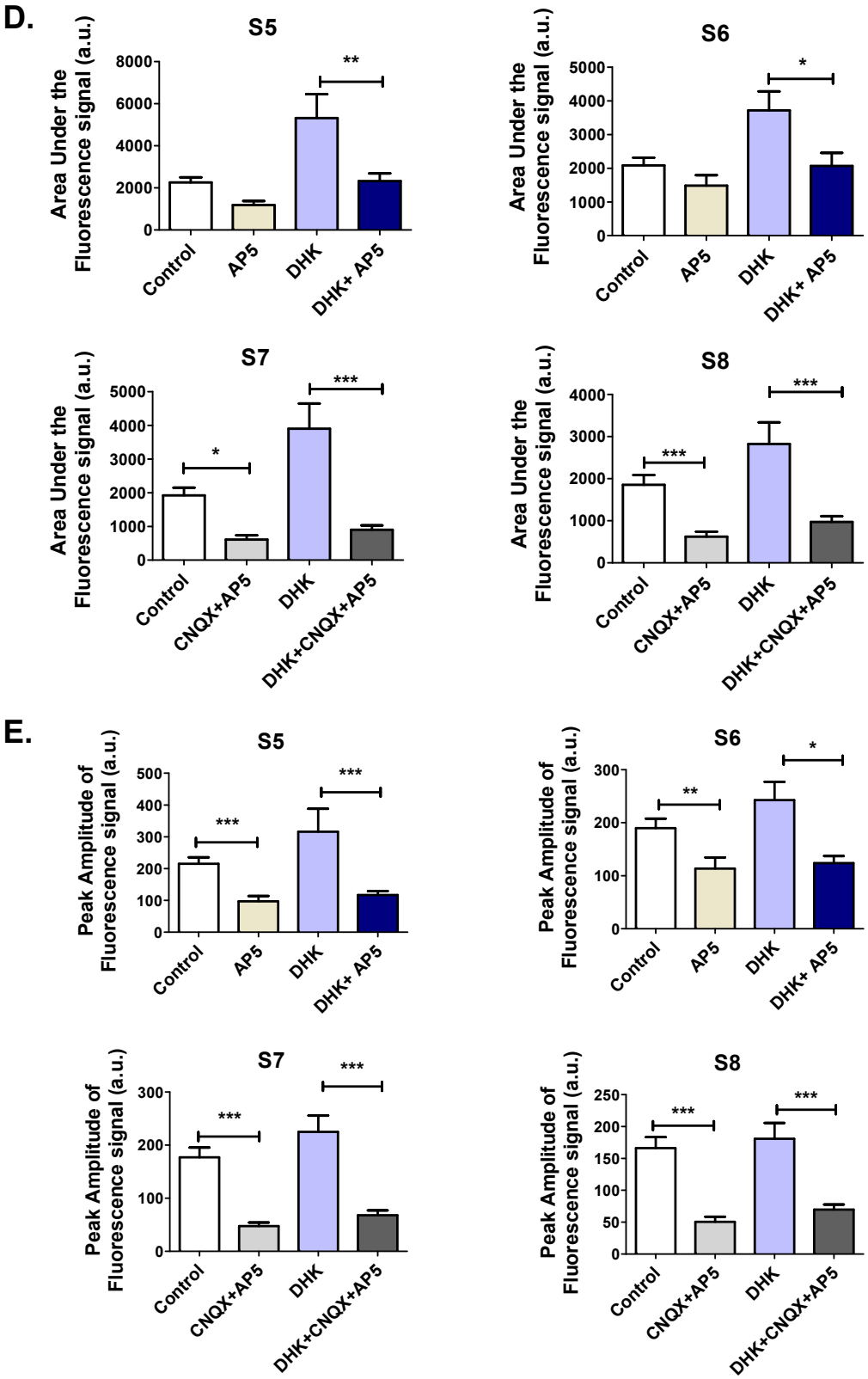
D.
S5
Area Under the Fluorescence signal (a.u.)
8000
6000
4000
2000
0
**
Control
AP5
DHK
DHK+ AP5
S6
Area Under the Fluorescence signal (a.u.)
5000
4000
3000
2000
1000
0
*
Control
AP5
DHK
DHK+ AP5
S7
Area Under the Fluorescence signal (a.u.)
5000
4000
3000
2000
1000
0
*
***
Control
CNQX+AP5
DHK
DHK+CNQX+AP5
S8
Area Under the Fluorescence signal (a.u.)
4000
3000
2000
1000
0
***
***
Control
CNQX+AP5
DHK
DHK+CNQX+AP5
E.
S5
Peak Amplitude of Fluorescence signal (a.u.)
500
400
300
200
100
0
***
***
Control
AP5
DHK
DHK+ AP5
S6
Peak Amplitude of Fluorescence signal (a.u.)
300
200
100
0
**
*
Control
AP5
DHK
DHK+ AP5
S7
Peak Amplitude of Fluorescence signal (a.u.)
300
200
100
0
***
***
Control
CNQX+AP5
DHK
DHK+CNQX+AP5
S8
Peak Amplitude of Fluorescence signal (a.u.)
250
200
150
100
50
0
***
***
Control
CNQX+AP5
DHK
DHK+CNQX+AP5

F.

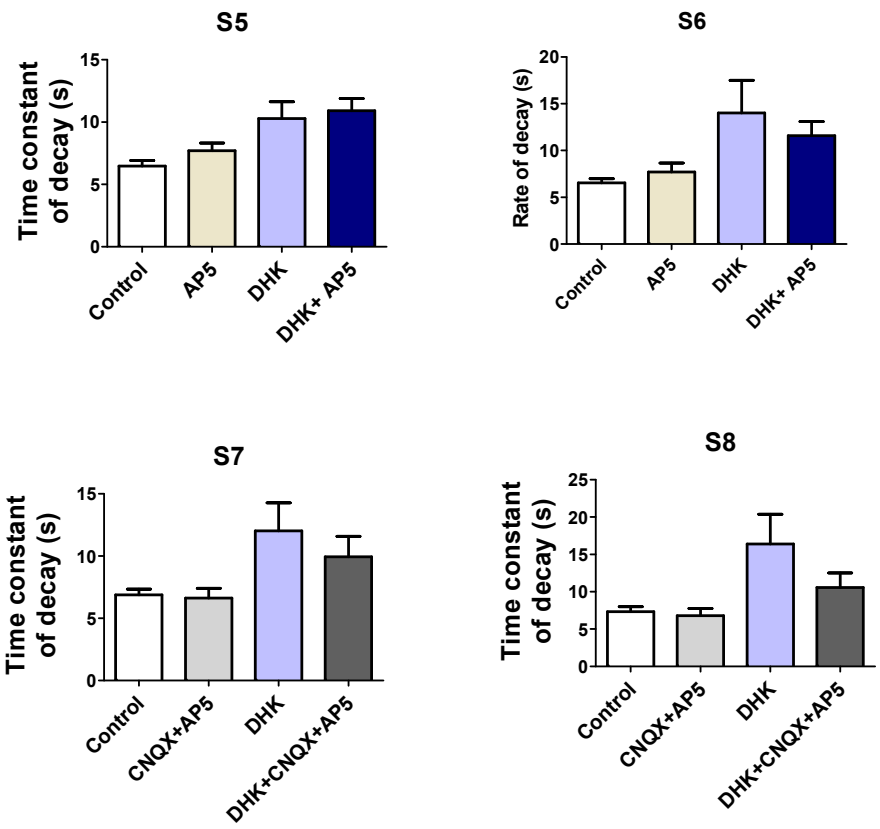
S5
Time constant of decay (s)
15
10
5
0
Control
AP5
DHK
DHK+ AP5
S6
Rate of decay (s)
20
15
10
5
0
Control
AP5
DHK
DHK+ AP5
S7
Time constant of decay (s)
15
10
5
0
Control
CNQX+AP5
DHK
DHK+CNQX+AP5
S8
Time constant of decay (s)
25
20
15
10
5
0
Control
CNQX+AP5
DHK
DHK+CNQX+AP5

Figure 4-2. Effects of DHK on Ca^{2+} permeable AMPA receptors.

A: Electrical stimulation protocol of application of IEM 1460 (50μM). AP5 (50μM) was administered after S1 to block NMDA receptors. IEM 1460 was administered after S4 for 5min and CNQX (10μM) was administered after S6 for 5min. B and C: Staggered fluorescent Ca^{2+} intensity traces from three dorsal horn neurons in the same untreated control (B, n=29, 6 DMOTCs) and DHK treated (C, 5-6d, n=33, 6 DMOTCs) DMOTC slice. D-F: S5 to S8 of area under the fluorescence Ca^{2+} signals (D), peak amplitude (E) and time constant of decay of fluorescence Ca^{2+} signals (F) evoked by electrical stimulations are indicated (unpaired t-test, *p<0.05, **p<0.01 ***p<0.001). S5-S8 of untreated control neurons following the application of IEM 1460 and CNQX were compared with another set of untreated control neurons that had been treated with AP5 (n=33, 3 DMOTCs) which are indicated as the "AP5" bars in D-F. S5-S8 of DHK treated neurons following the application of the antagonists were compared with the responses of DHK treated neurons applied with AP5 (n=34, 4 DMOTCs) which are indicated as the "DHK+AP5" bars in D-F. Scaling is in arbitrary units (A.U.) for area under the fluorescence signal and peak amplitude of fluorescence signal. Scaling is in seconds (s) for time constant of decay. Error bars indicate S.E.M..

Figure 4-2

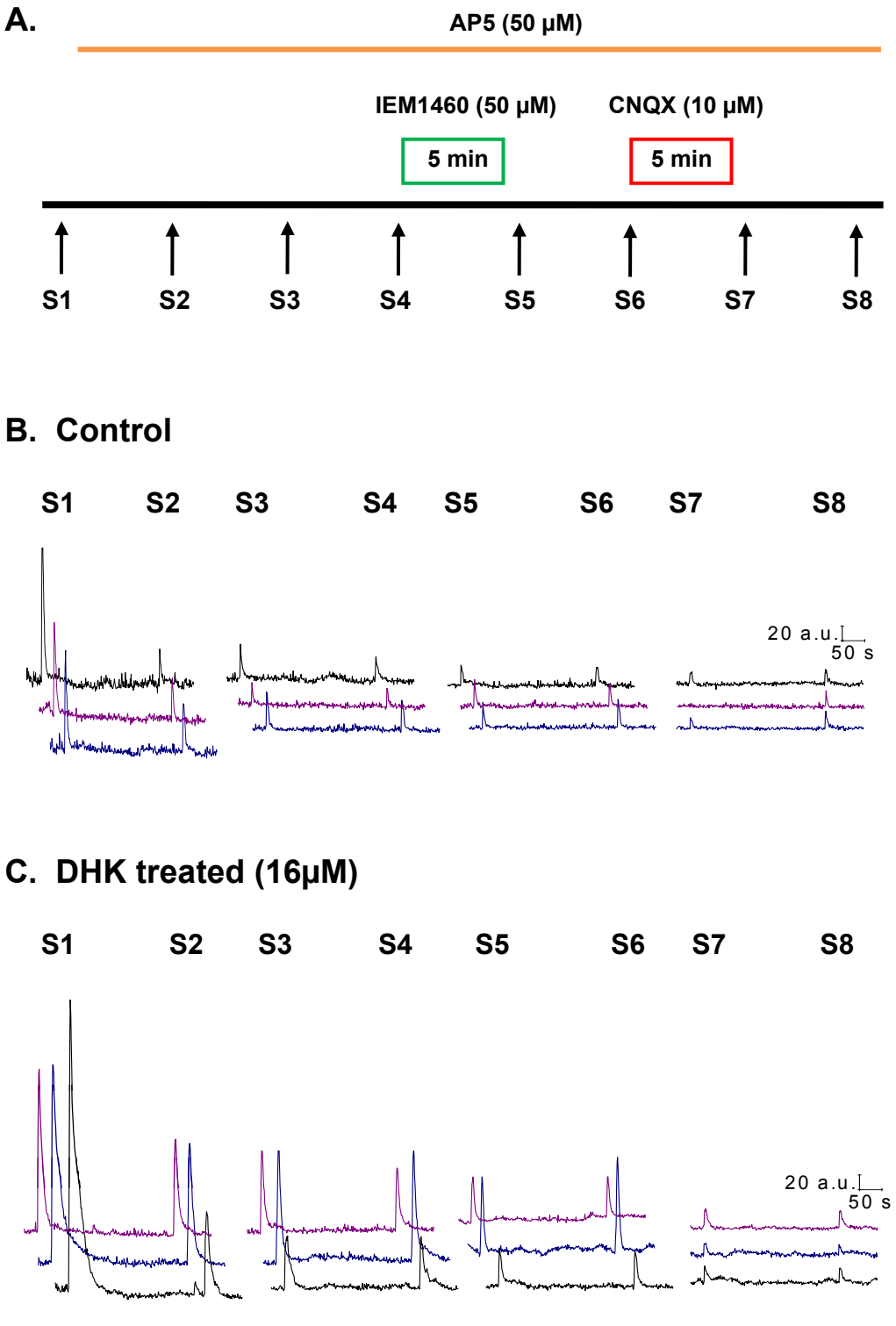
A.
AP5 (50 μM)
IEM1460 (50 μM)
CNQX (10 μM)
5 min
5 min
S1
S2
S3
S4
S5
S6
S7
S8
B. Control
S1
S2
S3
S4
S5
S6
S7
S8
20 a.u.
50 s
C. DHK treated (16μM)
S1
S2
S3
S4
S5
S6
S7
S8
20 a.u.
50 s

D.

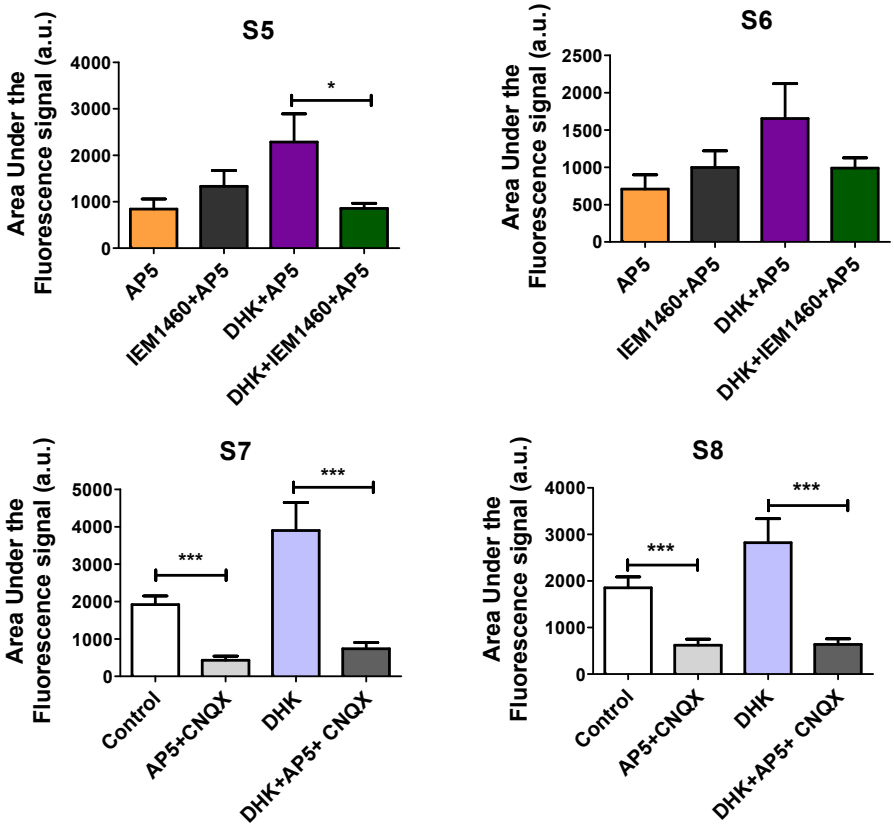
S5
Area Under the Fluorescence signal (a.u.)
4000
3000
2000
1000
0
*
AP5
IEM1460+AP5
DHK+AP5
DHK+IEM1460+AP5
S6
Area Under the Fluorescence signal (a.u.)
2500
2000
1500
1000
500
0
AP5
IEM1460+AP5
DHK+AP5
DHK+IEM1460+AP5
S7
Area Under the Fluorescence signal (a.u.)
5000
4000
3000
2000
1000
0
***
***
Control
AP5+CNQX
DHK
DHK+AP5+ CNQX
S8
Area Under the Fluorescence signal (a.u.)
4000
3000
2000
1000
0
***
***
Control
AP5+CNQX
DHK
DHK+AP5+ CNQX

E.

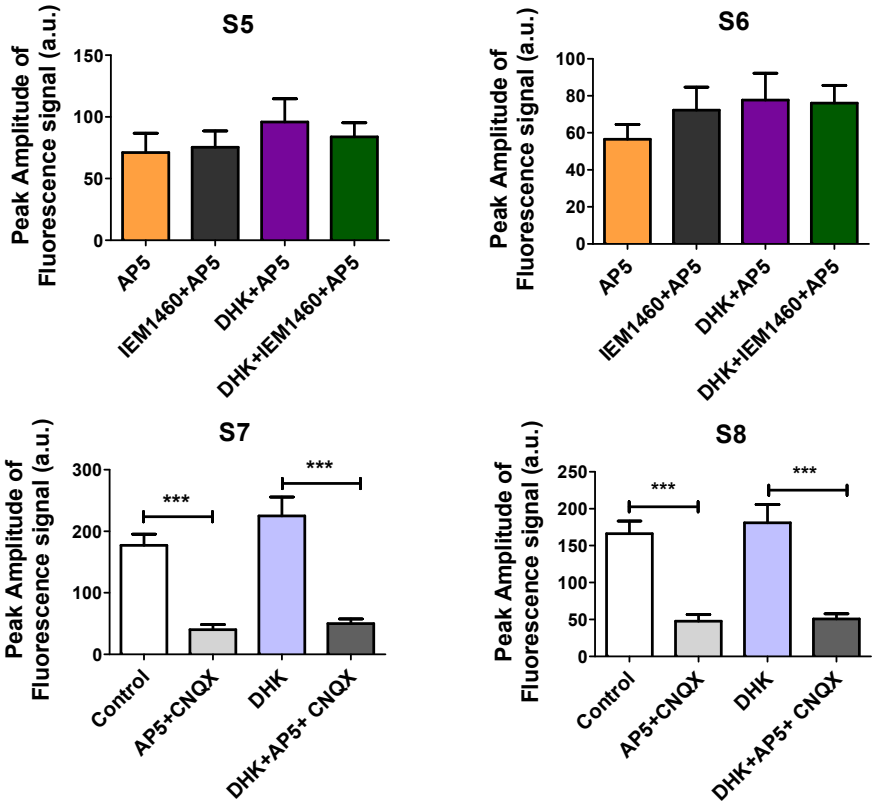
S5
Peak Amplitude of Fluorescence signal (a.u.)
150
100
50
0
AP5
IEM1460+AP5
DHK+AP5
DHK+IEM1460+AP5
S6
Peak Amplitude of Fluorescence signal (a.u.)
100
80
60
40
20
0
AP5
IEM1460+AP5
DHK+AP5
DHK+IEM1460+AP5
S7
Peak Amplitude of Fluorescence signal (a.u.)
300
200
100
0
***
***
Control
AP5+CNQX
DHK
DHK+AP5+ CNQX
S8
Peak Amplitude of Fluorescence signal (a.u.)
250
200
150
100
50
0
***
***
Control
AP5+CNQX
DHK
DHK+AP5+ CNQX

F.

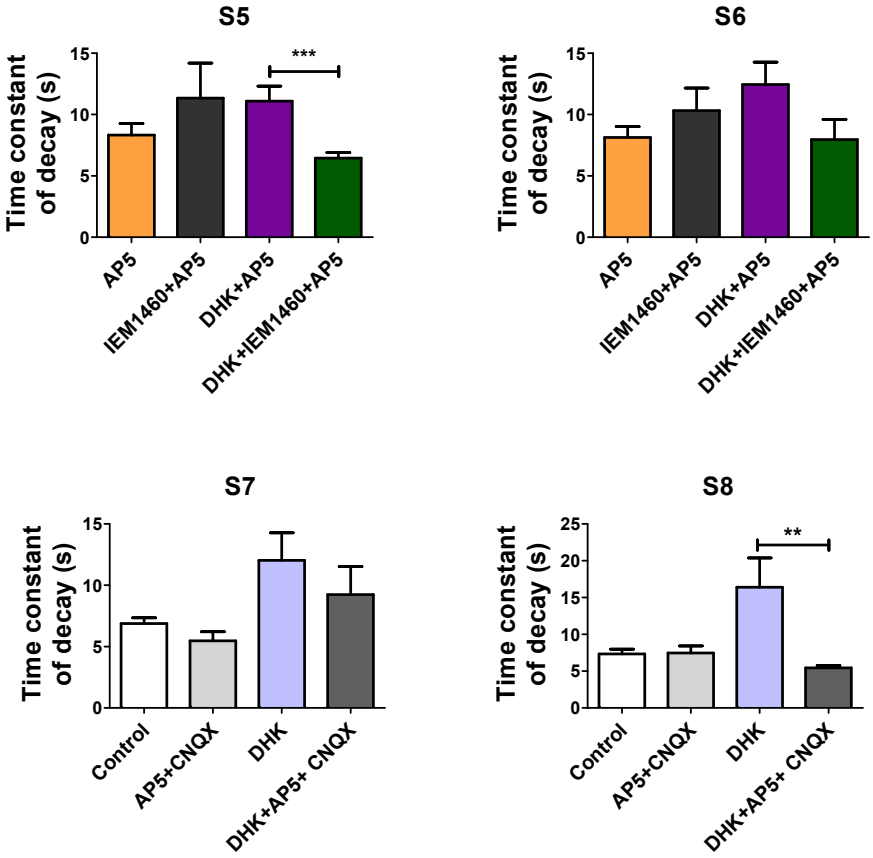
S5
Time constant of decay (s)
15
10
5
0
***
AP5
IEM1460+AP5
DHK+AP5
DHK+IEM1460+AP5
S6
Time constant of decay (s)
15
10
5
0
AP5
IEM1460+AP5
DHK+AP5
DHK+IEM1460+AP5
S7
Time constant of decay (s)
15
10
5
0
Control
AP5+CNQX
DHK
DHK+AP5+ CNQX
S8
Time constant of decay (s)
25
20
15
10
5
0
**
Control
AP5+CNQX
DHK
DHK+AP5+ CNQX

Figure 4-3. LY 367385 application protocol

A: Electrical stimulation protocol of application of LY 367385 (50μM). AP5 (50μM) and CNQX (10μM) were administered after S1 to block NMDA and AMPA/kanaite receptors, respectively. LY 367385 was administered after S4 for 5min. B and C: Staggered fluorescent Ca^{2+} intensity traces from three dorsal horn neurons in the same untreated control (B, n=30, 7 DMOTCs) and DHK treated (C, 5-6d, n=37, 5 DMOTCs) DMOTC slice. The peaks of S1 (DHK treated) are off the scale thus, they are not shown (C).

Figure 4-3

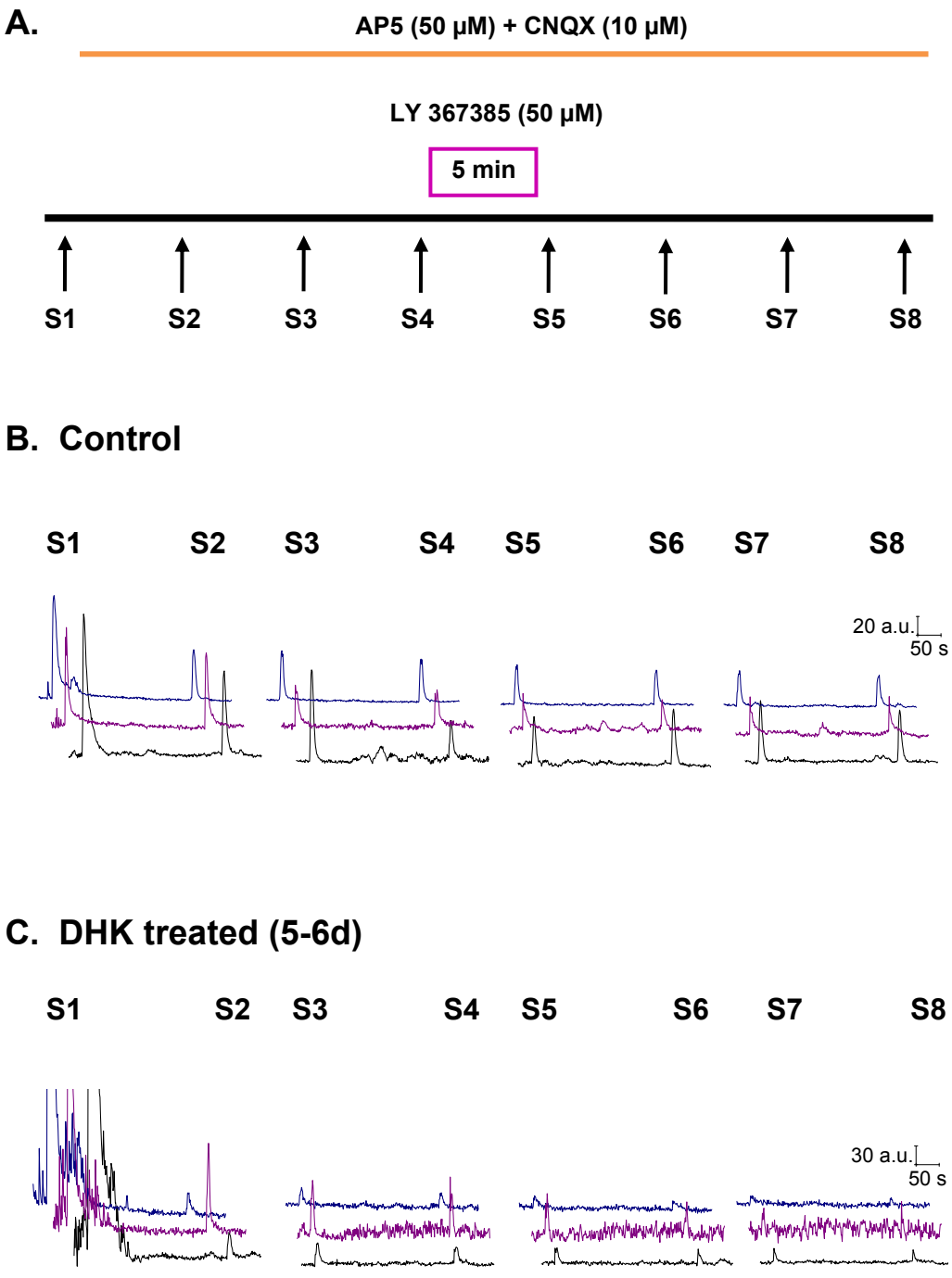
A.
AP5 (50 μM) + CNQX (10 μM)
LY 367385 (50 μM)
5 min
S1
S2
S3
S4
S5
S6
S7
S8
B. Control
S1
S2
S3
S4
S5
S6
S7
S8
20 a.u.
50 s
C. DHK treated (5-6d)
S1
S2
S3
S4
S5
S6
S7
S8
30 a.u.
50 s

Figure 4-4. MPEP application protocol

A: Electrical stimulation protocol of application of MPEP (10μM). AP5 (50μM) and CNQX (10μM) were administered after S1 to block NMDA and AMPA/kanaite receptors, respectively. MPEP was administered after S4 for 5min. B and C: Staggered fluorescent Ca^{2+} intensity traces from three dorsal horn neurons in the same untreated control (B, n=37, 5 DMOTCs) and DHK treated (C, 5-6d, n=33, 3 DMOTCs) DMOTC slice. The peaks of S1 are off the scale thus, they are not shown (B and C).

Figure 4-4

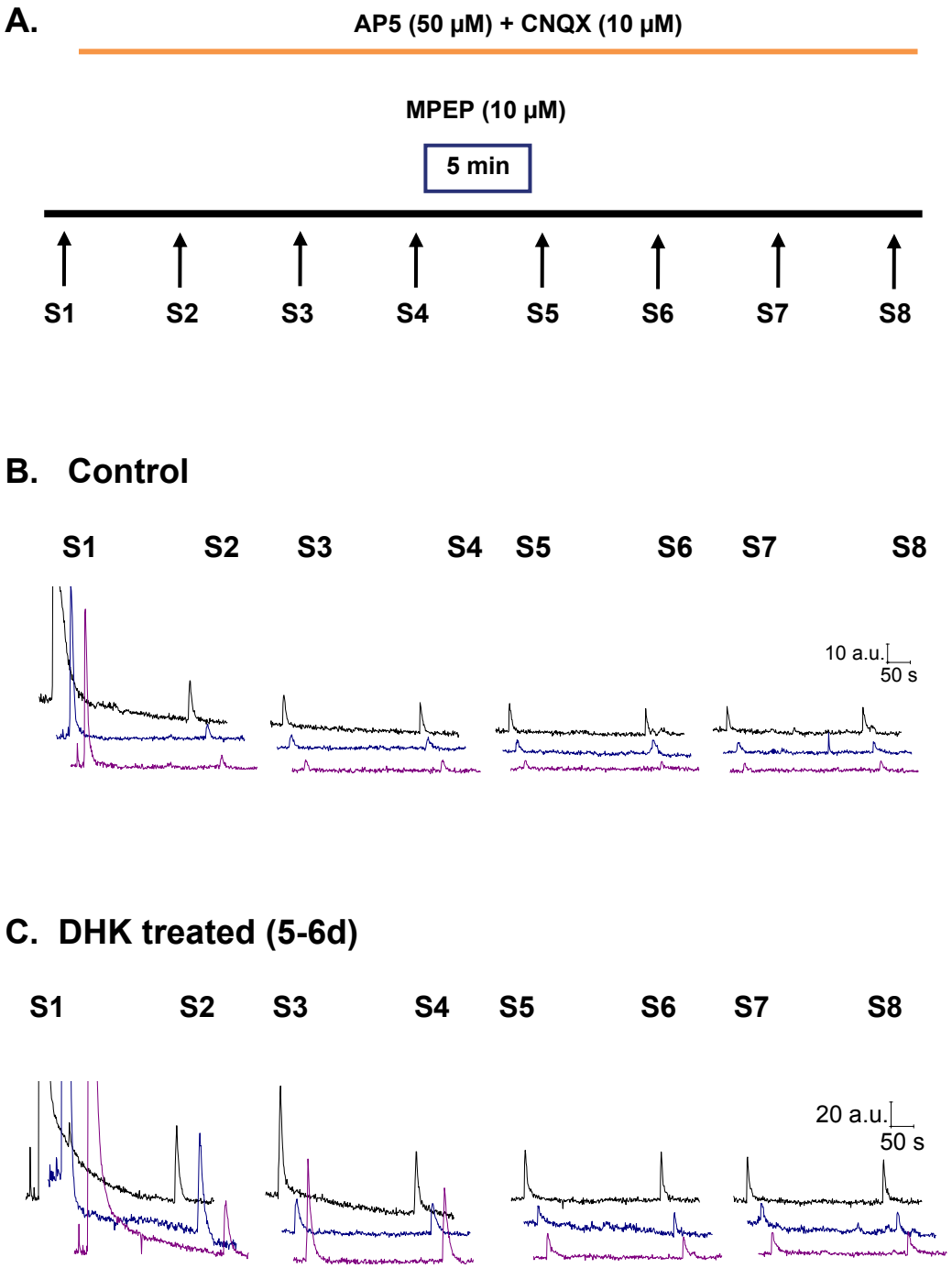
A.
AP5 (50 μM) + CNQX (10 μM)
MPEP (10 μM)
5 min
S1
S2
S3
S4
S5
S6
S7
S8
B. Control
S1
S2
S3
S4
S5
S6
S7
S8
10 a.u.
50 s
C. DHK treated (5-6d)
S1
S2
S3
S4
S5
S6
S7
S8
20 a.u.
50 s

Figure 4-5. Effects of DHK on $mGluR_1$ and $mGluR_5$

A-C: S5 area under the Ca^{2+} signal (A), peak amplitude (B) and time constant of decay of fluorescence Ca^{2+} signals (C) evoked by electrical stimulations following application of LY 367385 (50μM) and MPEP (10μM) are indicated (ANOVA, *p<0.05, **p<0.01, ***p<0.001). All of the control and DHK treated S5 responses were normalized to control (n=30, 7 DMOTCs) and DHK treated (n=37, 5 DMOTCs) CNQX+AP5 responses, respectively. Error bars indicate S.E.M..

Figure 4-5

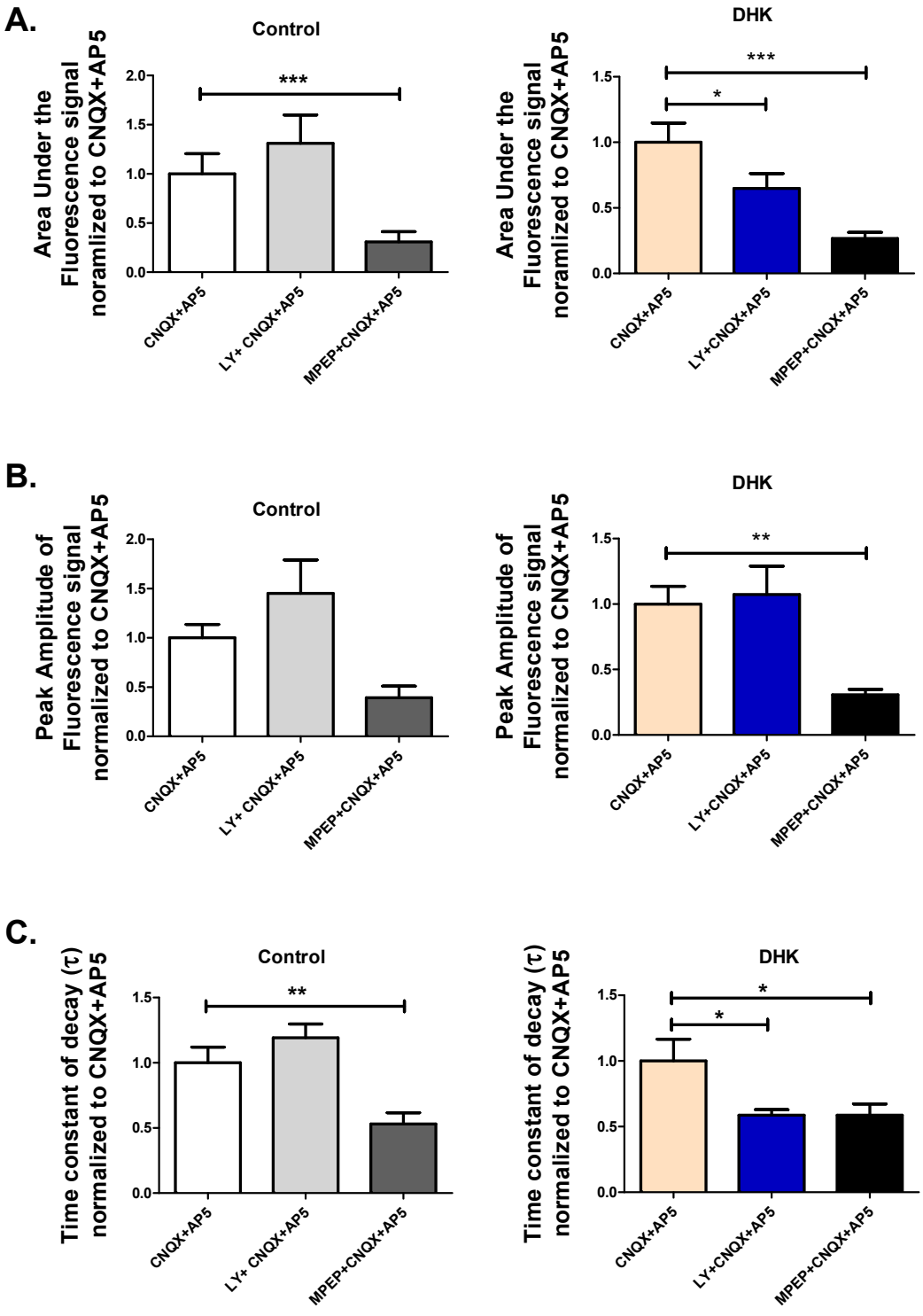
A.
Control
Area Under the Fluorescence signal noramlized to CNQX+AP5
***
2.0
1.5
1.0
0.5
0.0
CNQX+AP5
LY+ CNQX+AP5
MPEP+CNQX+AP5
DHK
Area Under the Fluorescence signal noramlized to CNQX+AP5
***
*
1.5
1.0
0.5
0.0
CNQX+AP5
LY+CNQX+AP5
MPEP+CNQX+AP5
B.
Control
Peak Amplitude of Fluorescence signal normalized to CNQX+AP5
2.0
1.5
1.0
0.5
0.0
CNQX+AP5
LY+ CNQX+AP5
MPEP+CNQX+AP5
DHK
Peak Amplitude of Fluorescence signal normalized to CNQX+AP5
**
1.5
1.0
0.5
0.0
CNQX+AP5
LY+CNQX+AP5
MPEP+CNQX+AP5
C.
Control
Time constant of decay (τ) normalized to CNQX+AP5
**
1.5
1.0
0.5
0.0
CNQX+AP5
LY+ CNQX+AP5
MPEP+CNQX+AP5
DHK
Time constant of decay (τ) normalized to CNQX+AP5
*
*
1.5
1.0
0.5
0.0
CNQX+AP5
LY+CNQX+AP5
MPEP+CNQX+AP5

Figure 4-6. Effects of DHK and BDNF on ionotropic and metabotropic glutamate receptors

A: Ionotropic and metabotropic receptor agonist application protocol is illustrated to examine agonist-evoked Ca^{2+} signals. A series of 35mM K^{+}, AMPA (10μM), NMDA (50μM), DHPG (50μM) and DHPG (50μM) and MPEP (10μM) were applied to untreated control (n=38, 4 DMOTCs), DHK (n=32, 4 DMOTCs) and BDNF (n=37, 5 DMOTCs) treated dorsal horn neurons. B-D: Sample fluorescent Ca^{2+} intensity traces from three dorsal horn neurons in the same untreated control (B), DHK (C) and BDNF treated (D) DMOTC slice. Each agonist was washed out for 15min prior to the subsequent agonist administration. E: Comparisons of area under the Ca^{2+} signal responses of control, DHK and BDNF treated neurons following the application of 35mM K^{+}, AMPA and NMDA (ANOVA, *$p<0.05$, **$p<0.01$). F: Comparisons of peak amplitude of Ca^{2+} signal responses of control, DHK and BDNF treated neurons following the application of 35mM K^{+}, AMPA and NMDA (ANOVA, *$p<0.05$, **$p<0.01$). G. Comparisons of time constant of decay of Ca^{2+} signal responses of control, DHK and BDNF treated neurons following the application of 35mM K^{+}, AMPA and NMDA (ANOVA, $p>0.05$). Scaling is in arbitrary units (A.U.) for area under the fluorescence signal and peak amplitude of fluorescence signal. Scaling is in seconds (s) for time constant of decay. Error bars indicate S.E.M..

Figure 4-6

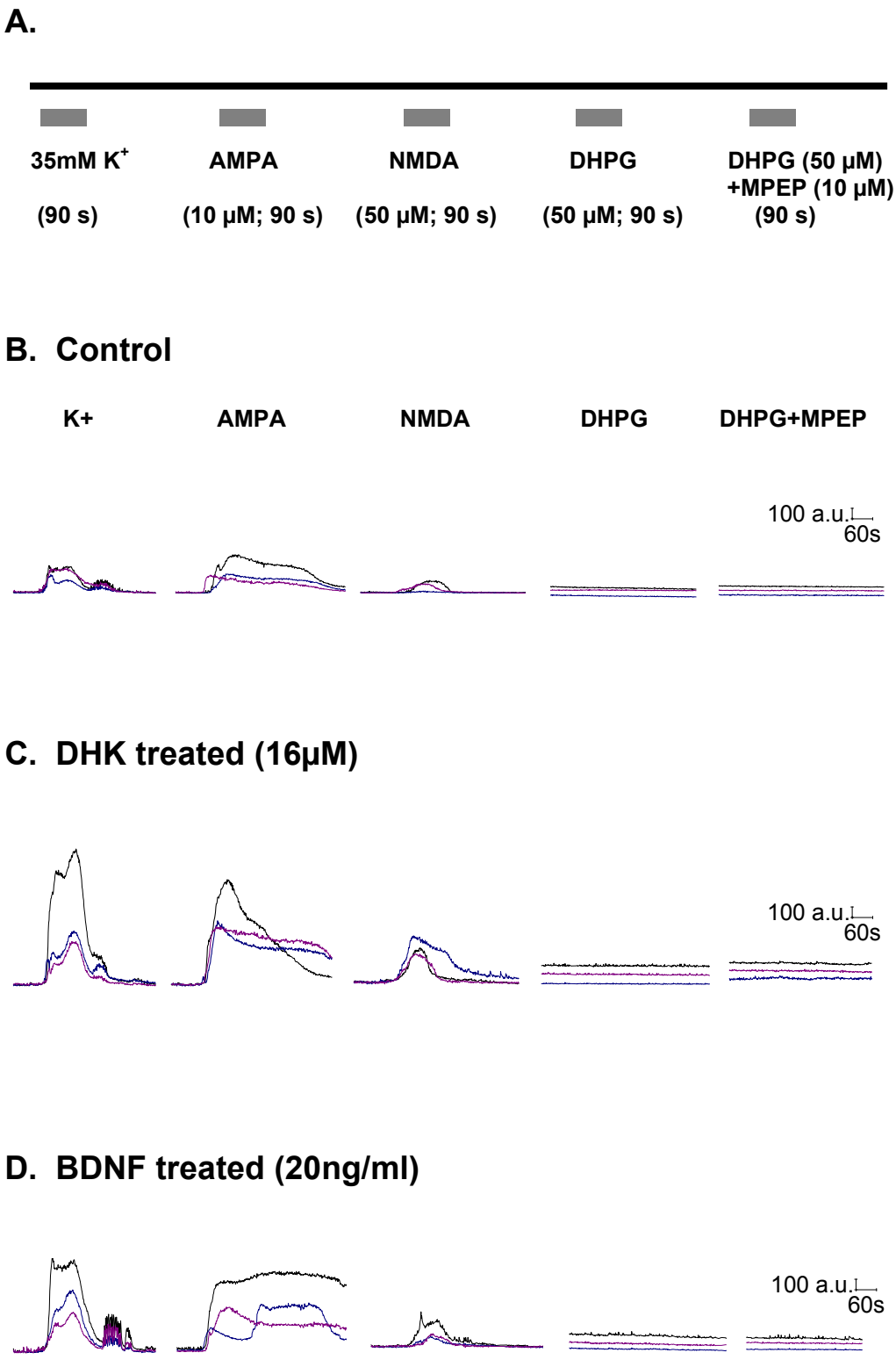
A.
35mM K+
(90 s)
AMPA
(10 µM; 90 s)
NMDA
(50 µM; 90 s)
DHPG
(50 µM; 90 s)
DHPG (50 µM)
+MPEP (10 µM)
(90 s)
B. Control
K+
AMPA
NMDA
DHPG
DHPG+MPEP
100 a.u.
60s
C. DHK treated (16µM)
100 a.u.
60s
D. BDNF treated (20ng/ml)
100 a.u.
60s

E. Area under the fluorescence Ca^{2+} signal

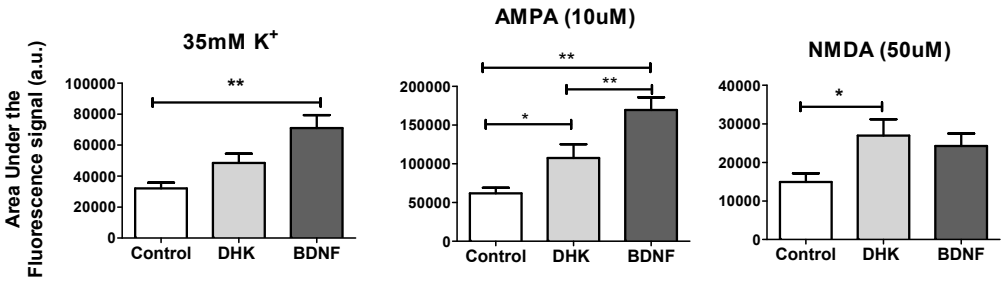

F. Peak amplitude of fluorescence Ca^{2+} signal

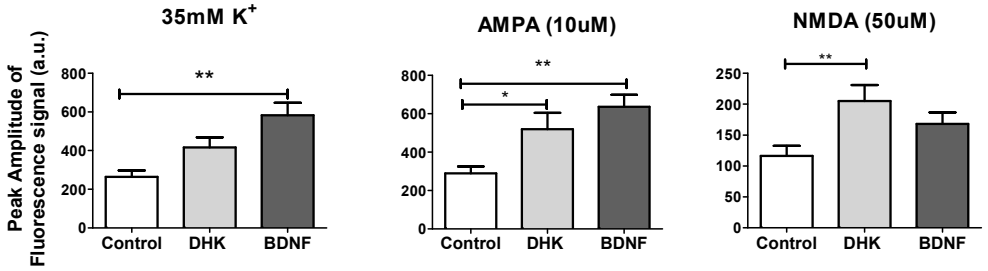

G. Time constant of decay

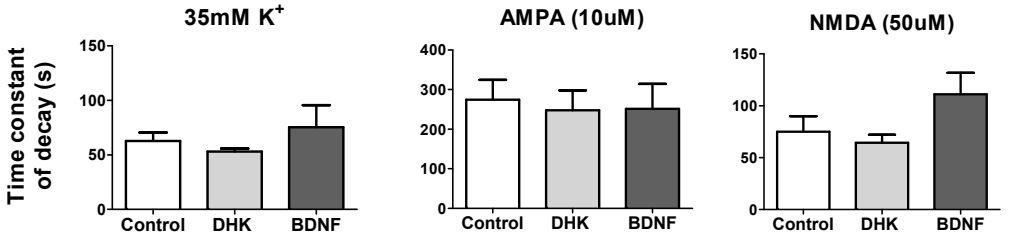

4.5 References

Fagni L, Ango F, Perroy J, & Bockaert J (2004). Identification and functional roles of metabotropic glutamate receptor-interacting proteins. *Semin Cell Dev Biol* **15**, 289-298.

Gasparini F, Lingenhohl K, Stoehr N, Flor PJ, Heinrich M, Vranesic I, Biollaz M, Allgeier H, Heckendorn R, Urwyler S, Varney MA, Johnson EC, Hess SD, Rao SP, Sacaan AI, Santori EM, Velicelebi G, & Kuhn R (1999). 2-Methyl-6-(phenylethynyl)-pyridine (MPEP), a potent, selective and systemically active mGlu5 receptor antagonist. *Neuropharmacology* **38**, 1493-1503.

Salt TE, Binns KE, Turner JP, Gasparini F, & Kuhn R (1999). Antagonism of the mGlu5 agonist 2-chloro-5-hydroxyphenylglycine by the novel selective mGlu5 antagonist 6-methyl-2-(phenylethynyl)-pyridine (MPEP) in the thalamus. *Br J Pharmacol* **127**, 1057-1059.

Salt TE & Turner JP (1998). Reduction of sensory and metabotropic glutamate receptor responses in the thalamus by the novel metabotropic glutamate receptor-1-selective antagonist S-2-methyl-4-carboxy-phenylglycine. *Neuroscience* **85**, 655-658.

Santos SF, Luz LL, Szucs P, Lima D, Derkach VA, & Safronov BV (2009). Transmission efficacy and plasticity in glutamatergic synapses formed by

excitatory interneurons of the substantia gelatinosa in the rat spinal cord. *PLoS One* **4**, e8047.

Schoepp DD, Goldsworthy J, Johnson BG, Salhoff CR, & Baker SR (1994). 3,5-dihydroxyphenylglycine is a highly selective agonist for phosphoinositide-linked metabotropic glutamate receptors in the rat hippocampus. *J Neurochem* **63**, 769-772.

CHAPTER 5 GENERAL DISCUSSION AND CONCLUSIONS

5.1 Summary of Results

The principal findings of this thesis project were that long-term inhibition of EAAT2 results in significant changes in the Ca^{2+} signals and activity of glutamate receptors in spinal dorsal horn neurons. No significant changes were observed following acute application of DHK via 35mM K^+ challenge method although the electrical stimulation method produced a significant increase in the time constant of decay of Ca^{2+} signal of dorsal horn neurons. In contrast, chronic treatment with DHK produced significant increase in area under the Ca^{2+} signal and time constant of decay of Ca^{2+} signal of dorsal horn neurons.

NMDA receptors appeared to have more prominent effects in terms of the area under the Ca^{2+} signal and AMPA receptors appeared to have greater effects on the area under the Ca^{2+} signal and time constant of decay of Ca^{2+} signal in DHK treated neurons. Although no significant changes were observed in Ca^{2+} signals mediated by $mGluR_5$, significant changes in the area under the Ca^{2+} signal and time constant of decay of Ca^{2+} signal mediated by $mGluR_1$ were found in DHK treated neurons compared to the control neurons. Ca^{2+} signals of DHK and BDNF treated neurons were significantly increased in response to application of AMPA. However, only chronic DHK treatment significantly increased Ca^{2+} signals following application of NMDA, therefore suggesting that the effects of chronic DHK and BDNF treatments may not the same. Moreover, $mGluR_1$ and $mGluR_5$ did not appear to have a significant role in both DHK and BDNF treated neurons as indicated by the lack of responses following administration of $mGluR_1$ and $mGluR_5$ agonists. Overall, these results suggest

that there may be changes in the pharmacological properties of $mGluR_1$, NMDA and AMPA receptors in the dorsal horn neurons following long-term inhibition of EAAT2.

5.2 Long-term treatment with DHK increases excitability of dorsal horn neurons

Following nerve injury, chemical mediators are released including BDNF (Woolf, 1991; Latremoliere and Woolf, 2009). Because the concentration of BDNF is elevated for several days subsequent to the injury (Cho *et al.*1998; Dougherty *et al.* 2000), studies have demonstrated that long-term exposure of BDNF to spinal dorsal horn neurons produces similar effects seen with CCI and significantly increases the area under the Ca^{2+} signal and peak amplitude of Ca^{2+} signal of dorsal horn neurons (Lu et al., 2007, Lu et al., 2009). The current project indicated that acute (5 min) application of DHK did not appear to affect the Ca^{2+} signals of dorsal horn neurons prominently. Thus acute administration of DHK likely does not correspond to the effects seen following a nerve injury. In contrast, long-term treatment with DHK in this project was carried out to correlate the time-course of the increased level of BDNF due to nerve injury and significantly modulated the excitability of the dorsal horn neurons similar to the results obtained by chronic treatment with BDNF (Lu et al., 2007; Lu et al., 2009).

The results from the present study indicated that although area and duration of the neuronal excitability were increased, the DHK treatment failed to increase peak amplitude of Ca^{2+} signal to a similar extent (Figure 3-3E,F and G).

One possibility for the lack of change in amplitude may be due to activation of presynaptic autoreceptors such as group II and III mGluRs. Upon activation, the autoreceptors suppress further release of glutamate from presynaptic terminals (Nester et al., 2001). Weng et al. (2007) have found that amplitudes of EPSC of *substantia gelatinosa* neurons were decreased with strong synaptic input after perfusion with DHK and suggested the cause as excess glutamate spilling over to presynaptic terminals, resulting in an activation of autoreceptors. Moreover, in hippocampal and spinal cord neurons, inhibition of glutamate transporters decreased EPSC amplitudes and the reduction was partially reversed after introducing mGluR II and III antagonists (Maki et al., 1994; Bird et al., 2001).

Another possibility is desensitization of postsynaptic AMPA receptors. Currents mediated by AMPA receptors have rapid onset and decay and the receptors desensitize rapidly (Nestler et al., 2001; Edmonds et al., 1995). Weng et al. (2007) have reported that administration of glutamate transporter blocker in presence of cyclothiazide (CTZ), which relieves AMPA receptors from desensitization, resulted in reversal of reduction in the amplitude of EPSP. Therefore, peak amplitude of Ca^{2+} signal of dorsal horn neurons by impairment of EAAT2 in this study may have been influenced by activation of presynaptic autoreceptors and desensitization of AMPA receptors.

5.3 Activity of NMDA receptors increases following long-term exposure to DHK

In this study, AP5 decreased area under the Ca^{2+} signal and peak amplitude of Ca^{2+} signal to a greater extent in DHK treated neurons (Figure 4-1D and E). Also, application of NMDA increased area under the Ca^{2+} signal and peak amplitude of Ca^{2+} signal of DHK treated neurons thereby indicating that long-term exposure to DHK has effects on NMDA receptors (Figure 4-6E and F). The involvement of NMDA receptors in chronic pain including neuropathic pain is well known (Bleakman et al., 2006; Nie and Weng, 2009). Inhibition of glutamate transporters contributes to increased activity of NMDA receptors as blockade of glutamate transporters in the dorsal horn increases rate of spontaneous EPSCs (sEPSCs) by activation of NMDA receptors (Thomson et al., 2006). Nie and Weng (2009) have reported that impaired glutamate transporters caused an increased amplitude and duration of NMDA EPSCs evoked by primary afferent inputs. Therefore, these support and are consistent with the results from this study, indicating that chronic exposure to DHK increases activity of NMDA receptors. It was observed that blockade of glutamate transporters increased open probability of NMDA receptors and led to glutamate spillover resulting in activation of synapses that are outside of the active synapses (Nie and Weng, 2009). Also, impairment of glutamate uptake leads to heightened activation of NMDA receptors and limiting glutamate spillover reduces abnormal activation of NMDA receptors in neuropathic rats (Nie and Weng, 2010). Moreover, it was reported that AP5 prevented pertussis

toxin (PTX)-induced (a neuropathic pain model) glutamate transporter downregulation (Wong et al., 2009). Thus, these suggest that actions of NMDA receptors and glutamate transporters may be tightly linked in neuropathic pain and the NMDA receptors likely have a prominent role in the development of central sensitization following downregulation of EAAT2. The present results indicated that the area under the Ca^{2+} signal and peak amplitude of the Ca^{2+} signal decreased following application of AP5 in DHK treated neurons but no changes in the rate of decay were found. This suggests that the rate of decay of Ca^{2+} signal in DHK treated neurons may not be affected by NMDA receptors to a great extent.

5.4 Activity of AMPA receptors increases following long-term exposure to DHK

The observation that the Ca^{2+}-permeable AMPA receptor antagonist, IEM1460 decreases area under the Ca^{2+} signal (Figure 4-2D) and time constant of decay of Ca^{2+} signal (Figure 4-2F) in DHK treated neurons indicated that chronic exposure to DHK has effects on Ca^{2+}-permeable AMPA receptors. The increase in the area under the Ca^{2+} signal and peak amplitude of Ca^{2+} signal following the application of AMPA in this study also contributed to such effects on AMPA receptors. In a study conducted by Weng et al. (2007), it was reported that inhibition of EAAT2 resulted in an increase in duration and area of primary afferent-evoked EPSCs and amplitude and duration of miniature EPSCs (mEPSCs). Also, studies have suggested that glutamate spillover due to

downregulation of glutamate transporters likely activates AMPA receptors located in the nearby synapses (Takayasu et al., 2004; Weng et al., 2007). These reports support the results obtained from this study as the changes in the area and rate of decay of Ca^{2+} signal may represent activation of nearby AMPA receptors outside the active synapses in addition to the subsynaptic AMPA receptors. Moreover, this study indicates that activation of AMPA receptors appeared to be affected as much as the NMDA receptors following inhibition of EAAT2.

In this study, no changes in the peak amplitude of Ca^{2+} signal were found in both control and DHK treated neurons following the application of IEM1460 (Figure 4-2E). As mentioned previously, application of glutamate transporter blocker in presence of CTZ led to reversal of reduction in the amplitude of EPSP following application of glutamate transporter blocker (Weng et al., 2007). Thus desensitization of postsynaptic AMPA receptors may account for the lack of change in peak amplitude observed from this study.

Furthermore, it was found that BDNF prominently increased the area under the Ca^{2+} signal and the peak amplitude of Ca^{2+} signal following administration of AMPA but not NMDA in this study (Figure 4-6E and F). This suggests that increased release of BDNF which can promote central sensitization may enhance the activation of glutamate receptors via mechanisms different from the mechanisms that follow inhibition of EAAT2. Thus impairment of EAAT2 may increase the activation of NMDA receptors more than BDNF to elicit central sensitization.

5.5 MGluR$_1$ is more affected by inhibition of EAAT2 than mGluR$_5$

In the present study, decreases in the area under the Ca^{2+} signal (Figure 4-5A) and an increase in the rate of decay of Ca^{2+} signal (Figure 4-5C) in DHK treated dorsal horn neurons following administration of mGluR$_1$ antagonist, LY 367385 were found. This is consistent with findings in cerebellar Purkinje cells where blockade of glutamate uptake resulted in an increase in amplitude and duration of mGluR$_1$-mediated EPSC (Reichelt and Knopfel, 2002). Also, Galik et al. (2008) reported that in dorsal horn neurons, mGluR$_1$ antagonist decreased amplitude and time constant of decay of slow EPSC elicited by stimulation of primary afferent fibres. These reports suggest that in addition to the ionotropic receptors, mGluR$_1$ also mediates the increase in excitability of dorsal horn neurons following long-term exposure to DHK. The two studies mentioned previously (Galik et al., 2008; Reichelt and Knopfel, 2002) have found that the amplitudes of slow EPSCs mediated by mGluR$_1$ were significantly affected by inhibition of glutamate transporters. However, the peak amplitude of Ca^{2+} signal of both control and DHK treated neurons was not affected by the mGluR$_1$ antagonist in this study. As previously discussed, such discrepancy may be due to activation of presynaptic autoreceptors. It is possible that long-term exposure to DHK may have resulted in much greater increase in extracellular Ca^{2+} level than acute application of the glutamate transporter blocker as demonstrated in the other two studies (Galik et al., 2008; Reichelt and Knopfel, 2002), thereby increasing the chance activating the autoreceptors.

In this study, the degree of activity of $mGluR_5$ appeared to be similar in both control and DHK treated neurons. This is consistent with a finding that intrathecal administration of $mGluR_1$ antagonist resulted in greater antinociceptive effects than $mGluR_5$ antagonist in formalin-induced nociceptive behaviour (Karim et al., 2001). Furthermore, knockdown of spinal $mGluR_1$ with intrathecal infusion of antisense oligonucleotides reduced mechanical allodynia, cold and heat hyperalgesia in neuropathic rats (Fundytus,et al., 2001). These studies indicate that $mGluR_1$ may have a greater role in nociceptive processing than $mGluR_5$. Thus these reports suggest that long-term inhibition of EAAT2 may increase the activity of $mGluR_1$ more than $mGluR_5$.

No responses in control, DHK and BDNF treated neurons were observed following administration of $mGluR_1$ and $mGluR_5$ agonists in this study. This may be due to the nature of mGluRs. Unlike ionotropic receptors which allow ions such as Ca^{2+} to pass through, mGluRs are G-protein coupled receptors that couple signal transduction cascades (Nestler et al., 2001). Group I mGluRs couple via G_q/G_{11} protein to PLC and result in release of Ca^{2+} from intracellular stores and generate slow postsynaptic currents evoked by trains of stimuli (Fagni et al., 2004; Bhave et al., 2001, Nestler et al., 2001; Galik et al., 2008). Therefore, it is likely that acute application of mGluR agonist may not have been a strong stimulus to activate $mGluR_1$ and $mGluR_5$ in this project.

5.6 EAAT2 and synaptic plasticity

LTP is defined as long-lasting increase in synaptic strength and its mechanisms are thought to underlie learning and memory (Nestler et al., 2001). LTP is a type of synaptic plasticity and can also be occur in the spinal cord (Neves et al., 2008; Ikeda et al., 2009). Central sensitization, which has a major role in development of neuropathic pain, is considered as another type of synaptic plasticity and involves activity-dependent increase in excitability of dorsal horn neurons (Ji et al., 2003). It has been suggested that mechanisms of central sensitization are analogous to mechanisms involved in LTP (Woolf and Salter 2000; Ji et al., 2003). For example, NMDA receptors have a crucial role in development of LTP and central sensitization (Ji et al., 2003) and phosphorylation of NMDA receptor subunit 2B occurred in both LTP and dorsal horn neurons in a chronic pain model (Rosenblum et al., 1996; Guo et al., 2002). Also, NMDA receptors induced trafficking and insertion of AMPA receptors to postsynaptic membrane in both LTP and dorsal horn neurons (Luscher et al., 2000; Ji et al., 2003; Li et al., 1999). Therefore, it is possible that long-term impairment of EAAT2 enhances trafficking and insertion of AMPA receptors. The results obtained from this study indicated that in DHK treated neurons, both AMPA and NMDA receptors were highly involved. Thus the increased activity of NMDA receptors in DHK treated neurons may induce the AMPA receptor trafficking and insertion. Furthermore, the increased area under the Ca^{2+} signal and peak amplitude of Ca^{2+} signal following application of AMPA in DHK treated neurons may represent the inserted AMPA receptors.

5.7 Limitations

There are some limitations involved in this study. First, glutamate receptors may be upregulated to a different extent in different neuron types in the dorsal horn. Five types of neurons in lamina II have been classified (Grudt and Perl, 2002). It is possible that changes in specific glutamate receptors following long-term treatment with DHK observed in this study occur more in certain types of neurons. If so, then some of the responses following the administration of receptor antagonist or agonist might have been underestimated because types of neurons cannot be identified by Ca^{2+} imaging technique. Also, the results from this study do not inform whether there were changes in the expression level of glutamate receptors. For instance, if chronic inhibition of EAAT2 leads to insertion of new AMPA receptors as observed in LTP, AMPA receptors will be upregulated in the dorsal horn neurons. Therefore, a different technique should be used to determine whether the expression of specific types of glutamate receptors is increased to support the findings from this study.

Furthermore, there were also a few limitations regarding the electrical stimulation protocol. As previously mentioned in Chapter 2, the amplitudes of S1-S4 appeared to be more variable than the amplitudes of S5-S8. However, only a series of 4 stimulations (S1-S4) were given in acute (5 min) DHK experiments. This indicates that the S3 and S4 responses following the acute DHK application may not represent the actual acute effect of DHK. Thus, the best approach to check whether the results obtained are valid would be to run the

same experiments but with a series of 8 stimulations. In these experiments, the acute DHK application should be done after S6.

5.8 Future Directions

The present study involved a long-term inhibition of EAAT2 using Ca^{2+} imaging technique. The Ca^{2+} imaging technique has enabled to observe the overall excitability of dorsal horn neurons. However, this technique does not distinguish between different types of neurons. Therefore, whole-cell recordings should be used to determine which types of dorsal horn neurons are involved the most and the least in changes in glutamate receptors following chronic inhibition of EAAT2. Also, Western blot could be used to determine whether expression level of glutamate receptors, AMPA receptors in particular, is increased following inhibition of EAAT2. Antibodies to subunits of the glutamate receptors should be used in the Western blotting process to compare the expression level of the receptors in dorsal horn neuron in control and exposed to DHK (5-6d).

Furthermore, due to the involvement of EAAT2 in neuropathic pain conditions, examining the excitability of dorsal horn neurons with administration of glutamate transporter activator, (*R*)-(−)-5-methyl-1-nicotinoyl-2-pyrazoline (MS-153), could be another approach to study EAAT2. This could be done by observing changes in the excitability of dorsal horn neurons following chronic treatment with MS-153 in BDNF treated (5-6d) DMOTCs using the Ca^{2+} imaging technique.

5.9 Conclusion

This study shows that chronic inhibition of EAAT2 produces a series of enduring changes in the spinal dorsal horn that appear consistent with the involvement of EAAT2 downregulation in the development of central sensitization. Thus, long-term exposure to DHK appeared to increase the activity of NMDA and AMPA receptors. It was also indicated that activity of $mGluR_1$ was more affected than $mGluR_5$ following chronic exposure to DHK. Lastly, more NMDA receptors of dorsal horn neurons appeared to be affected by inhibition of EAAT2 than chronic exposure to BDNF. This indicates that the pathways to promote central sensitization may be different in inhibition of EAAT2 and release of BDNF following nerve injury. Overall, this study suggests that further investigation on EAAT2 may be a novel therapeutic approach for neuropathic pain.

5.10 References

Bhave G, Karim F, Carlton SM, & Gereau RW (2001). Peripheral group I metabotropic glutamate receptors modulate nociception in mice. *Nat Neurosci* **4**, 417-423.

Bird GC, Asghar AU, Ackley MA, & King AE (2001). Modulation of primary afferent-mediated neurotransmission and Fos expression by glutamate uptake inhibition in rat spinal neurones in vitro. *Neuropharmacology* **41**, 582-591.

Bleakman D, Alt A, & Nisenbaum ES (2006). Glutamate receptors and pain. *Semin Cell Dev Biol* **17**, 592-604.

Cho HJ, Kim JK, Park HC, Kim JK, Kim DS, Ha SO, & Hong HS (1998). Changes in brain-derived neurotrophic factor immunoreactivity in rat dorsal root ganglia, spinal cord, and gracile nuclei following cut or crush injuries. *Exp Neurol* **154**, 224-230.

Dougherty KD, Dreyfus CF, & Black IB (2000). Brain-derived neurotrophic factor in astrocytes, oligodendrocytes, and microglia/macrophages after spinal cord injury. *Neurobiol Dis* **7**, 574-585.

Edmonds B, Gibb AJ, & Colquhoun D (1995). Mechanisms of activation of glutamate receptors and the time course of excitatory synaptic currents. *Annu Rev Physiol* **57**, 495-519.

Fagni L, Ango F, Perroy J, & Bockaert J (2004). Identification and functional roles of metabotropic glutamate receptor-interacting proteins. *Semin Cell Dev Biol* **15**, 289-298.

Fundytus ME, Yashpal K, Chabot JG, Osborne MG, Lefebvre CD, Dray A, Henry JL, & Coderre TJ (2001). Knockdown of spinal metabotropic glutamate receptor 1 (mGluR(1)) alleviates pain and restores opioid efficacy after nerve injury in rats. *Br J Pharmacol* **132**, 354-367.

Galik J, Youn DH, Kolaj M, & Randic M (2008). Involvement of group I metabotropic glutamate receptors and glutamate transporters in the slow excitatory synaptic transmission in the spinal cord dorsal horn. *Neuroscience* **154**, 1372-1387.

Grudt TJ & Perl ER (2002). Correlations between neuronal morphology and electrophysiological features in the rodent superficial dorsal horn. *J Physiol* **540**, 189-207.

Guo W, Zou S, Guan Y, Ikeda T, Tal M, Dubner R, & Ren K (2002). Tyrosine phosphorylation of the NR2B subunit of the NMDA receptor in the spinal

cord during the development and maintenance of inflammatory hyperalgesia. *J Neurosci* **22**, 6208-6217.

Ikeda H, Kiritoshi T, & Murase K (2009). Synaptic plasticity in the spinal dorsal horn. *Neurosci Res* **64**, 133-136.

Ji RR, Kohno T, Moore KA, & Woolf CJ (2003). Central sensitization and LTP: do pain and memory share similar mechanisms? *Trends Neurosci* **26**, 696-705.

Karim F, Wang CC, & Gereau RW (2001). Metabotropic glutamate receptor subtypes 1 and 5 are activators of extracellular signal-regulated kinase signaling required for inflammatory pain in mice. *J Neurosci* **21**, 3771-3779.

Latremoliere A & Woolf CJ (2009). Central sensitization: a generator of pain hypersensitivity by central neural plasticity. *J Pain* **10**, 895-926.

Li P, Kerchner GA, Sala C, Wei F, Huettner JE, Sheng M, & Zhuo M (1999). AMPA receptor-PDZ interactions in facilitation of spinal sensory synapses. *Nat Neurosci* **2**, 972-977.

Lu VB, Ballanyi K, Colmers WF, & Smith PA (2007). Neuron type-specific effects of brain-derived neurotrophic factor in rat superficial dorsal horn and their relevance to 'central sensitization'. *J Physiol* **584**, 543-563.

Lu VB, Biggs JE, Stebbing MJ, Balasubramanyan S, Todd KG, Lai AY, Colmers WF, Dawbarn D, Ballanyi K, & Smith PA (2009). Brain-derived neurotrophic factor drives the changes in excitatory synaptic transmission in the rat superficial dorsal horn that follow sciatic nerve injury. *J Physiol* **587**, 1013-1032.

Luscher C, Nicoll RA, Malenka RC, & Muller D (2000). Synaptic plasticity and dynamic modulation of the postsynaptic membrane. *Nat Neurosci* **3**, 545-550.

Maki R, Robinson MB, & Dichter MA (1994). The glutamate uptake inhibitor L-trans-pyrrolidine-2,4-dicarboxylate depresses excitatory synaptic transmission via a presynaptic mechanism in cultured hippocampal neurons. *J Neurosci* **14**, 6754-6762.

Neves G, Cooke SF, & Bliss TV (2008). Synaptic plasticity, memory and the hippocampus: a neural network approach to causality. *Nat Rev Neurosci* **9**, 65-75.

Nie H & Weng HR (2009). Glutamate transporters prevent excessive activation of NMDA receptors and extrasynaptic glutamate spillover in the spinal dorsal horn. *J Neurophysiol* **101**, 2041-2051.

Nie H & Weng HR (2010). Impaired glial glutamate uptake induces extrasynaptic glutamate spillover in the spinal sensory synapses of neuropathic rats. *J Neurophysiol* **103**, 2570-2580.

Reichelt W & Knopfel T (2002). Glutamate uptake controls expression of a slow postsynaptic current mediated by mGluRs in cerebellar Purkinje cells. *J Neurophysiol* **87**, 1974-1980.

Rosenblum K, Dudai Y, & Richter-Levin G (1996). Long-term potentiation increases tyrosine phosphorylation of the N-methyl-D-aspartate receptor subunit 2B in rat dentate gyrus in vivo. *Proc Natl Acad Sci U S A* **93**, 10457-10460.

Takayasu Y, Iino M, & Ozawa S (2004). Roles of glutamate transporters in shaping excitatory synaptic currents in cerebellar Purkinje cells. *Eur J Neurosci* **19**, 1285-1295.

Thomson LM, Zeng J, & Terman GW (2006). Differential effect of glutamate transporter inhibition on EPSCs in the morphine naive and morphine tolerant neonatal spinal cord slice. *Neurosci Lett* **407**, 64-69.

Weng HR, Chen JH, Pan ZZ, & Nie H (2007). Glial glutamate transporter 1 regulates the spatial and temporal coding of glutamatergic synaptic transmission in spinal lamina II neurons. *Neuroscience* **149**, 898-907.

Wong CS, Wu GJ, Chen WF, Jean YH, Hung CH, Lin CS, Huang SY, & Wen ZH (2009). N-Methyl-D-aspartate receptor antagonist d-AP5 prevents pertussis toxin-induced alterations in rat spinal cords by inhibiting increase in concentrations of spinal CSF excitatory amino acids and downregulation of glutamate transporters. *Brain Res Bull* **80**, 69-74.

Woolf CJ (1991). Generation of acute pain: central mechanisms. *Br Med Bull* **47**, 523-533.

Woolf CJ & Salter MW (2000). Neuronal plasticity: increasing the gain in pain. *Science* **288**, 1765-1769.